Estimation of Groundwater Seepage and Nitrogen Load from Septic Systems to Lakes Marshall, Roberts, Weir, and Denham

Manuscript Completed: February 2014

Update 1: October, 2014

ArcNLET flow model was calibrated against the seepage measurements of Lake Roberts.

Update 2: January, 2015

Septic tank locations were adjusted to meet the 150-feet setback distance for Lake Roberts.

Update 3: April, 2015

Impacts of watershed boundary was discussed for Lake Roberts.

Update 4: May, 2015

ArcNLET flow model was calibrated against hydraulic head measurements near Lake Weir, and more septic tanks were included in the Lake Weir modeling.

Prepared by

Ming Ye, Yan Zhu, and Mohammad Sayemuzzaman

Department of Scientific Computing, Florida State University, Tallahassee, FL 32306

Rick Hicks, FDEP Contract Manager

Prepared for

Florida Department of Environmental Protection

Tallahassee, FL

EXECUTIVE SUMMARY

The ArcGIS-based Nitrate Load Estimation Toolkit (ArcNLET), which was developed for the Florida Department of Environmental Protection (FDEP) by the Florida State University (FSU), was used in this study to the watersheds of Lake Marshall, Lake Roberts, Lake Weir, and Lake Denham. The ArcNLET modeling is to estimate groundwater seepage velocity into the four lakes and nitrogen load from septic systems within the watershed to the four lakes. While ArcNLET is based on a simplified model of groundwater flow and nitrogen transport, the model considers heterogeneous hydraulic conductivity and porosity as well as spatial variability of septic system locations, surface water bodies, and distances between septic systems and surface water bodies. ArcNLET also considers key mechanisms controlling nitrogen transport, including advection, dispersion, and denitrification. After preparing model input files (e.g., raster file of hydraulic conductivity) in the ArcGIS format, setting up an ArcNLET model run is easy through a graphic user interface. The modeling results are readily available for post-processing and visualization within ArcGIS. The modeling results include Darcy velocity, groundwater flow paths from septic systems to surface water bodies, spatial distribution of nitrogen plumes, and nitrogen load estimates to individual surface water bodies; these results can be used directly for environmental management and regulation of nitrogen pollution.

The ArcNLET flow and transport models of this study were established using the data downloaded from public-domain websites and provided by colleagues from FDEP. Site-specific data of DEM, waterbodies, septic locations, hydraulic conductivity, and porosity were used in the ArcNLET modeling. Literature-based smoothing factor for flow modeling and transport parameters, including longitudinal dispersivity (α_L), transverse horizontal dispersivity (α_{TH}), decay coefficient (k), inflow mass to groundwater (M_{in}), and source plane concentration (C_0) were used in the transport modeling. These parameter values are listed in Table ES-1. Due to lack of observations of hydraulic head and nitrogen concentration, only flow model calibration was conducted for Lake Roberts and Lake Weir. Using the seepage measurements available for Lake Roberts, the smoothing factor and hydraulic conductivity are calibrated, and the calibrated smoothing factor increases from 50 to 400 to match the small values of measured seepage rate (Table ES-0-1). However, the smoothing factor remains 50, after the flow model was calibrated against the hydraulic head data available at a landfill site near Lake Weir.

Table ES-0-1. Literature-based ArcNLET model parameters for the four watersheds. The smoothing factor is changed to 400 for Lake Roberts after calibrating the ArcNLET flow model using seepage rate measurements.

Parameter	Lake Marshall	Lake Roberts	Lake Weir	Lake Denham
Smoothing factor	50	50 (400)	50	50
M_{in} (g/d)	24.22	24.22	21.31	22.19
C_0 (mg/L)	40	40	40	40
α_L (m)	10	10	10	10
α_{TH} (m)	1	1	1	1
k (d^{-1})	0.001	0.001	0.001	0.001

ArcNLET can simulate directions and magnitude of groundwater flows at each raster cell; using ArcGIS extraction tools to extract the simulated seepage velocity along lake perimeters can estimate groundwater seepage velocity to the lakes. Table ES-2 lists the statistics of the simulated seepage velocity to the four lakes. The average estimates is the largest for Lake Weir (3.244 m/d) and the smallest for Lake Denham (0.021 m/d). The estimates are consistent with the lake geometry. For example, the average seepage estimate is 0.391 m/d for Lake Marshall but only 0.121 m/d for Lake Roberts. This is consistent with the deeper slope of land surface around Lake Marshall than around Lake Roberts. For Lake Roberts, the simulated groundwater flows become significantly smaller when the calibrated smoothing factor and hydraulic conductivity are used.

Table ES-0-2. Simulated groundwater seepage velocity into the four lakes.

Statistics	Lake Marshall	Lake Roberts		Lake Weir	Lake Denham
		Uncalibrated	Calibrated		
Min	0.154	0.018	0.0009	0.000	0.005
Max	0.627	0.196	0.0104	14.224	0.061
Sum	99.199	41.429	1.700	10762.250	13.819
Mean	0.391	0.121	0.005	3.244	0.021
Std. Dev.	0.096	0.048	0.0018	2.817	0.011

Table ES-3 lists the numbers of septic systems, the ArcNLET-estimated total loads (in the units of g/d and lb/yr), load (g/d) per septic system to the surface water bodies, and the reduction ratios for the four watersheds. The reduction ratio is the amount of denitrified nitrogen (i.e., the difference between the load to groundwater and the load to surface waterbodies) divided by the load to groundwater (i.e., the inflow mass, M_{in}). The table shows that, while the total load is proportional to the number of septic systems, the relation between total load and number of septic systems is not linear. The relation depends on the amount of denitrification. For example, because of the small reduction ratio, the load per septic system is the largest for the Lake Roberts watershed. As a result, the total load in the Lake Roberts watershed is about half of the total load in the Lake Weir watershed, although the number of septic systems in the Lake Roberts watershed is only 1/8 of that in the Lake Weir watershed. After the model calibration, the load to Lake Roberts becomes 35.9% smaller, and the reduction ratio becomes larger, which is attributed to the decrease of the simulated groundwater flow to match the observations of seepage rate.

Table ES-0-3. Simulated nitrogen loads to surface waterbodies and nitrogen reduction ratios for the four watersheds.

Name	Septic number	Total load (g/d)	Total load (lb/yr)	Load per septic systems (g/d)	Reduction ratio (%)
Lake Marshall	47	319.92	257.43	6.81	62.26
Lake Roberts (before calibration)	83	1413.54	1137.46	17.03	16.62
Lake Roberts (after calibration)	83	906.51	729.46	10.92	47.28
Lake Weir	2081	16141.05	12990.72	7.76	59.89
Lake Denham	28	262.87	211.53	9.39	37.65

The reduction ratios estimated in this study are comparable with those reported literature and those obtained in our modeling practice. The reduction ratios are determined by the flow path and flow velocity; large flow path and small flow velocity always lead to large amount of denitrification and thus large reduction ratio. Ye and Sun (2013) showed that flow paths and velocities are closely related to soil drainage conditions given in the SSURGO database. The relation however has not been evaluated in this study. Another way to evaluate reasonableness of the estimates is to compare the load estimate from septic systems with the total nitrogen load estimate. For example, a recent study (USEPA, 2013) for the Chesapeake Bay watershed indicates that septic systems contribute about 5% of the total nitrogen load. The comparison should be straightforward when the total load estimates are available.

The seepage rate measurements at Lake Roberts are important to calibrate the ArcNLET flow model for estimating the smoothing factor and hydraulic conductivity. The results of flow and solute transport modeling before the calibration are significantly different from those after the calibration. Generally speaking, after the calibration, the ArcNLET-simulated flow velocity and nitrogen load become smaller. However, the calibrated smoothing factor is not used for the other three watersheds, because the measured seepage rate is suspiciously small and it is unknown why the measurements at one site are significantly larger than those at other sites. If the seepage rate measurements are considered to be reasonable, it is straightforward to use the calibrated smoothing factor for the other three watersheds. It is also possible to use small values of hydraulic conductivity for the other three watersheds, if necessary.

CONTENTS

LIST OF FIGURES

LIST OF TABLES

1. INTRODUCTION

This report summarizes the modeling effort of the Florida State University (FSU) to support management of nutrient pollution of the Florida Department of Environmental Protection (FDEP) for Lake Roberts and Lake Marshall in Orange County, Lake Weir in Marion County, and Lake Denham in Lake County. Locations of the four lakes are shown in Figure 1-1, provided by Kyeongsik Phew at FDEP. The ArcGIS-Based Nitrate Load Estimation Toolkit (ArcNLET) (Rios et al. 2013a; Wang et al., 2013), developed by FSU, is used in this study to simulate groundwater flow and nitrate transport from septic systems in surficial aquifers. With the assumption that ammonium transports in the same way as nitrate, ArcNLET can be used to simulate nitrogen fate and transport. ArcNLET provides the following outputs:

(1) Approximation of water table shape in the modeling domains that includes lakes,
(2) Magnitude and direction of Darcy velocity at raster cells of the modeling domains,
(3) Nitrogen plumes from individual septic systems to nearby water bodies including lakes, and
(4) Nitrogen load estimates to the individual water bodies including the lakes.

The resulting Darcy velocity can be used to estimate groundwater seepage velocity to the individual lakes by extracting the velocity at the lake perimeters.

ArcNLET modeling requires the following raster and polygon files that are available in the public domain:

(1) Digital elevation model (DEM) of tomography that is available at the USGS National Map Viewer and Download Framework (http://nationalmap.gov/viewer.html). The DEM data is smoothed to generate the shape of water table, based on the assumption that water table is subdued replica of tomography. The smoothed DEM is used to evaluate groundwater flow magnitude and direction by using the Darcy's law.
(2) Water body locations that is available from USGS National Hydrography Database (http://nhd.usgs.gov/). Flow lines from septic systems are terminated at the water bodies.
(3) Locations of septic systems that is available from FDEP database. Xueqing Gao and Kyeongsik Phew at FDEP provided the location files to FDEP.
(4) Hydraulic conductivity and porosity of the modeling domains download from the Soil Survey Geographic Database (SSURGO).

The data above is site specific. ArcNLET modeling also involves the following parameters of groundwater flow and solute transport that are obtained from literature in this study:

(1) Dispersivities in the longitudinal and horizontal transverse directions, and
(2) Decay coefficient of denitrification.

Site-specific values of these parameters can be obtained by model calibration, in which the literature-based parameter values are adjusted to match simulations of hydraulic head and nitrogen concentration to corresponding field observations. However, due to the lack of field observations in this study, the model calibration was not performed. Instead, the ArcNLET simulation of this study is conducted using the parameter values obtained from literature and other sites, e.g., the City of Jacksonville, the City of Stuart, St. Lucie County, and Martin County. Justification of using the parameter values is given in the report.

In the remainder of this report, the conceptual model of groundwater flow and nitrogen transport used in ArcNLET and its computational implementation are briefly described in Section 2. Sections 3-6 present the modeling practice and results for the four lakes. The summary and conclusions of this study are discussed in Section 7.

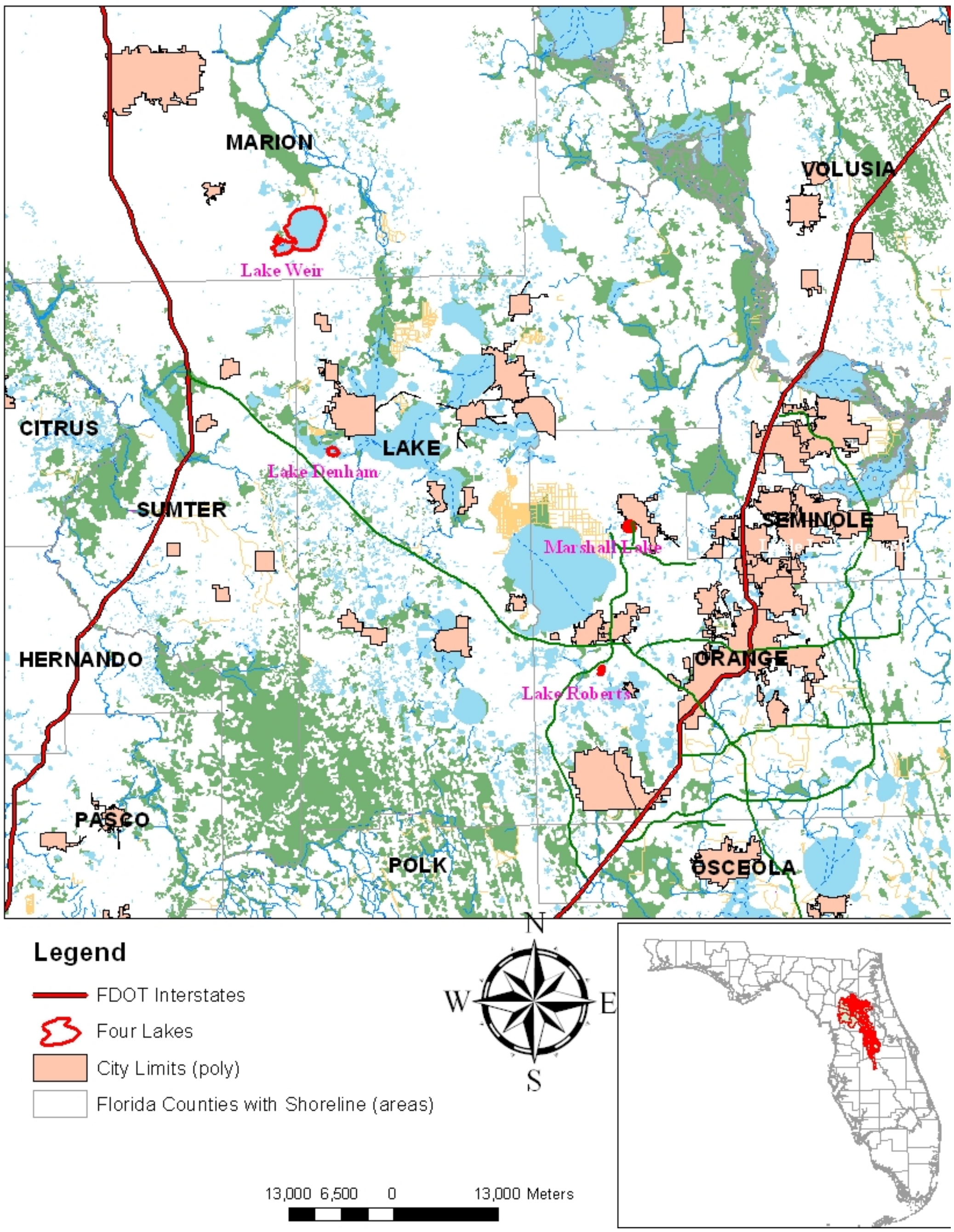

Figure 1-1. Location of Lake Robert and Lake Marshall in Orange County, Lake Weir in Marion County, and Lake Denham in Lake County.

2. SIMPLIFIED CONCEPTUAL MODEL OF ArcNLET

ArcNLET is based on a simplified conceptual model of groundwater flow and nitrate transport. The model has three sub-models: groundwater flow model, nitrate transport model, and nitrate load estimation model. The results from the flow model are used by the transport model, whose results are in turn utilized by the nitrate load estimation model. By invoking assumptions and simplifications to the system being modeled, computational cost is significantly reduced, which enables ArcNLET to provide quick estimates of nitrate loads from septic systems to surface water bodies. The three submodels are briefly described here; more details of them can be found in Rios (2010) and Rios et al. (2013a). Ammonium is not explicitly simulated in ArcNLET. Instead, it is assumed in this study that ammonium transport is the same as nitrate transport so that ArcNLET can simulate nitrogen transport and estimate nitrogen load, not merely nitrate load, from septic systems to surface water bodies. This assumption however may overestimate nitrogen loads.

The groundwater flow model of ArcNLET is simplified by assuming that the water table is a subdued replica of the topography in the surficial aquifer. According to Haitjema and Mitchell-Bruker (2005), the assumption is valid if

$$\frac{RL^2}{mKHd} > 1 , \tag{1}$$

where R [m/day] is recharge, L [m] is average distance between surface waters, m is a dimensionless factor accounting for the aquifer geometry, and is between 8 and 16 for aquifers that are strip-like or circular in shape, K [m/day] is hydraulic conductivity, H [m] is average aquifer thickness, and d [m] is the maximum distance between the average water level in surface water bodies and the elevation of the terrain. The criterion, as a rule of thumb, can be met in shallow aquifers in flat or gently rolling terrain. Based on the assumption, the shape of water table can be obtained by smoothing land surface topography given by DEM of the study area. In ArcNLET, the smoothing is accomplished using moving-window average via a 7 × 7 averaging window. The smoothing process needs to be repeated for multiple times, depending on discrepancy between the shapes of topography and water table. The number of the smoothing process, called smoothing factor, is specified by ArcNLET users as an input parameter of ArcNLET. This parameter needs to be calibrated against measured hydraulic heads in the study area, as explained in detail in Section 4.

With the assumption that smoothed DEM has the same shape (not the same elevation) of water table, hydraulic gradients can be estimated from the smoothed DEM. Subsequently, groundwater seepage velocity, v, can be obtained by applying Darcy's Law

$$\begin{aligned} v_x &= -\frac{K}{\phi}\frac{\partial h}{\partial x} \approx -\frac{K}{\phi}\frac{\partial z}{\partial x} \\ v_y &= -\frac{K}{\phi}\frac{\partial h}{\partial y} \approx -\frac{K}{\phi}\frac{\partial z}{\partial y} \end{aligned} , \tag{2}$$

where K is hydraulic conductivity [LT^{-1}], ϕ is porosity, h is hydraulic head, and hydraulic gradient ($\partial h/\partial x$ and $\partial h/\partial y$) is approximated by the gradient of the smoothed topography ($\partial z/\partial x$ and $\partial z/\partial y$). Implementing the groundwater flow model in the GIS environment yields the magnitude and direction of the flow velocity for every discrete cell of the modeling domain, which are used to estimate flow paths originating from individual septic systems and ending in surface water bodies. The calculation considers spatial variability of hydraulic conductivity, porosity, hydraulic head, and septic system locations. Because hydraulic gradients and water bodies are not hydraulically linked in the model, ArcNLET users need to evaluate whether the resulting shape of the water table is consistent with the drainage network associated the water bodies. The values of hydraulic conductivity and conductivity can be obtained from field measurements, literature data, and/or by calibration against measurements of hydraulic head and groundwater velocity.

Additional assumptions and approximations of the flow model are made as follows: (1) the Dupuit-Forchheimer assumption is used so that the vertical flow can be ignored and only two-dimensional (2-D) isotropic horizontal flow is simulated; (2) the steady-state flow condition is assumed, since this software is used for the purpose of long-term environmental planning; (3) the surficial aquifer does not include karsts or conduits so that Darcy's Law can be used; (4) mounding on water table due to recharge from septic systems and rainfall is not explicitly considered (but assumed to be reflected by the steady-state water table); (5) the flow field is obtained from the water table without explicit consideration of a water balance; (6) groundwater recharge from the estuary is disregarded. While these assumptions may not be ideal, especially the assumption of steady-state, they are needed to make model complexity compatible with available data and information and to make the model run efficient in the GIS modeling environment.

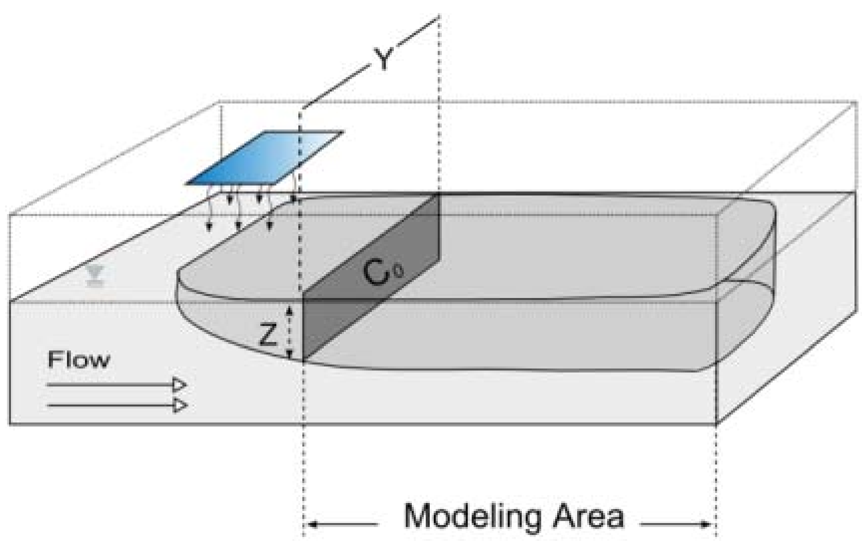

Figure 2-1. Conceptual model of nitrate transport in groundwater adapted from Aziz et al. (2000). The unsaturated zone is bounded by the rectangular box delineated by the dotted lines; the groundwater zone is bounded by the box delineated by the solid lines

Figure 2-1 shows the conceptual model of nitrate transport in ArcNLET, which is similar to that of BIOSCREEN (Newell et al. 1996) and BIOCHLOR (Aziz et al. 2000) developed by the U.S. EPA. In the conceptual model, nitrate enters the groundwater zone with a uniform and steady flow in the direction indicated. The Y−Z plane in Figure 2-1 is considered as a source plane (with a constant concentration C_0 [ML^{-3}]) through which nitrate enters the groundwater system. Two-dimensional (2-D) nitrate transport in groundwater is described using the advection-dispersion equation

$$\frac{\partial C}{\partial t} = D_x \frac{\partial^2 C}{\partial x^2} + D_y \frac{\partial^2 C}{\partial y^2} - v\frac{\partial C}{\partial x} - kC \tag{3}$$

where C is the nitrate concentration [M/L^3], t is time [T], D_x and D_y are the dispersion coefficients in the x and y directions, respectively [L^2T^{-1}], v is the constant seepage velocity in the longitudinal direction [L], and k is the first-order decay coefficient [T^{-1}]. This equation assumes homogeneity of parameters (e.g., dispersion coefficient) and uniform flow in the longitudinal direction. The last term in Eq. 3 is to simulate the denitrification, in which nitrate is transformed into nitrogen gas through a series of biogeochemical reactions. Following McCray et al. (2005) and Heinen (2006), the denitrification process is modeled using first-order kinetics and included as the decay term, which can also be used to take into account other loss processes. The steady-state form, semi-analytical solution of Eq. 3 is derived based on that of West et al. (2007), which is of 3-D, steady-state form and similar to the work of Domenico (1987). The analytical solution used in this study is (Rios, 2010; Rios et al., 2013a)

$$\begin{aligned} C(x,y) &= \frac{C_0}{2} F_1(x) F_2(y,x) \\ F_1 &= \exp\left[\frac{x}{2\alpha_x}\left(1-\sqrt{1+\frac{4k\alpha_x}{v}}\right)\right] \\ F_2 &= erf\left(\frac{y+Y/2}{2\sqrt{\alpha_y x}}\right) - erf\left(\frac{y-Y/2}{2\sqrt{\alpha_y x}}\right) \end{aligned} \tag{4}$$

where α_x and α_y [L] are longitudinal and horizontal transverse dispersivity, respectively, Y [L] is the width of the source plane, and C_0 [M/L^3] is the constant source concentration at the source plane. A review of analytical solutions of this kind and errors due to assumptions involved in their derivation is provided by Srinivasan et al. (2007).

The 2-D concentration plume is extended downwards to the depth Z of the source plane (Figure 2-1); the pseudo three-dimensional (3-D) plume is the basis for estimating the amount of nitrate that enters into groundwater and loads to surface water bodies. While each individual septic system has its own source concentration, C_0, drainfield width, Y, and average plume thickness, Z, the information and data of these variables are always unavailable in a management project. Therefore, constant values are used for all septic systems in this study. ArcNLET allows using different C_0 values for different septic systems, if the data are available. Despite of the constant values used for all the septic systems, each individual septic system has its own concentration plume, because flow velocity varies between the septic systems. Since the flow velocity estimated in the groundwater flow model is not uniform but varies in space, in order to use the analytical solution with uniform velocity, the harmonic mean of velocity (averaged along the flow path of a plume) is used for evaluating each individual plume. The plumes either end at surface water bodies or are truncated at a threshold concentration value (usually very small, e.g., 10^{-6}). After the plumes for all septic systems are estimated, by virtue of linearity of the advection-dispersion equation with respect to concentration, the individual plumes are added together to obtain the spatial distribution of nitrate concentration in the modeling domain. The superposition however may result in higher and shallower concentrations than exist in the field unless the averaging depth is deep enough.

The nitrate load estimation model evaluates the amount of nitrate loaded to target surface water bodies. For the steady-state model, this is done using the mass balance equation, $M_{out} = M_{in} - M_{dn}$, where M_{out} [MT^{-1}] is mass load rate to surface water bodies, M_{in} [MT^{-1}] is mass inflow rate from septic systems to groundwater, and M_{dn} [MT^{-1}] is mass removal rate due to denitrification. The mass inflow rate, M_{in}, consists of inflow due to advection and dispersion, and is evaluated via

$$M_{in} = YZ\phi\left(vC_0 - \alpha_x v \left.\frac{\partial C}{\partial x}\right|_{x=0} \right) = YZ\phi v C_0 \frac{1+\sqrt{1+\frac{4k\alpha_x}{v}}}{2} \quad . \tag{5}$$

The derivative, $\partial C/\partial x$, used for calculating the dispersive flux is evaluated using an analytical expression based on the analytical expression of concentration in equation (4). When the mass inflow rate is known, it can be specified within ArcNLET. Otherwise, the mass inflow rate is calculated by specifying the Z value. The mass removal rate due to denitrification, M_{dn}, is estimated via

$$M_{dn} = \sum_i kC_i V_i \phi_i \ , \tag{6}$$

where C_i and V_i are concentration and volume of the i-th cell of the modeling domain, and kC_i is denitrification rate assuming that denitrification is the first-order kinetic reaction (Heinen 2006). If a plume does not reach any surface water bodies, the corresponding nitrate load is theoretically zero.

The simplified groundwater flow and nitrate transport model is implemented as an extension of ArcGIS using the Visual Basic .NET programming language. In keeping with the object oriented paradigm, the code project is structured in a modular fashion. Development of the graphical user interface (GUI) elements is separated from that of the model elements; further modularization is kept within the development of GUI and model sub-modules. The main panel of the model GUI is shown in Figure 2-2; there are four tabs, each of which represents a separate modeling component. For example, the tab of Groundwater Flow is for estimating magnitude and direction of groundwater flow velocity, and the tab of Particle Tracking for estimating flow path from each septic system. Each tab is designed to be a self-contained module and can be executed individually within ArcGIS. Five ArcGIS layers are needed for running ArcNLET. They are DEM, hydraulic conductivity, and porosity in raster form, septic system locations in point form, and surface water bodies in polygon form. These ArcGIS files need to be prepared outside ArcNLET. The output files are also ArcGIS layers that can be readily post-processed and visualized within ArcGIS. More details of the software development, including verification and validation, are described in Rios (2010) and Rios et al. (2013a).

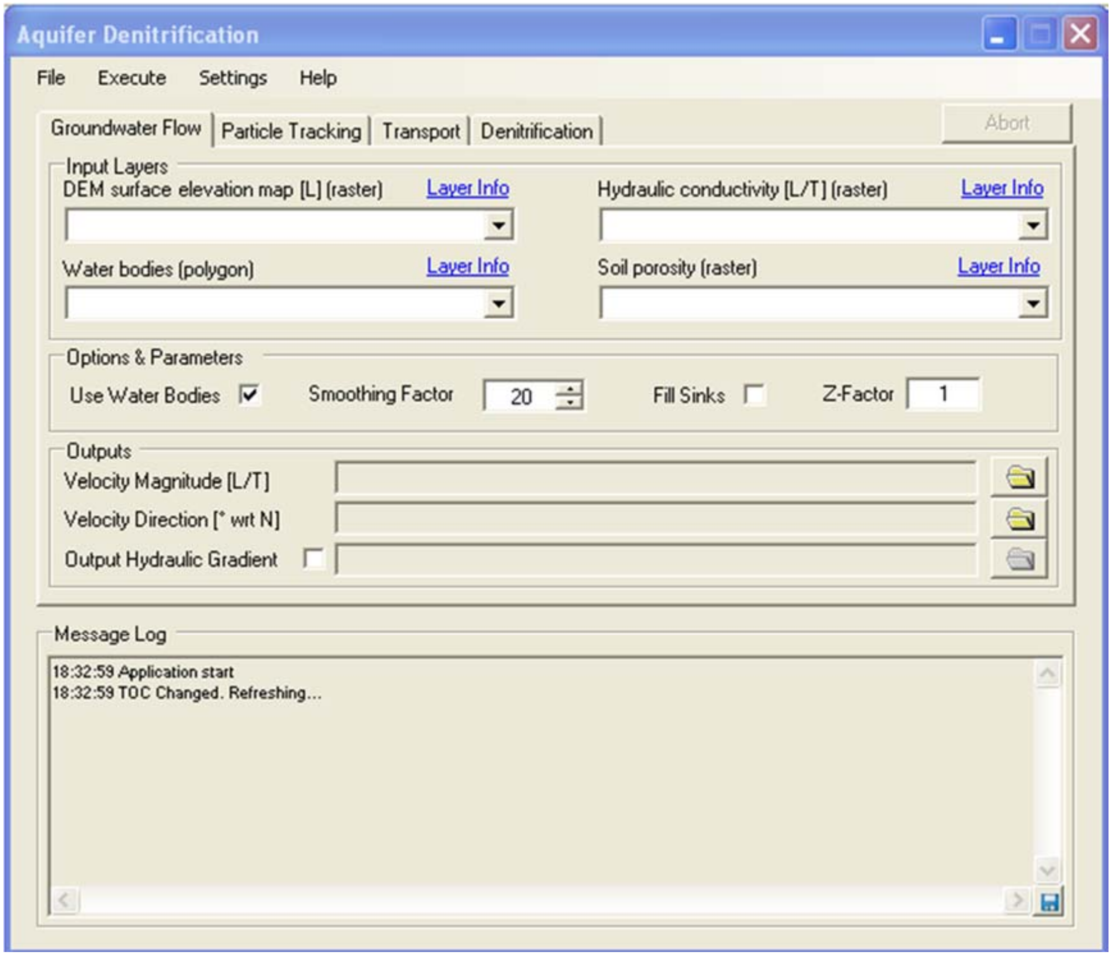

Figure 2-2. Main Graphic User Interface (GUI) of ArcNLET with four modules of Groundwater Flow, Particle Tracking, Transport, and Denitrification

Before ArcNLET is used for estimating nitrogen load to surface water bodies, calibrating the model parameters is always needed to match model simulations to field observations. However, in many projects of nitrogen pollution management, field observations are scarce. This is the reason of developing ArcNLET whose complexity is compatible with available data. As shown in the next section, observation data is extremely limited in the modeling area, and the conceptual model based on the limited data should be simple. On the other hand, the calibrated ArcNLET model is able to reasonably match field observations, as shown in Section 4.

3. ARCNLET MODELING FOR LAKE MARSHALL

3.1. Modeling Site and Geographic Data

Lake Marshall is located in the Orange County and at the northeast side of Lake Apopka (Figure 3-1). Figure 3-2 shows the boundary of the watershed where Lake Marshall resides; the watershed boundary was downloaded from FDEP database and provided by Xueqing Gao at FDEP. In addition to Lake Roberts, the watershed also includes several small waterbodies and a few swamps and marshes as shown in Figure 3-2; the polygon files of waterbodies and swamps and marshes were also provided by Xueqing Gao. The swamps and marshes were merged into waterbodies so that they also receive nitrogen load from the septic systems. The merge is considered to be reasonable, because the swamps and marshes are of low elevation and should be discharge areas of groundwater flow.

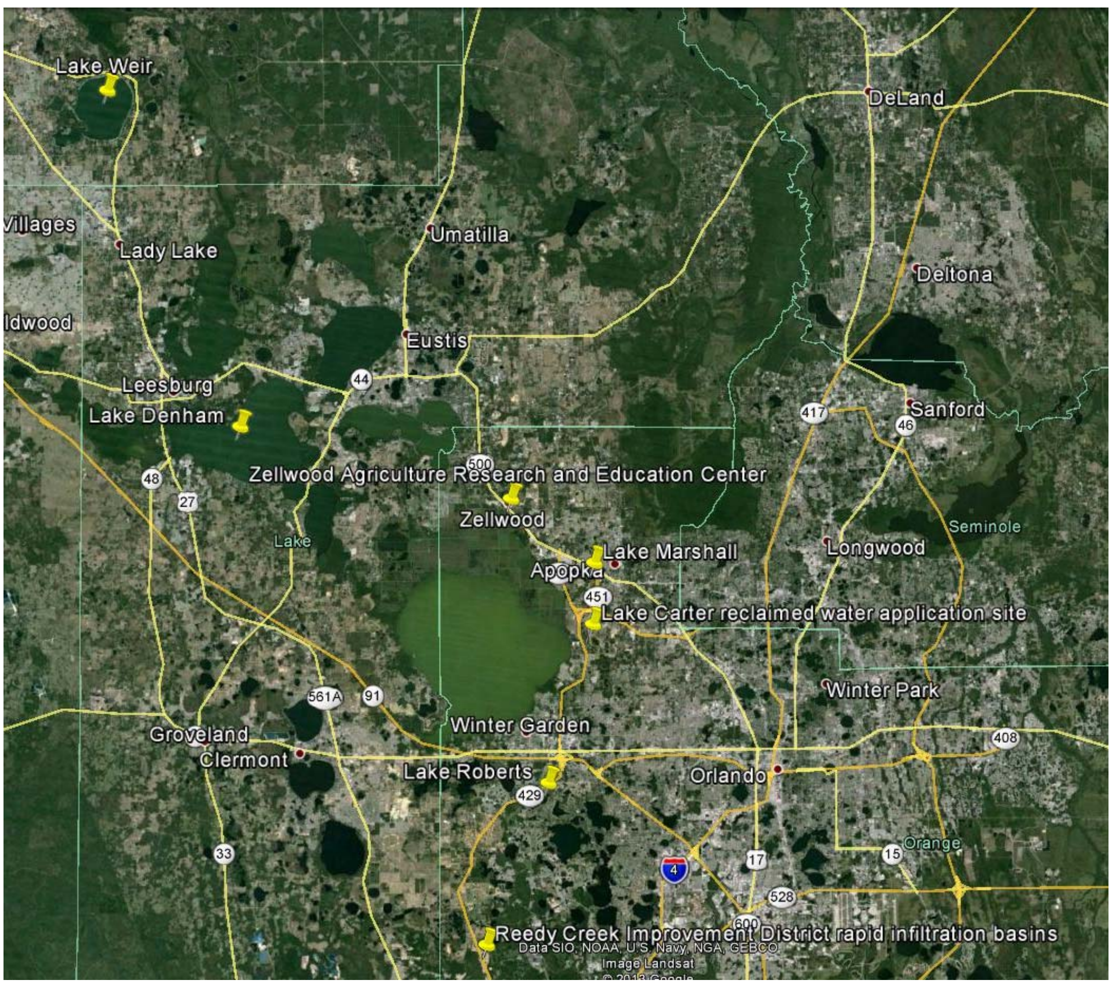

Figure 3-1. Locations of Lake Roberts, Lake Marshall, Lake Denham, and Lake Weir. The figure also shows two sites: Reedy Creek Improvement District and Lake Carter reclaimed water application site; hydraulic and transport parameter values at the two sites were used in the ArcNLET modeling of Lake Roberts and Lake Marshall.

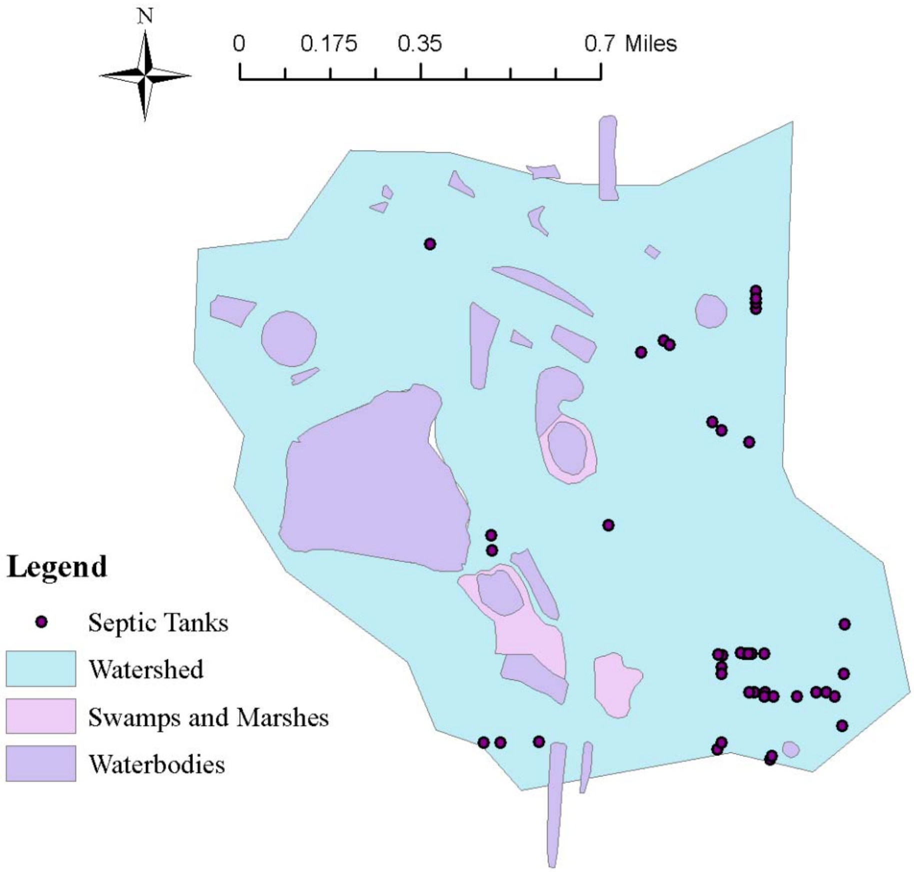

Figure 3-2. Watershed of Lake Marshall and locations of septic systems, waterbodies, and swamps and marshes. The swamps and marshes were merged into waterbodies later on for calculation of nitrogen load.

Figure 3-3 plots the DEM of the watershed and its vicinity downloaded from the USGS National Map Viewer and Download Framework (http://nationalmap.gov/viewer.html). Comparing Figures 3-2 and 3-3 shows that the major waterbodies (e.g., Lake Marshall) are reflected on the DEM with resolution of 10m × 10m (not as fine as that of LiDAR DEM). However, the small waterbodies in the watershed cannot be reflected on the DEM, due to its relatively coarse resolution. The elevation in the watershed decreases from west to east. The elevation difference of the Lake Marshall watershed is relatively large, in comparison with that of the Lake Roberts watershed, which will be discussed in the next chapter. It should be noted that the trough of low elevation left to Lake Marshall is outside of the watershed boundary. According to our ArcNLET modeling experience at the City of Jacksonville, the DEM resolution of 10m × 10m may require a relatively small value of smoothing factor such as 50. This value was used in this study.

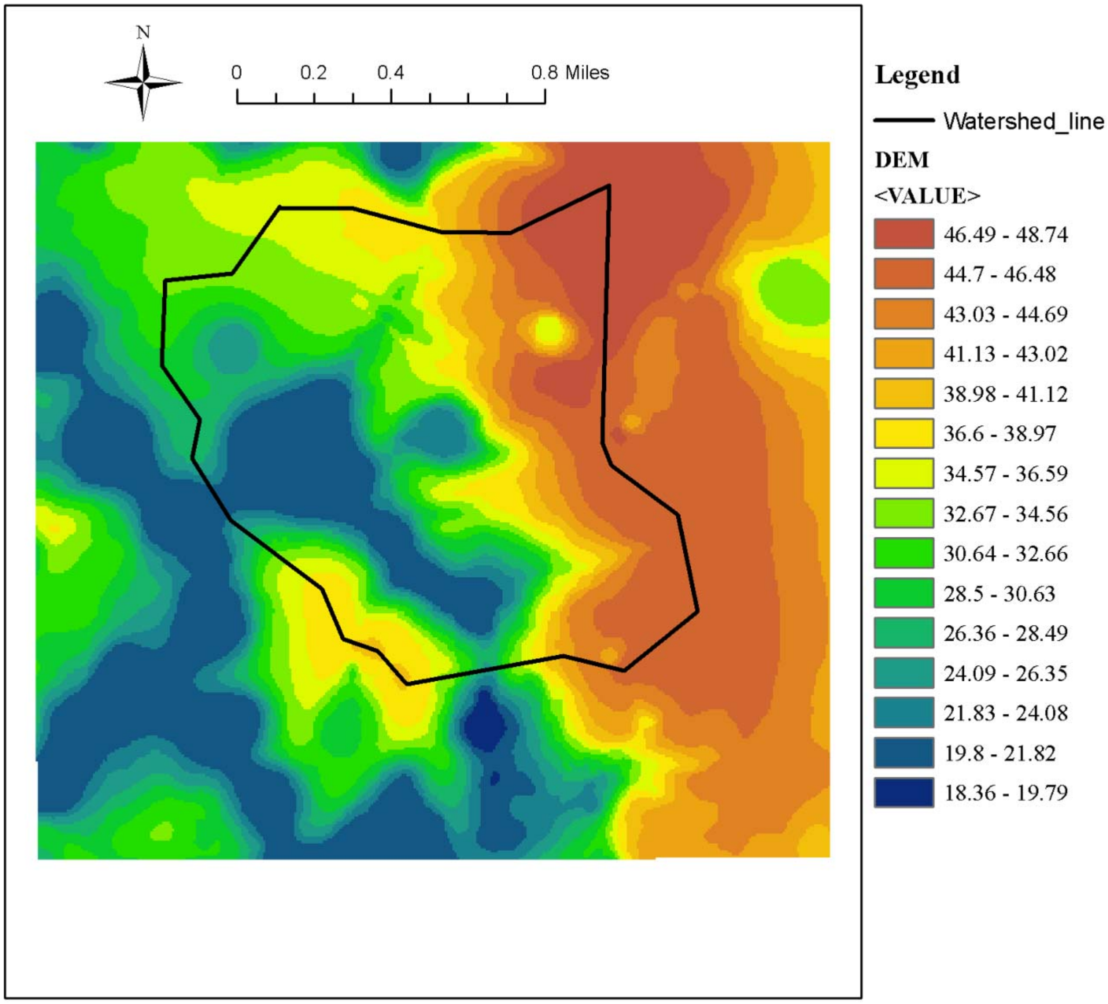

Figure 3-3. DEM of the Lake Marshall watershed and its vicinity.

3.2. Parameters of Groundwater Flow Parameters

For groundwater flow modeling, values of hydraulic conductivity and porosity are needed. The hydraulic conductivity values are obtained directly from the Soil Survey Geographic database (SSURGO) database, i.e., the representative values contained in the database. Since the database does not include porosity data, the data was evaluated as 1 – (D_B/D_P), where D_B and D_p are bulk density and particle density, respectively; bulk density was obtained directly from the SSURGO database and particle density was assumed to be 2.65 gcm^{-3} that is commonly used in soil physics. The SSURGO database contains data at the horizon levels; they need to be aggregated to the component and subsequently unit levels, because the hydraulic conductivity and porosity at the soil units are used in ArcNLET modeling. Figure 3-4 shows the soil units of the Lake Marshall watershed. The aggregation was completed by following the procedure described in Wang et al. (2011) and was assisted by Xueqing Gao at FDEP. Figures 3-5 and 3-6 plot the heterogeneous hydraulic conductivity and porosity values for the soil units in the Lake Marshall watershed. The figures show that, at the vicinity of Lake Marshall, the parameter values are relatively homogeneous

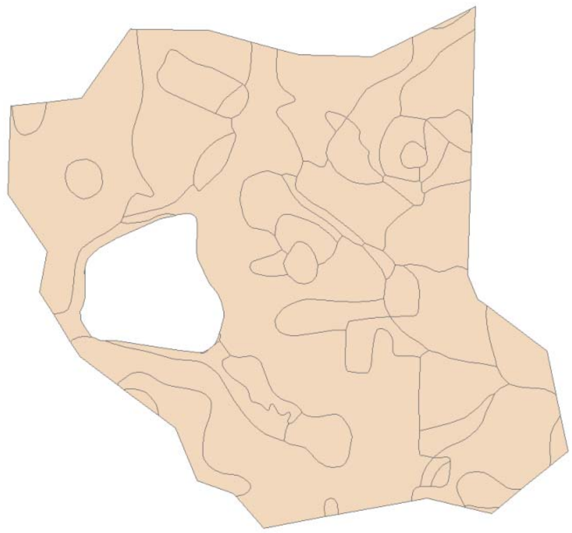

Figure 3-4. SSURGO soil units of the watershed of Lake Marshall.

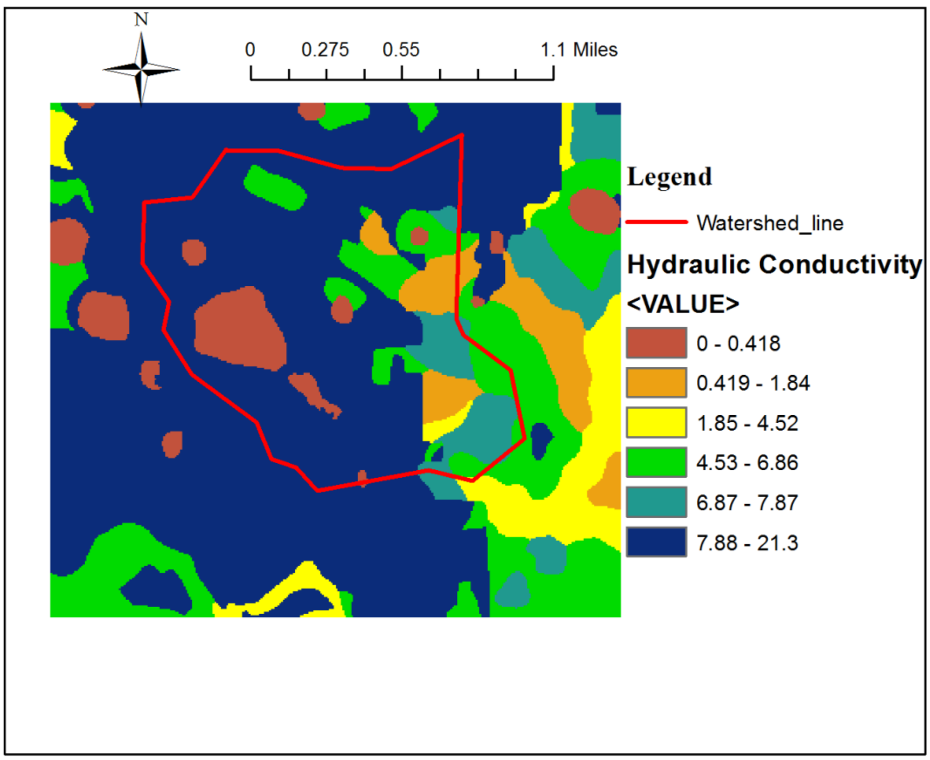

Figure 3-5. Heterogeneous hydraulic conductivity (m/d) of soil units of the Lake Marshall watershed.

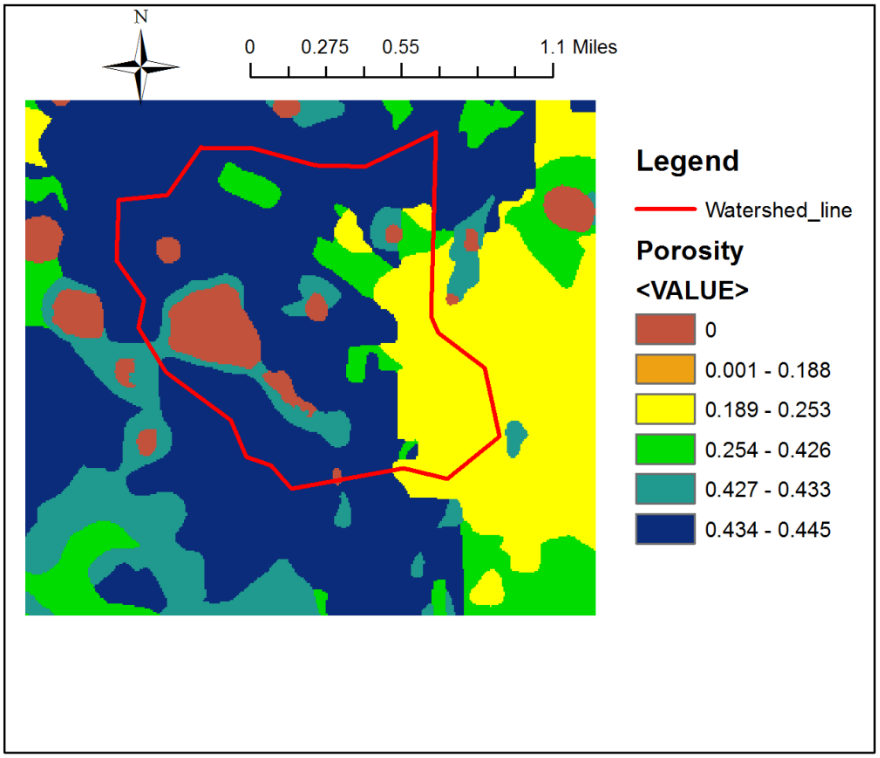

Figure 3-6. Heterogeneous porosity ([-]) of soil units of the Lake Marshall watershed.

The values of hydraulic conductivity and porosity are comparable with those obtained from model calibration at a nearby site. Sumner et al. (1996) conducted a numerical modeling of unsaturated and saturated flow at the Reedy Creek Improvement District in Orange County to simulate infiltration of reclaimed water. As shown in Figure 3-1, the Reedy Creek Improvement District is about 32.85 km (20.41miles) south to Lake Marshall and 14.02 km (8.71 miles) south to Lake Robert. Sumner et al. (1996) separated the modeling domain into three layers based on soil texture, and conducted model calibration to yield estimates of hydraulic parameters for the three layers. The calibrated parameter values are shown in Figure 3-8. As shown in Figure 3-6, the porosity value of the Lake Marshall watershed is close to that of Layer 3 of Sumner et al. (1996). This is not surprising, because, when aggregating the soil data, the data of the deepest horizons were used and the corresponding depth is about 2.3 meters. However, the hydraulic conductivity values (Figure 3-5) of the Lake Marshall watershed are smaller than that of Layer 3 of Sumner et al. (1996). For instance, for most of the watershed, the hydraulic conductivity value is about 8m/d, which is smaller than the horizontal (45 m/d) and vertical (14 m/d) hydraulic conductivity of Layer 3 of Sumner et al. (1996). The site-specific values are desired and used in this study. It should be note that larger hydraulic conductivity leads to faster flow and less denitrification, which results in larger nitrogen load from septic systems to surface waterbodies.

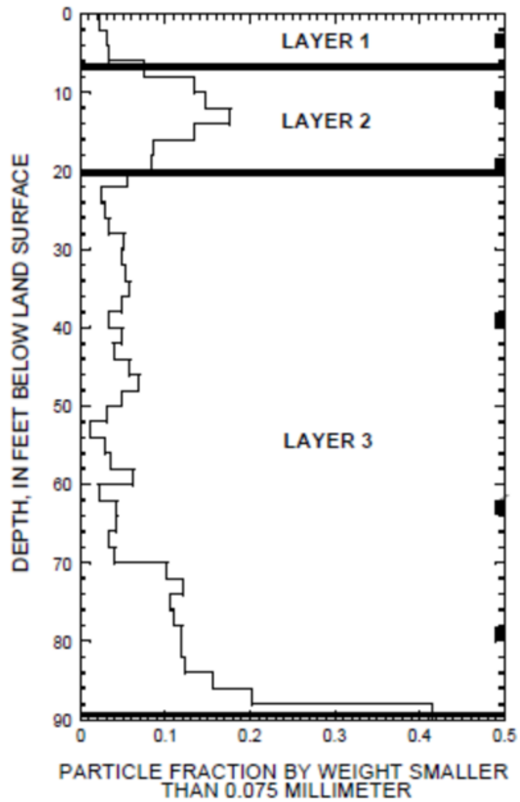

Figure 3-7. Soil texture description and delineation of three model layers in the modeling of Sumner et al. (1996) for the Reedy Creek Improvement District in Orange County. The figure is copied from Figure 6 of Sumner et al. (1996).

Layer	$(K_c)_r$ (ft/d)	$(K_c)_z$ (ft/d)	θ_s (ft^3/ft^3)	θ_r (ft^3/ft^3)	α (ft^{-1})	n (dimen-sion-less)
1	--	5.1	0.28	0.06	1.1	7
2	--	5.1	.35	.13	1.1	4
3	150	45	.45	.04	1.1	7

Figure 3-8. Calibrated hydraulic parameters reported in Sumner et al. (1996). The table is copied from Table 7 of Sumner et al. (1996).

3.3. Parameters of Nitrogen Transport Parameters

For longitudinal and horizontal transvers dispersivities, Blandford and Birdie (1992) reported the calibrated values of 50 feet and 5 feet used in their groundwater flow and solute transport modeling study for eastern Orange County. The longitudinal dispersivity of 15.24m is larger than that of 2.134m used in Davis (2000) for a groundwater flow and solute transport modeling in the City of Jacksonville. In addition, considering the scaling effect of dispersivity (i.e., dispersivity increases with spatial scale), for the modeling domain that is a small watershed of this study, the values of 10m and 1m were used for longitudinal and horizontal transverse dispersivities, respectively, for the entire watershed.

The decay coefficient of denitrification is also subject to uncertainty. Sumner et al. (1996) reported that nitrogen removal due to denitrification appeared to be minimal in their study, which was attributed to possible lack of reducing conditions and low amounts of organic carbon. However, the low magnitude of denitrification may be considered as an exception. A series of laboratory experiments of Reddy et al. (1980) using soil samples at the Zellwood Agricultural Research and Education Center indicated that the flooded organic soil can be used as an effective sink for reducing nitrogen levels of agricultural drainage waters. This conclusion should be applicable to the Lake Roberts watershed, because the distance between Lake Roberts and Lake Apopka is similar to that between Zellwood and Lake Apopka. The denitrification coefficient reported in Reddy et al. (1980) is between 0.038 d^{-1} and 0.75 d^{-1}. This range is comparable with the range of 0.004 – 2.27 d^{-1} reported in McCray et al. (2005) and the range of 0.004 – 1.08 d^{-1} used in the recently developed ArcNLET Monte Carlo simulation package (Rios et al., 2013b).

A more recent laboratory study of Byrne et al. (2012) based on water samples from Upper Floridan aquifer and spring water led to a similar conclusion that “results of the study indicate that denitrifying bacteria are present in the groundwater and spring water samples, and that these bacteria can readily denitrify the waters when suitable geochemical conditions exist.” Byrne et al. (2012) gave the rate of zeroth-order kinetics in the unit of mg L^{-1} day^{-1} (Figure 3-9). A rough way of converting the rate of zeroth-order kinetic to that of the first-order kinetics is to divide the rate of zeroth-order kinetics to nitrate concentration. This leads to the range of 0.042 – 0.089 d^{-1} for the results of the second treatment, 0.014 – 0.045 d^{-1} for the third treatment, and 0.46 – 0.88 d^{-1} for the fourth treatment. These ranges are comparable with that 0.038 – 0.75 d^{-1} reported in Reddy et al. (1980).

However, it should be noted that Byrne et al. (2012) evaluated the potential rate of denitrification. i.e., the capacity of denitrifying bacteria present in the water to reduce nitrate concentrations when certain optimal conditions exist, e.g., presence of denitrifying bacteria, ample supply of carbon to act as an electron donor source, and reducing conditions related to a low concentration of dissolved oxygen. For example, the denitrification rate of the fourth treatment was for the condition that carbon was added in the form of glucose. For the ambient water sample, denitrification did not occur for aquifer samples MW-2, MW-5R, MW-8B (this is the reason of adding nitrate in the other three treatments), which suggests denitrification in groundwater. Considering that the optimal conditions may not exist in reality, small value of decay rate should be used.

[(mg/L)/d N, milligrams nitrogen per liter per day; mg/L nitrate, milligrams nitrate-nitrogen per liter; NA, not applicable]

Site name	Date	1st treatment ambient denitrification rate, in (mg/L)/d N	2nd treatment ambient sample amended with 1.4 mg/L nitrate denitrification rate, in (mg/L)/d N	3rd treatment ambient sample amended with 5.0 mg/L nitrate denitrification rate, in (mg/L)/d N	4th treatment ambient sample amended with 5.0 mg/L nitrate and 10 mg/L glucose denitrification rate, in (mg/L)/d N	Nitrate consumption rate sample amended with 1.4 mg/L nitrate, in (mg/L)/d N
MW-2	11/10/09	NA	0.059	0.087	2.3	-0.227
MW-5R	11/10/09	NA	0.083	0.071	4.0	-0.090
MW-8B	12/15/08	NA	0.120	NA	NA	NA
MW-8B	11/10/09	NA	0.118	0.127	2.3	-0.205
Phipps Well	12/01/09	0.050	0.099	0.105	4.4	-0.173
Wekiwa Spring	12/01/09	0.072	0.124	0.142	2.4	-0.269
Rock Spring	12/01/09	0.071	0.095	0.226	3.4	-0.218

Figure 3-9. Denitrification rates measured by Byrne et al. (2012). The table is copied from Table 2 of Byrne et al. (2012).

Based on our experience of ArcNLET modeling, the value of 0.001 d^{-1} was used in this study. It is close to the value used in our modeling for St. Lucie and Martin Counties. Using this value is justified by the comparable magnitude of soil organic matter content (%) at the two sites, considering that soil organic matter content can be used as a measure of the extent of denitrification. We qualitatively compared the soil organic matter content of the soil units in the Lake Marshall watershed and its vicinity (Figure 3-10) and the Port St. Lucie area (Figure 3-11). The organic matter contents are obtained from the USDA soil survey website (http://websoilsurvey.sc.egov.usda.gov/App/HomePage.htm). The areas shown in Figures 3-10 and 3-11 are approximate, and large organic matter content values were excluded from the data analysis. Figure 3-12 plots the histograms of soil organic matter content for the two sites, and it shows that the soil organic matter content at the Port St. Lucie area is larger than that of the Lake Marshall watershed. Therefore, it is reasonable to use the decay coefficient calibrated at the Port St. Lucie area. Further study is warranted to select appropriate values of the decay coefficient, because it is significantly influential to the nitrogen load estimation.

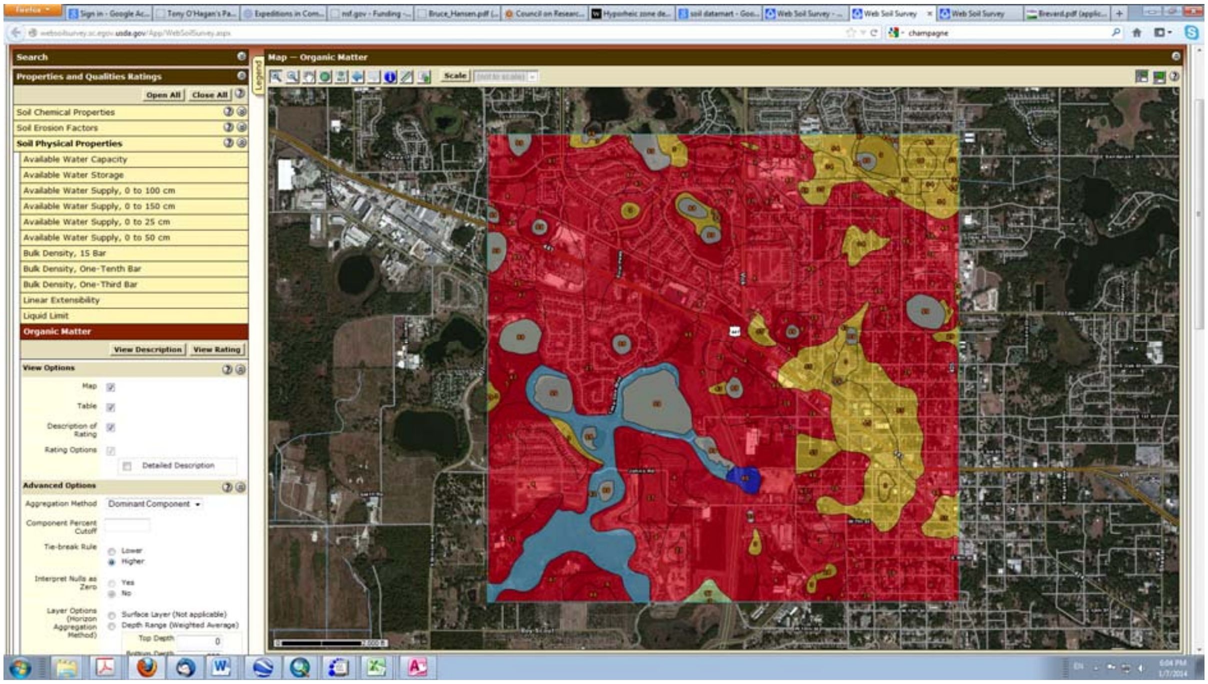

Figure 3-10. Soil units in the Lake Marshall watershed and its vicinity. The figure was generated from the USDA soil survey website (http://websoilsurvey.sc.egov.usda.gov/App/HomePage.htm).

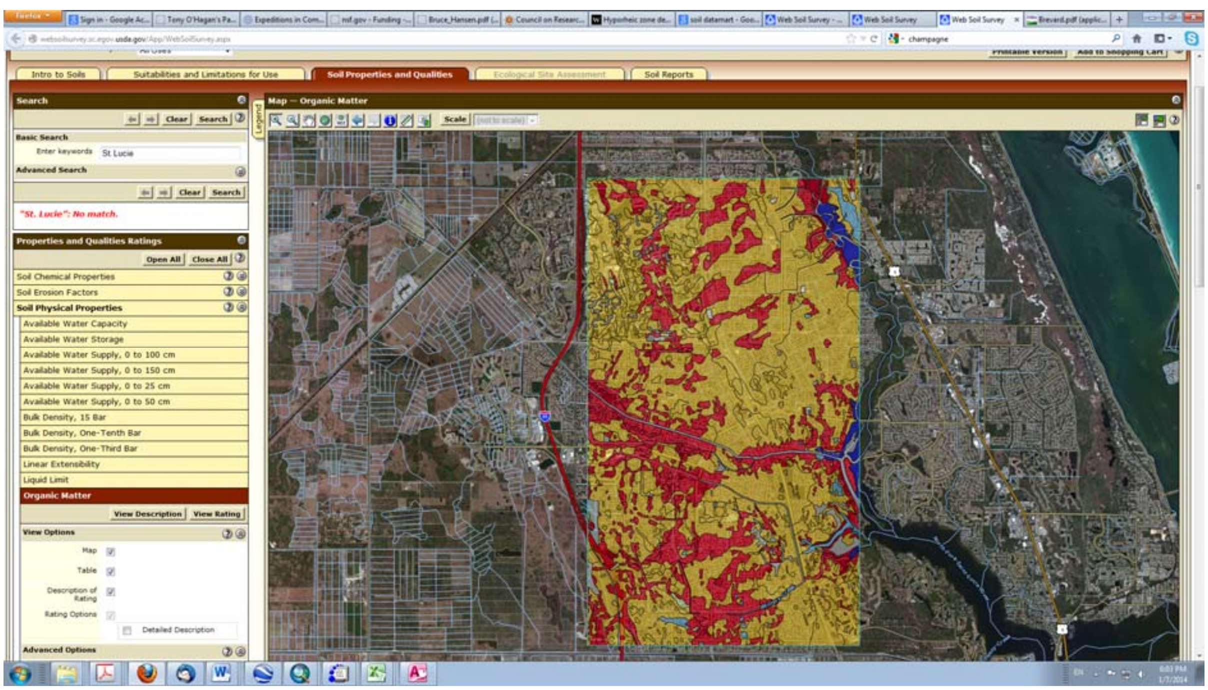

Figure 3-11. Soil units in the Port St. Lucie area. The figure was generated from the USDA soil survey website (http://websoilsurvey.sc.egov.usda.gov/App/HomePage.htm).

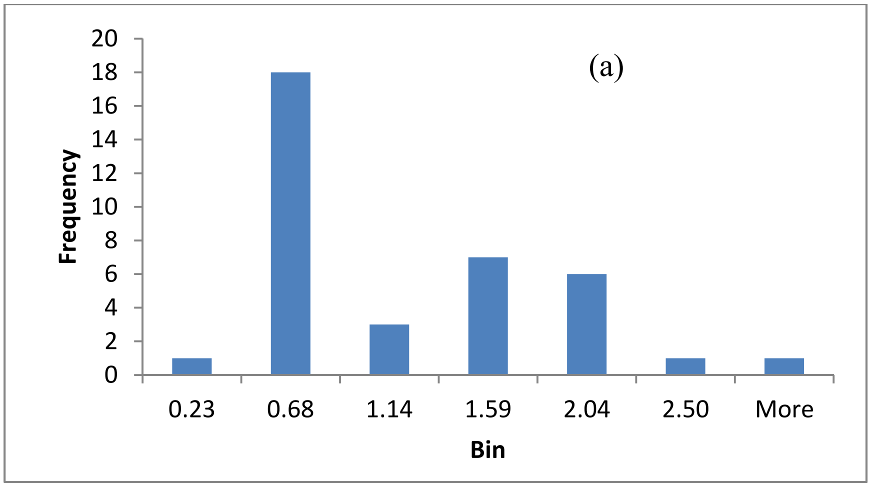

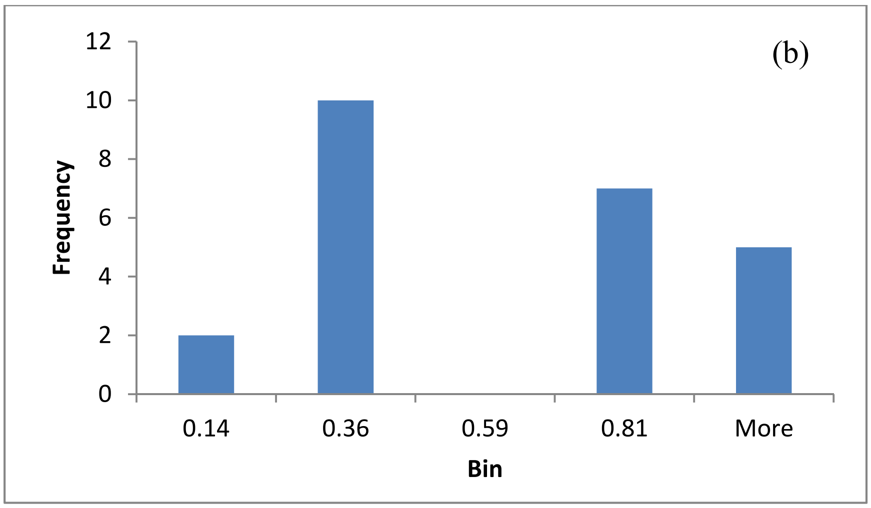

Figure 3-12. Histograms of soil organic matter contents at (a) Port St. Lucie area and (b) Lake Marshall watershed and its vicinity.

3.4. Nitrogen Load to Groundwater

Nitrogen load from a septic system to groundwater, which is the inflow mass (M_{in} (g/d) of equation 5, is an important parameter in ArcNLET modeling. There are two equivalent ways of handling the inflow mass: (1) to fix M_{in} and evaluate Z using equation 5 (Z is the source plan height needed for calculating the mass of denitrification and load), and (2) to fix Z and calculate M_{in} using equation 5. In this study, the first option is used, and the value of inflow mass is approximated as nitrogen release per person per day × people/household × 0.7 (the amount of nitrogen not lost in septic tanks). According to Xueqing Gao at FDEP (personal communication, November 2013), the average total nitrogen (TN) load is 4.61kg per person per year, i.e., 12.63g per person per day. The U.S. Census Bureau website (http://quickfacts.census.gov/qfd/states/12/12095.html) reported that there are 2.74 persons per household in Orange County. It is a general consensus that about 30% of nitrogen is removed in Septic tank (e.g., MACTEC, 2007). Therefore, the input mass from septic to groundwater is 24.22 g/d, which is slightly larger than 21.7 g/d reported in the Wekiva study (Roeder, 2008). This value is used for all the individual septic systems in the modeling sites.

Another quantity needed to use equation (5) for evaluating the inflow mass is the source plane concentration (C_0). It ranges between 0 mg/L and 80 mg/L (McCray et al., 1995), and the average of 40 mg/L was used in this study.

3.5. Groundwater Flow Modeling Results

With the data and information described above, ArcNLET groundwater flow module and particle tracking module were executed. The flow model provides magnitude and direction of seepage velocity (Darcy velocity divided by porosity) at the individual raster cells in the modeling domain. They are used in the particle tracking module to evaluate flow paths between individual septic systems and receiving waterbodies of particles placed at the septic system locations.

In this study, calculation of the seepage velocity was conducted for the area shown in Figures 3-3, 3-5, and 3-6, which is larger than the Lake Marshall watershed to eliminate effect of boundary (e.g., the watershed boundary) on the smoothing. Figure 3-13 plots the simulated flow paths obtained using smoothing factor of 50. Accuracy of the simulated water table shape and flow paths can be quantitatively evaluated, if monitoring data of hydraulic head are available in the modeling area. This can be done by comparing the smoothed DEM with measured water table elevation, as described in Wang et al. (2011, 2013).

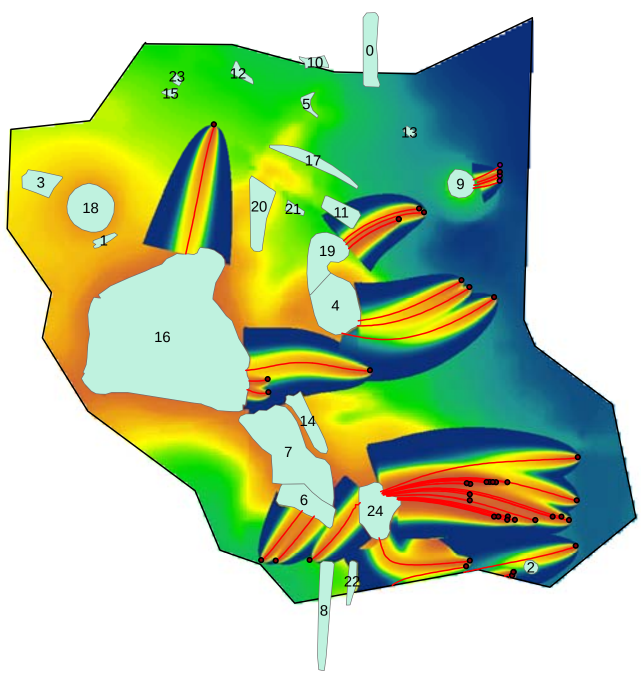

Figure 3-13. Simulated flow paths and nitrogen plumes from septic systems to surface waterbodies. The background color is for DEM.

To obtain the groundwater seepage to Lake Marshall (one of the objectives of this modeling), velocity magnitude (m/d) is extracted along the perimeter of the lake by using the ArcGIS clip function. The velocity direction is not considered, because groundwater velocity converges to the lake. Figure 3-14 shows a number of locations (green circles) where seepage velocity magnitude was extracted. While the green circles mimic the shape of the lake perimeter (the red line), the green circles are not smooth, because seepage velocity was calculated at raster cells; the shape of green circles should be smoother if the DEM raster file has higher resolution. An alternative improvement is to extract the velocity magnitude along points on the perimeter. It however requires placing a large number of points manually and thus was not attempted.

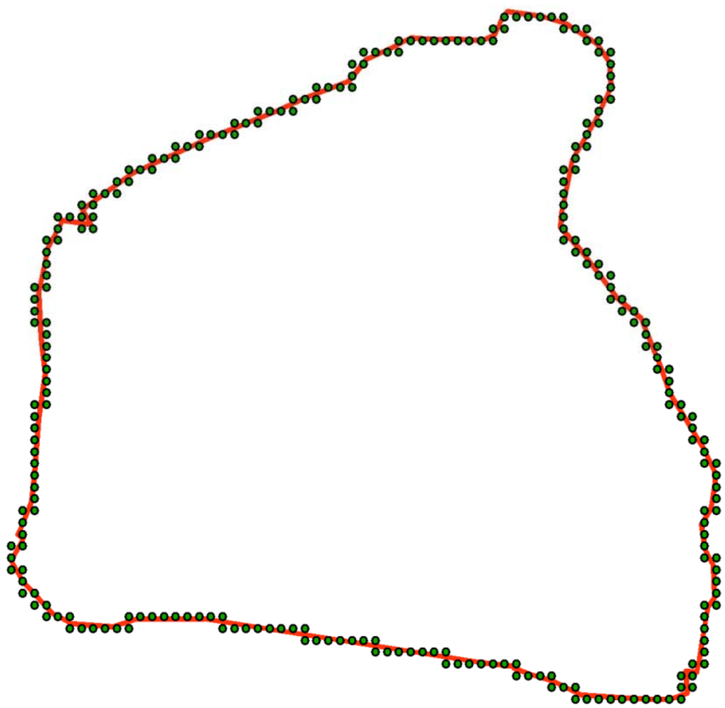

Figure 3-14. Locations (green circles) groundwater seepage velocity magnitude extracted along the perimeter of Lake Marshall (red line).

The extracted seepage velocity magnitude can be analyzed within or outside of ArcGIS. Figure 3-15 shows the summary statistics and histogram of the extracted seepage velocity magnitude obtained in ArcGIS. Figure 3-16 plots the same histogram using EXCEL. While Figure 3-15 lists descriptive statistics, more advanced statistical analysis of the data can be done using other professional statistical software such as MINITAB and SPSS. These data can be used to help TMDL modeling.

It should be noted that the extracted data is seepage velocity, not flow rate that is needed for TMDL modeling. To obtain the flow rate, the seepage velocity should be divided by porosity to obtain Darcy velocity. Subsequently, the resulting Darcy velocity is multiplied by the seepage area, i.e., multiplication of the perimeter and seepage depth. ArcNLET does not provide the seepage depth, and it has to be evaluated using independent information.

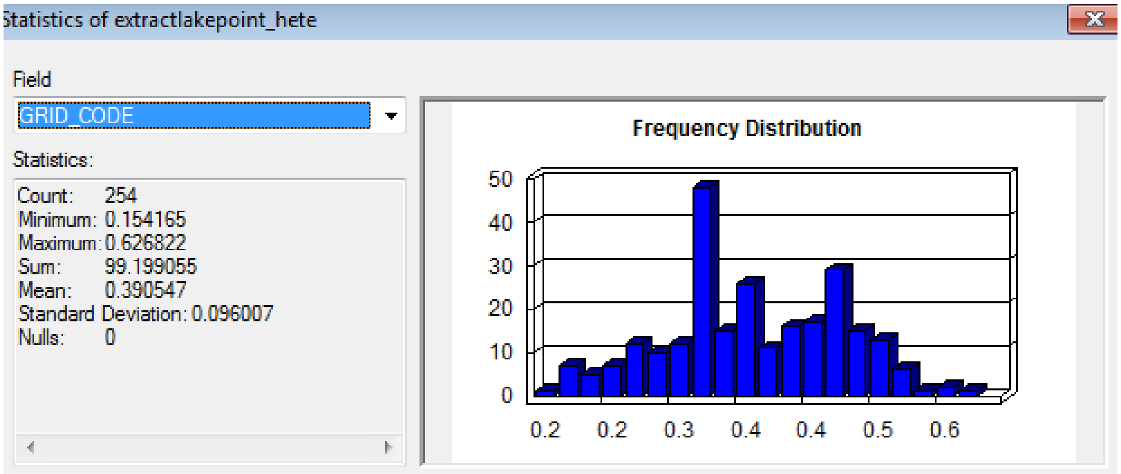

Figure 3-15. ArcGIS-provided statistics and histogram of extracted seepage velocity magnitude (m/d) along the perimeter of Lake Marshall.

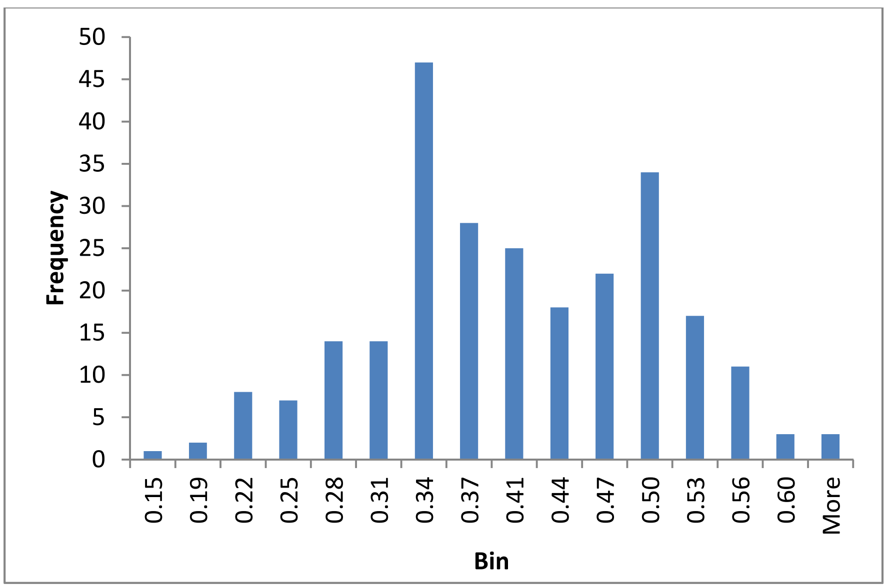

Figure 3-16. EXCEL-based histogram of extracted seepage velocity magnitude (m/d) along the perimeter of Lake Marshall.

3.6. Nitrogen Transport Modeling Results

Using the nitrogen transport parameter values discussed above, ArcNLET transport module was executed. The simulated nitrogen plumes are plotted in Figure 3-13. Table 3-1 lists the nitrogen load estimates to the receiving waterbodies; FID of the waterbodies can be found in Figure 3-13, which also shows the septic tanks contributing the load to each waterbody. The table also lists the inflow mass to groundwater from the septic tanks that contributing load to surface waterbodies. For example, there are four septic systems that contribute load to Lake Marshall; considering that the load from a septic system to water table is 24.22 g/d (see Section 3.4), the inflow mass to groundwater from the four septic systems is 24.22 × 4 = 96.88 g/d. The difference between the inflow load (to groundwater) and outflow load (to surface waterbodies) is the removed mass due to denitrification, and the removal ratio (to the inflow load) is listed in Table 3-1. The overall removal ration (the total amount of removal divided by the total amount of inflow load) is 62%, which is comparable with the value of 70% obtained in the Wekiva study (Roeder, 2008). The removal ratio varies between 34% and 94%, depending mainly on the distance between the waterbodies and their contributing septic systems. For example, the small reduction ratios for watersheds 6 and 16 are mainly because of the short flow paths. Reasonableness of the modeling results can be evaluated more quantitatively when observations of nitrogen concentration are available in the modeling domain.

Table 3-1. Simulated nitrogen loads to surface waterbodies and groundwater (inflow mass) in the Lake Marshall watershed. Locations of the waterbodies are shown in Figure 3-13.

Waterbody FID	Load (g/d)	Load (lb/yr)	Inflow Mass (g/d)	Reduction Ratio (%)
24	199.37	160.43	532.84	62.58
4	3.94	3.17	72.66	94.58
19	34.45	27.72	96.88	64.44
16	50.20	40.40	96.88	48.18
6	31.95	25.71	48.44	34.04
Sum	319.92	257.433	847.70	62.26

4. ARCNLET MODELING FOR LAKE ROBERTS

Lake Roberts is also located in Orange County and near Lake Apopka (Figures 1-1 and 3-1). Due to the geographic similarity, the parameter values used for the Lake Marshall modeling were also used for the Lake Roberts modeling. Therefore, this chapter only includes data specific to Lake Roberts in Section 4.1. The materials in Sections 4.2 – 4.5 are organized as follows:

(1) Section 4.2 includes the ArcNLET-based modeling results without model calibration but using parameter values from literature and previous ArcNLET modeling experience.
(2) Section 4.3 presents the ArcNLET-based modeling results after calibrating the ArcNLET flow model against field measurements of seepage velocity provided by the Orange County. The calibration changes the values of smoothing factor and hydraulic conductivity dramatically, and yield acceptable match between ArcNLET-simulated and measured seepage velocity.
(3) Section 4.4 includes the ArcNLET-based modeling results (after the calibration) with adjusted locations of several septic tanks to meet the 150-feet setback distance between septic systems and surface waterbodies used in the Orange County. Impacts of the adjusted septic tank locations on the simulation results are negligible.
(4) Section 4.5 compares the old watershed boundary used in Sections 4.1 – 4.4 and the new watershed boundary used the TMDL report of Kang (2015). It is concluded that the modeling results of nitrogen loading is not affected by the watershed boundary. This is unsurprising, because the change of the watershed boundary does not affect any step of the ArcNLET modeling.

Comparing all the modeling results at the different stages of the modeling procedure makes it easier for the readers to understand the impacts of the various factors (i.e., model calibration, setback distance, and watershed boundary) on the ArcNLET-simulated seepage velocity and nitrogen loading.

4.1. Geographic Data for Lake Roberts

Using the ArcGIS data of watershed, swamps and marshes, and waterbodies (downloaded from FDEP database and provided by Xueqing Gao at FDEP), Figure 4-1 shows the boundary of the Lake Roberts watershed as well as waterbodies and swamps and marshes within the watershed. Similar to the Lake Marshall modeling, the swamps and marshes were merged into waterbodies so that they also receive nitrogen load from the septic systems. Comparing Figure 4-1 with Figure 3-2 shows that the number of small waterbodies in the Lake Roberts watershed is smaller than that of the Lake Marshall watershed. In addition to Lake Roberts, the watershed also includes Lake Reaves. A field trip of Xueqing Gao revealed that there was no clear boundary between the two lakes, because the two lakes were connected by the swamps and marshes between them (personal communication, November, 2013).

The watershed boundary was change in 2015. Figure 4-1 shows the original watershed boundary delineated by the black polyline and the new watershed area in the blue polygon. As discussed in Section 4.5, the change of watershed boundary has no impacts on the ArcNLET-simulated seepage velocity and nitrogen loading, because the modeling domain is larger than the watershed, as shown in Figure 4-2. In addition, the watershed boundary is not used in any step of the ArcNLET modeling, but only in the post-processing of presenting the modeling results. Although Figure 4-1 shows that certain septic tanks are located outside of the new watershed boundary, it should be noted that groundwater flow is determined not by the watershed boundary but by hydraulic gradient (elevation gradient in the ArcNLET flow model). The groundwater flow toward Lake Roberts is supported by the seepage measurements provided by the Orange County (Section 4.3). Therefore, nitrogen from the septic tanks outside of the new watershed boundary will also flow into Lake Roberts, since the hydraulic (or elevation) gradient is toward the lake. This is shown in the sections below.

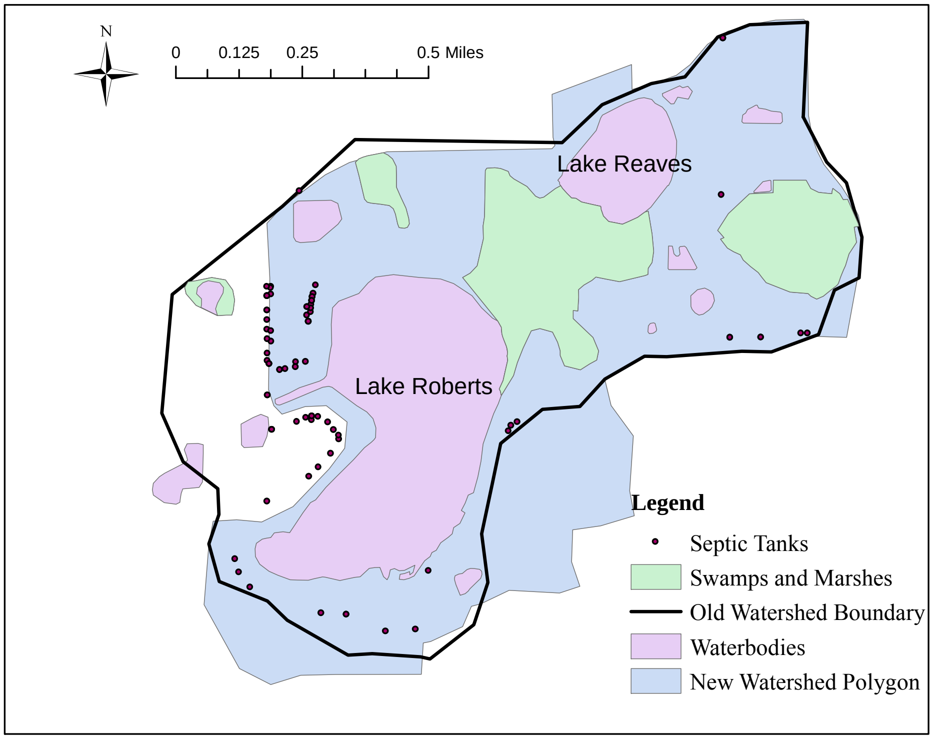

Figure 4-1. Watershed of Lake Roberts and locations of septic tanks, waterbodies, and swamps and marshes. The swamps and marshes are merged into waterbodies later on for calculation of nitrogen load. The black polyline denotes the old watershed boundary used in Sections 4.1 – 4.4. The blue polygon is the new watershed boundary used in the TMDL report of Kang (2015). As explained in Section 4.5, the change of watershed boundary has no impacts on the ArcNLET modeling results.

Figure 4-2 plots the DEM of the watershed and its vicinity. The DEM data only reflects the locations of the two lakes, but not the locations of small waterbodies and swamps. In comparison with the Lake Marshall watershed, the Lake Roberts watershed is relatively flat with the elevation ranging from 30.29m to 38.49m; the elevation ranges between 18.36m and 48.74m in the Lake Marshall watershed. It should be noted that, while Lake Roberts is the lowest location within the watershed, a lake outside of the watershed has even lower elevation at the southeast corner of the clipped DEM (Figure 4-3). Therefore, it is possible that groundwater flow may flow out of the watershed to the lake of lower elevation.

Figure 4-2 shows that the modeling domain is substantially larger than the original and the new watershed boundaries delineated by the black and red polylines, respectively. Therefore, the modeling results are not affected by the watershed boundaries. This point is made clearer below when the ArcNLET-simulated flow paths and plumes are presented.

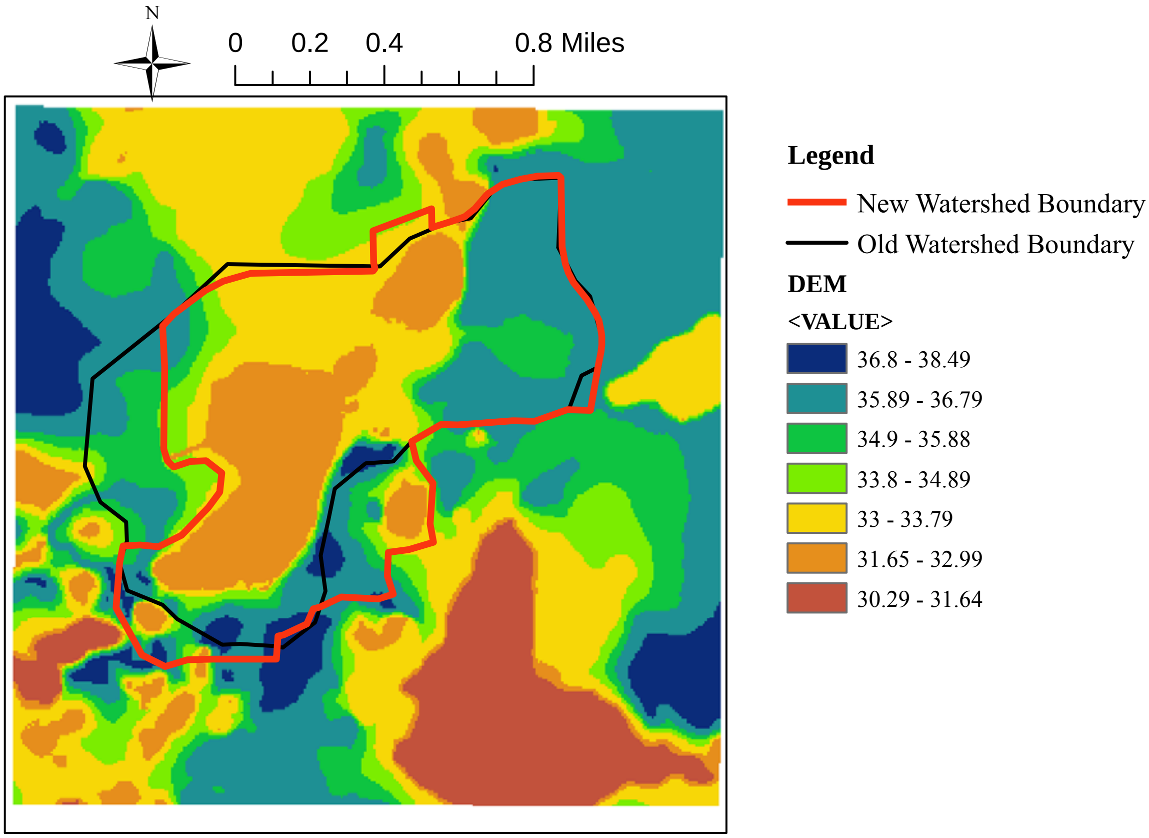

Figure 4-2. DEM of the Lake Marshall watershed and its vicinity. The original and new watershed boundary are delineated by the back and red polylines, respectively.

Figures 4-3 and 4-4 plot the heterogeneous hydraulic conductivity and porosity values for the soil units in the Lake Roberts watershed. The figures show that, at the vicinity of Lake Marshall, the parameter values are relatively homogeneous. This spatial pattern is similar to that of the Lake Marshall watershed. The values of hydraulic conductivity and porosity in the Lake Roberts watershed are similar to those of the Lake Marshall watershed. Figures 4-3 and 4-4 show again that the modeling domain is larger than the original and new watershed boundaries.

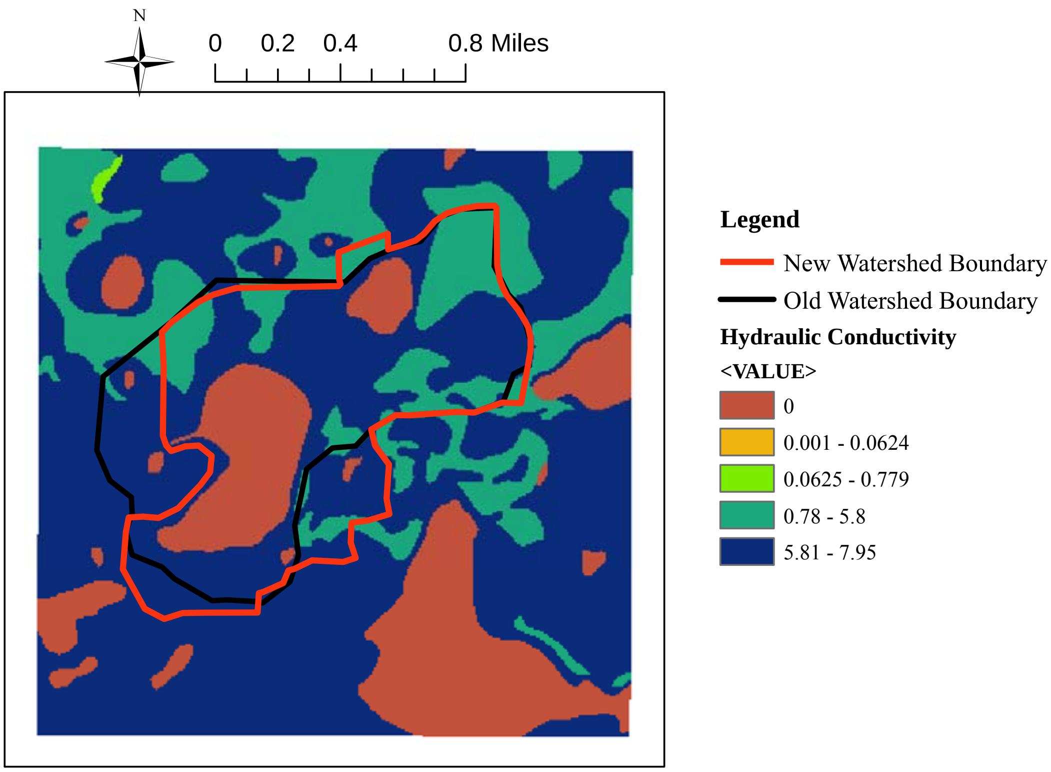

Figure 4-3. Heterogeneous hydraulic conductivity (m/d) of soil units of the Lake Roberts watershed.

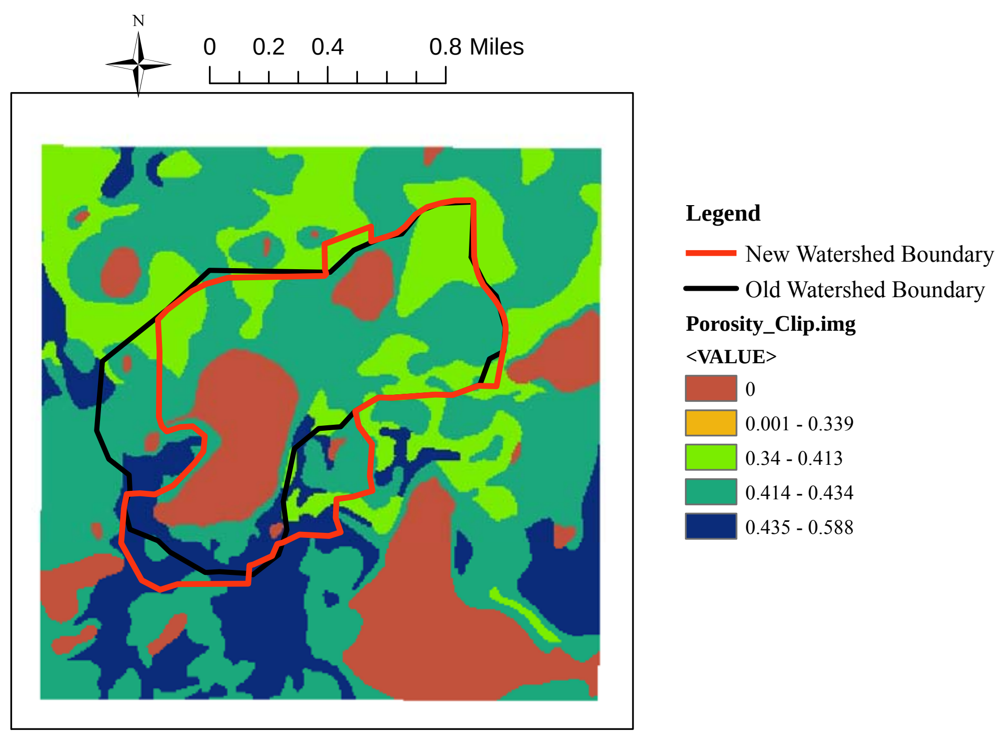

Figure 4-4. Heterogeneous porosity ([-]) of soil units of the Lake Roberts watershed.

4.2. Modeling Results without Flow Model Calibration Using Seepage Data

With the data discussed above and information of model parameters described in Chapter 3, ArcNLET modeling was conducted. Figure 4-5 plots the simulated flowpaths obtained using smoothing factor of 50. Among the 83 septic systems, the flow paths from 76 septic systems are terminated at Lake Roberts. For the other seven flow paths, two of them are terminated at Lake Reaves and a swamp. For the flow path terminating at the swamp, the septic tank location is suspicious. As shown in Google Earth (Figure 4-6), there is no septic system at the northwest corner of the pond. This is not surprising, since the locations of septic tanks are approximated at the center of the parcels. For the five septic systems located on or near the boundary of the east side of the watershed, their flow paths are extended out of the watershed. This is reasonable, because, near the five septic systems, there are waterbodies with lower elevation outside of the watershed, as shown in Figure 4-2. Accuracy of the simulated water table shape and flow paths can be evaluated, if monitoring data of hydraulic head are available in the modeling area. This can be done by comparing the smoothed DEM with measured water table elevation, as described in Wang et al. (2011, 2013).

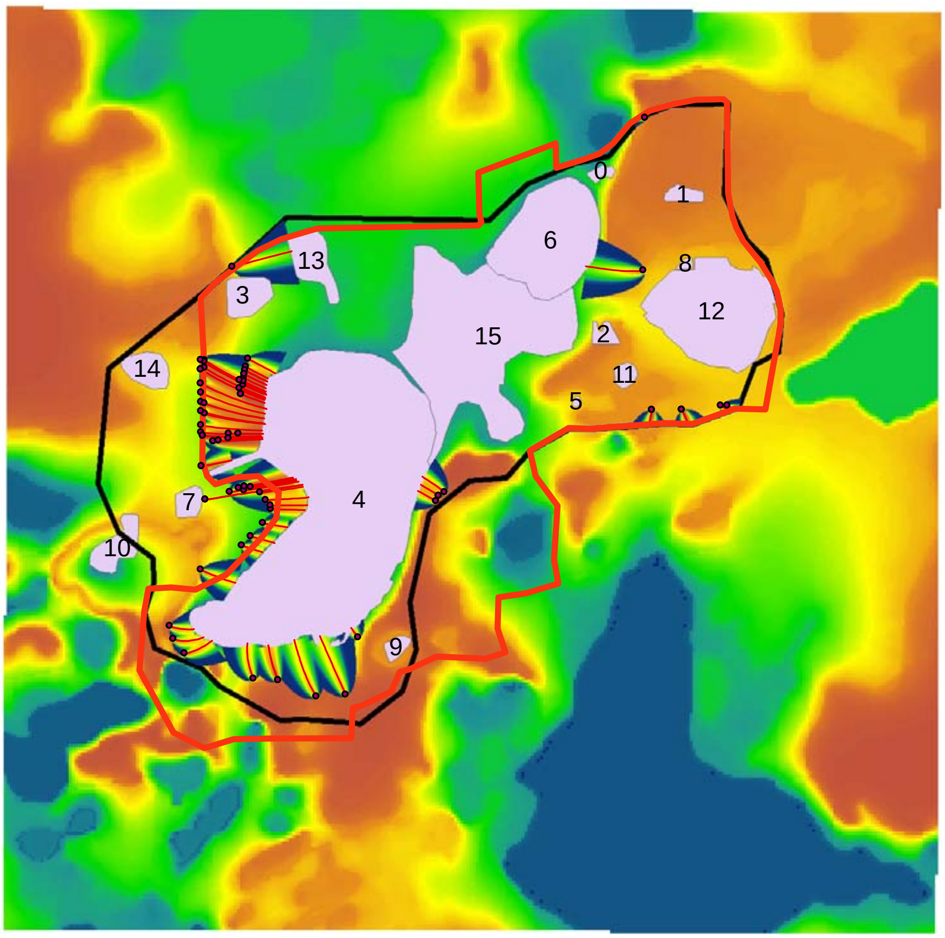

Figure 4-5. Simulated flow paths and nitrogen plumes from septic systems to surface waterbodies. The background is DEM. The waterbodies (including marshes and swamps) are labeled with their FIDs. The original and new watershed boundaries are delineated by the black and red polylines, respectively.

Figure 4-6. Bird view of the northwest corner of the modeling domain where a flow path is terminated at the swamp.

Figure 4-7 shows the ArcGIS-generated descriptive statistics of the extracted seepage velocity magnitude along the perimeter of Lake Roberts. The seepage velocity magnitude varies in one order of magnitude from 0.005 to 0.06 m/d. Comparing the statistics in Figure 4-7 with those in Figure 3-15 for Lake Marshall shows that the magnitude of seepage to Lake Roberts is significantly smaller than that to Lake Marshall. This is not surprising, because the elevation gradient in the Lake Marshall watershed (Figure 3-3) is larger than that in the Lake Roberts watershed (Figure 4-2). This manifests importance of considering spatial variation in the TMDL analysis. It should be noted that the seepage estimates are substantially reduced after calibrating the ArcNLET flow model against seepage measurements provided by the Orange County, as discussed in Section 4.3 below.

The histogram generated by ArcGIS (Figure 4-7) is not desired, because the x-axis of the histogram does not reflect the data range. A histogram was plotted in Figure 4-8 using the data analysis function of EXCEL, after the data was exported as a dBASE file that can be opened by EXCEL. More advanced statistical analysis of the data can be done using other professional statistical software such as MINITAB and SPSS.

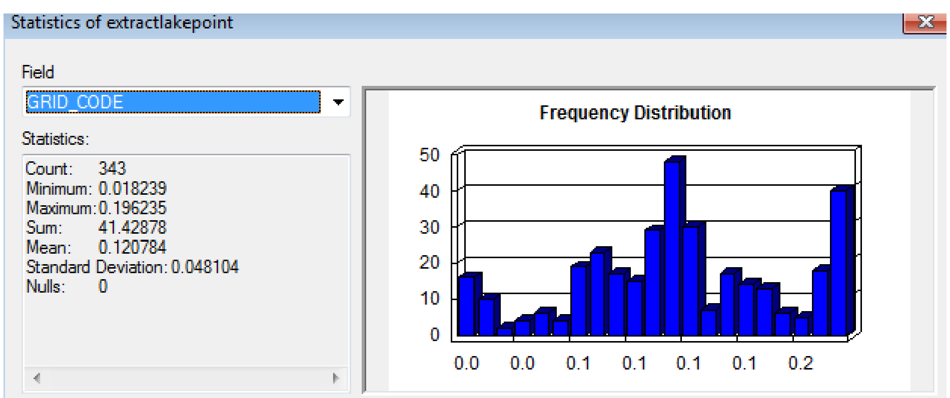

Figure 4-7. Statistics of extracted seepage velocity magnitude (m/d) along the perimeter of Lake Roberts. The estimates are substantially reduced after the model calibration, as shown in Figure 4-17.

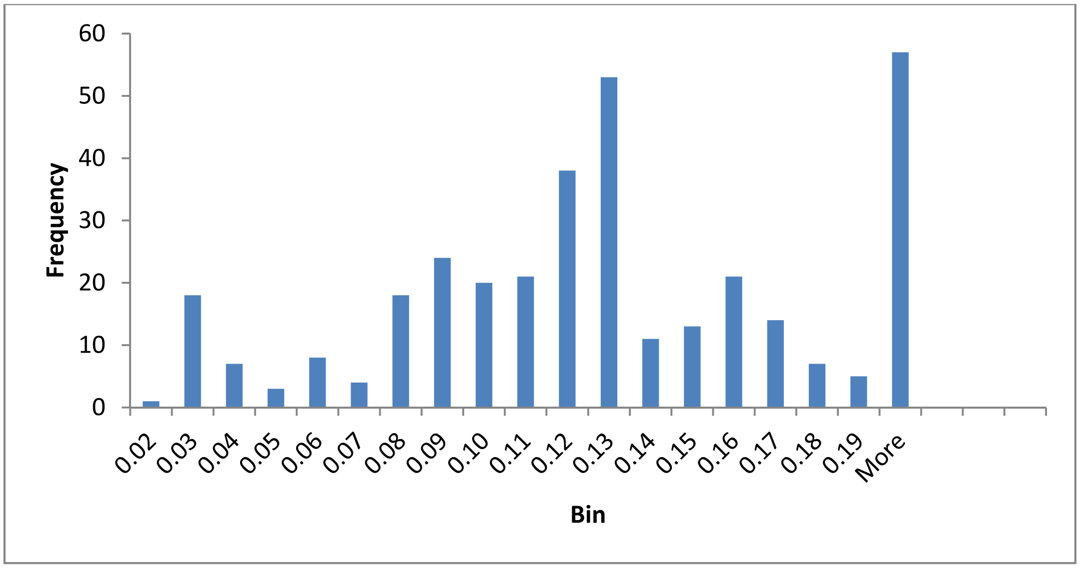

Figure 4-8. EXCEL-based histogram of extracted seepage velocity magnitude (m/d) along the perimeter of Lake Roberts.

Longitudinal and horizontal transvers dispersivities of 10m and 1m are used in the Lake Roberts Watershed, which are the same as those used for Lake Marshalls. The decay coefficient of denitrification is 0.001 d^{-1}, also the same as that used for Lake Marshalls. The input mass from septic to groundwater (M_{in}) is fixed at 24.22g/d. The source plane concentration (C_0) of 40 mg/L was adopted from the modeling of Lake Marshalls.

Figure 4-5 plots the simulated nitrogen plumes, and Table 4-1 lists the waterbodies that receive nitrogen load. The total amount of load is 1413.54 g/d, i.e., 1137.46 lb/year, which is significantly larger than the load at the Lake Marshall watershed. Lake Roberts (with FID of 4) receives most of the load. In addition, the reduction ratio is only 15.28% for Lake Roberts, which is significantly smaller than those of the Lake Marshall watershed. This is attributed to the small distance between Lake Roberts and its nearby septic systems. For Lake Reaves and the pond at the northwest corner of the watershed, each of them receives load from only one septic system, and the reduction ratio is similar for the two waterbodies.

Table 4-1. Simulated nitrogen loads to surface waterbodies and groundwater (inflow mass) in the Lake Marshall watershed. Locations of the waterbodies are shown in Figure 4-5.

Waterbody FID	Load (g/d)	Load (lb/yr)	Inflow Mass (g/d)	Reduction Ratio (%)
4	1395.38	1122.84	1646.96	15.28
6	9.18	7.39	24.22	62.08
13	8.98	7.23	24.22	62.92
Sum	1413.54	1137.458	1695.40	16.62

4.3. Flow Model Calibration Using Seepage Data

As explained in Chapter 2, the ArcNLET groundwater flow modeling involves three parameters: smoothing factor, hydraulic conductivity, porosity. Since porosity always has small uncertainty, the SSURGO values are used directly in the ArcNLET modeling without model calibration. As a common practice in groundwater modeling, hydraulic conductivity is calibrated in this section. It is always ideal to calibrate the smoothing factor using site-specific measurements of hydraulic head. Our previous practice of calibrating smoothing factor for the ArcNLET flow model is to adjust the smoothing factor until that measured hydraulic heads and corresponding smoothed DEM values fall on the 1:1 line, indicating that the shape of smoothed DEM matches the shape of water table. This calibration however is not conducted here, because head observations are unavailable.

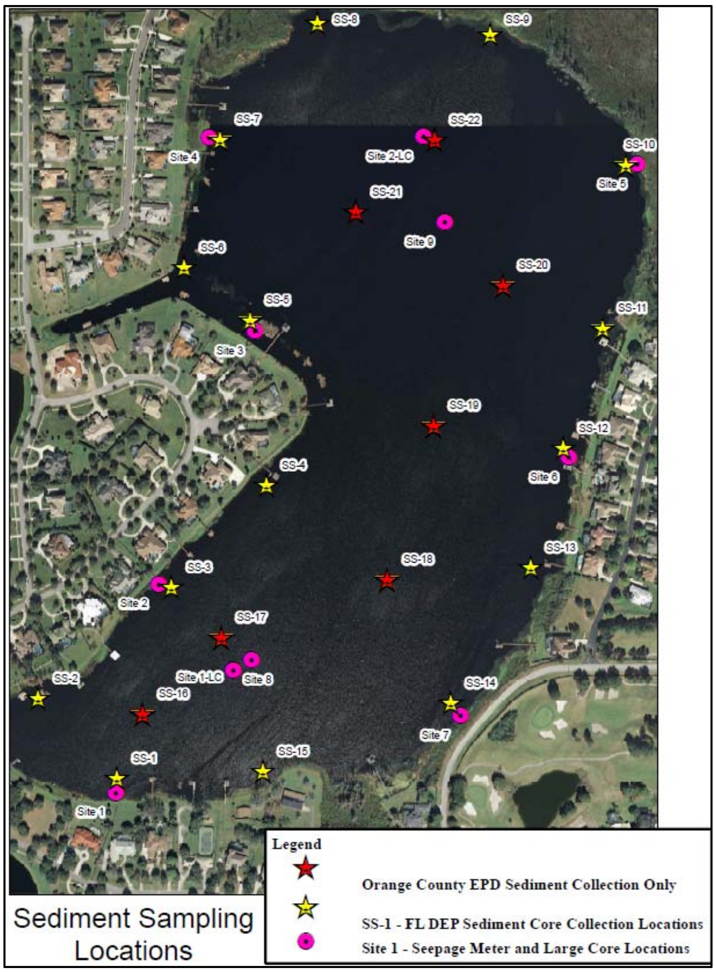

Figure 4-9. Locations of seepage meters and sediment core samples. Sites 1 – 9 are the nine locations of seepage meter installation; Sites 8 and 9 are located in the lake and thus not used for model calibration. Sites SS-1 – SS-15 are the fifteen locations of sediment cores. The sediments are loamy sand at SS-2, SS-7, SS-10, and SS-12, but sand at other sites.

Instead, measurements of groundwater discharge to the lake and sediment particle distributions are available and used in the calibration. Figure 4-9 shows the locations of the nine seepage meter installations. The seepage meters were installed by the Orange County, and the seepage meter measurements listed in Table 4-2 are provided by Mitchell Katz at the county Environmental Protection Division for the period of 10/2013 – 8/2014 (August, 2014, personal communication). The measurements are significantly smaller than those listed in Table 4-3 at four lakes in the City of Winter Haven (also located in the Orange County) reported in PBSJ (2009). For example, the averages listed in Table 4-2 are generally one order of magnitude smaller than those listed in Table 4-3. In addition, the ratios of Average/Min and Max/Min in Table 4-2 are about one or two orders of magnitude smaller than those listed in Table 4-3. The significant difference has not been fully understood, and the reasons for the small seepage measurements at Lake Roberts are unknown. Another unknown factor is the large seepage measured at Site 2 shown in Figure 4-9. In the analysis below, only the measurements at Sites 1-7 are used, because Sites 8 and 9 are inside the lake.

Table 4-2. Measurements of groundwater seepage rate (m/d) at the nine sites shown in Figure 4-9.

Time	Site 1	Site 2	Site 3	Site 4	Site 5	Site 6	Site 7	Site 8	Site 9
10/15/2013	0.00047	0.01893	-----	0.00037	0.00037	0.00071	0.00074	0.00132	0.00037
11/12/2013	0.00056	0.00261	0.00192	0.00050	0.00109	0.00076	0.00076	0.00036	0.00122
01/10/2014	0.00133	0.00785	0.00085	0.00046	0.00061	0.00140	0.00055	0.00009	0.00102
03/15/2014	0.00094	0.00118	0.00040	0.00065	0.00051	0.00075	0.00117	0.00026	0.00019
05/19/2014	0.00000	0.00375	0.00054	0.00056	0.00064	0.00060	0.00050	0.00037	0.00036
06/16/2014	0.00000	0.00327	0.00083	0.00129	0.00112	0.00129	0.00136	0.00016	0.00069
07/11/2014	0.00122	0.00319	0.00219	0.00167	0.00122	0.00170	0.00100	0.00033	0.00100
08/08/2014	0.00096	0.00526	0.00179	0.00142	0.00109	0.00152	0.00103	0.00010	0.00046
Average	0.00069	0.00576	0.00122	0.00086	0.00083	0.00109	0.00089	0.00037	0.00066
Max	0.00133	0.01893	0.00219	0.00167	0.00122	0.00170	0.00136	0.00132	0.00122
Min	0.00000	0.00118	0.00040	0.00037	0.00037	0.00060	0.00050	0.00009	0.00019
Average/Min	---	5	3	2	2	2	2	4	4
Max/Min	---	16	5	4	3	3	3	14	7
	Statistics after the measurements are corrected by multiplying a factor of 1.3								
Average	0.00090	0.00749	0.00159	0.00112	0.00108	0.00142	0.00116	0.00048	0.00086
Max	0.00173	0.02461	0.00285	0.00217	0.00159	0.00221	0.00177	0.00172	0.00159
Min	0.00000	0.00153	0.00052	0.00048	0.00048	0.00078	0.00065	0.00012	0.00025

When using the seepage data for the model calibration, the average values are used. The measurements need to be corrected by multiplying them to a correction factor, as suggested in literature (Erickson, 1981; Cherkauer and McBride, 1988; Belanger and Montgomery, 1992). Rosenberry and Menheer (2006) reviewed the correction factors and suggested a range between 1.05 and 1.74. The correction factor of 1.3 is used in this study, because Belanger and Montgomery (1992) reported a ratio of 0.77 between measured and actual seepage rates for seepage rates below 20 mm h^{-1} (equals to 0.48 m/d). A similar correction factor was used to correct the seepage velocities at Lake Hampen, Western Denmark, by Kidmose et al. (2011). Table 4-2 lists the corrected average values together with the corrected maximum and minimum values. The corrected averages are used for the model calibration.

Both the raw and corrected data indicate significant groundwater seepage at Sites 2 – 4 located on the west side of Lake Roberts, in comparison with the seepage measurements from the other sites. It suggests that, at the west side of the lake, groundwater flows cross the new watershed boundary, given the narrow distance between the boundary and lake shore at the west side of the lake. This indicates again that the watershed boundary does not affect the ArcNLET modeling results of groundwater flow and nitrogen transport.

Table 4-3. Measurements of groundwater seepage rate (m/d) at four lakes in Winter Heaven, Orange County.

Lake	Site	Min	Max	Average	Max/Min	Average/Min
Haines	LH-ES	0.0001	0.00771	0.00368	77	37
	LH-NS	0.00041	0.00869	0.00235	21	6
	LH-WS	0.00377	0.01564	0.00735	4	2
	LH-WD	0.00021	0.01564	0.00254	74	12
Rochelle	LR-WS	0.0001	0.00742	0.00234	74	23
	LR-SS	0.00014	0.01575	0.00403	113	29
	LR-NS	0.00013	0.00337	0.00168	26	13
	LR-ND	0.00007	0.01019	0.00257	146	37
Smart	LS-NS	0.00001	0.00482	0.00191	482	191
	LS-WS	0.00003	0.00356	0.00161	119	54
	LS-SS	0.00118	0.01083	0.00335	9	3
	LS-SD	0.00013	0.00356	0.00126	27	10
Conine	LC-SS	0.00057	0.03171	0.01666	56	29
	LC-NS	0.00007	0.00384	0.00131	55	19
	LC-ES	0.00004	0.00476	0.00153	119	38
	LC-ED	0.00016	0.00696	0.00233	44	15

Figure 4-9 also shows the locations of fifteen lake sediment cores. The core samples were collected by the Orange County, and the particle size distributions were measured by the Florida Department of Environmental Protection. The particle sizes measurements and the soil types of the 15 cores are listed in tables A-1 – A-15 of Appendix A. The four soil samples at SS-2, SS-7, SS-10, and SS-12 are loamy sand, and the rest of the samples are sand. It suggests relatively homogeneous distribution of the lake sediment.

The values of hydraulic conductivity of the sand and loamy sand samples are determined based on the database of Carsel and Parrish (1998) that includes 216 sand soil samples and 315 loamy sand soil samples. The average hydraulic conductivity of the two soil types reported in Carsel and Parrish (1998) are listed in Table 4-4. The average of 7.13 m/d for sand is close to that of 7.95 m/d given in the SSURGO database. The minimum and maximum values listed in Table 4-4 are evaluated using the statistical analysis of Carsel and Parrish (1998). For each soil type, Carsel and Parrish (1998) conducted the Johnson transformations and fitted the transformed data to the standard normal distribution. The specific Johnson transformation for sand and loamy sand is $Y = \ln [(X-A)/(B-X)]$, where Y is the transformed variable and X denotes an un-transformed variable with limits of variation from A to B. For the sand samples, the values of A and B given in Carsel and Parrish (1998) are 0 cm/h and 70 cm/h, respectively; for the loamy sand samples, A and B are 0 cm/h and 51 cm/h, respectively. Since over 95% of data are included within [-2, 2] for a standard normal distribution, the Y value is taken as -2 and 2, and the corresponding X values are treated as the minimum and maximum value of hydraulic conductivity, and they are listed in Table 4-4.

Table 4-4. Average, maximum, and minimum values of hydraulic conductivities of loamy sand and sand studied by Carsel and Parrish (1988).

	Loamy Sand		Sand	
	cm/h	m/d	cm/h	m/d
Average	14.59	3.50	29.70	7.13
Min	6.08	1.46	8.34	2.00
Max	44.92	10.78	61.66	14.80

Because hydraulic conductivity and smoothing factor jointly determine the simulated groundwater seepage (smoothing factor determines hydraulic gradient), during the ArcNLET calibration, the two variables are adjusted to match simulated with observed groundwater seepage. Since the simulated seepage rates (reported in Section 4.2) are significantly larger than the observations, the calibration is to use small hydraulic conductivity and large smoothing factor values (corresponding to small hydraulic gradient). The final values of the two variables are determined in an empirical manner to simulate groundwater seepage using the same hydraulic conductivity value but different smoothing factor values. Figure 4-10 plots the simulated seepage rates with the smoothing factor values up to 500 but with the average value of sand hydraulic conductivity. The figure shows that the simulated seepage rate reduces dramatically when the smoothing factor increases from 150 to 500. However, the simulated seepage rates are still larger than the observed, suggesting the need of using smaller hydraulic conductivity values. This is done by using the values of 2.0 (the minimum hydraulic conductivity value of sand), 3.5 m/d and 1.46 m/d; the latter two are the average and minimum values of hydraulic conductivity of loamy sand. The simulated seepage rates are plotted in Figure 4-11 – Figure 4-13, respectively. The three figures show that, when hydraulic conductivity is small and smoothing factor is large, the simulated groundwater seepage can match the observed values.

Figure 4-14 plots the final model seepage simulation with the smoothing factor of 400 and the hydraulic conductivity of 2.0 and 1.46 m/d, i.e., the minimum values of sand and loamy sand. The value of 1.46 m/d is used for Sites 4 – 6 where the sediment samples are loamy sand; the value of 2 m/d is used for the other sites. The figure shows that, except at Sites 2 and 4, the ArcNLET-simulated seepage rates are within the minimum and maximum of the observed seepage rates, suggesting that the simulations are acceptable. Therefore, the smoothing factor of 400 is used for the load estimation. For the hydraulic conductivity, the value of 2.0 m/d is used, since the two values of 1.46 m/d and 2 m/d are similar and there is no information to delineate a separate zone of loamy sand. In other words, the SSURGO soil zones are used in the load estimation, but the hydraulic conductivity value in the soil zone surrounding the lake is changed from 7.95 m/d to 2.0 m/d. Figure 4-15 plots the heterogeneous field of hydraulic conductivity with the updated value of 2.0 m/d obtained after using the seepage data.

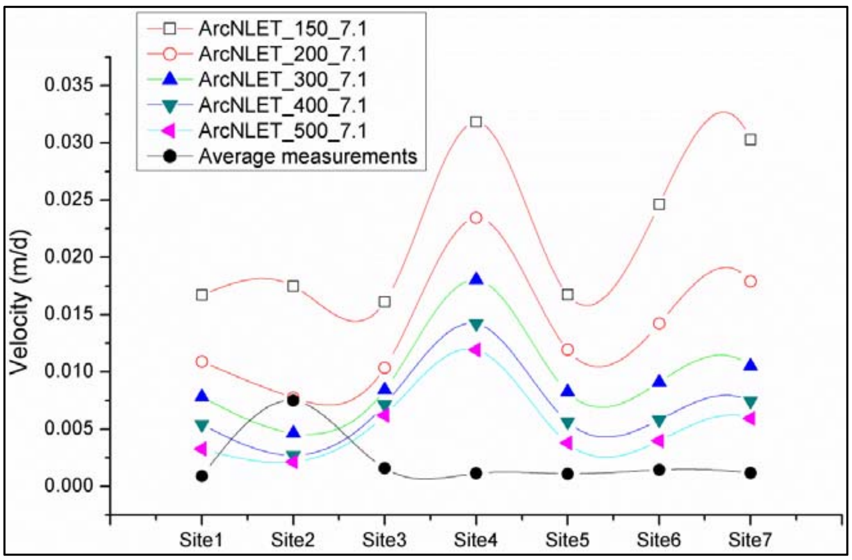

Figure 4-10. Average of observed seepage rates and simulated seepage rates with different smoothing factors (150 – 500) but the same hydraulic conductivity of 7.1 m/d, the average value for sand.

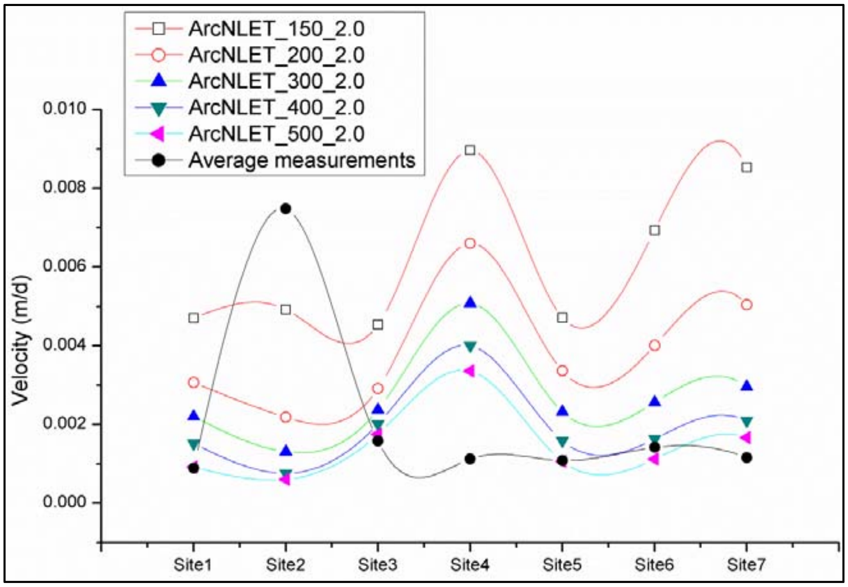

Figure 4-11. Average of observed seepage rates and simulated seepage rates with different smoothing factors (150 – 500) but the same hydraulic conductivity of 2.0 m/d, the minimum value for sand.

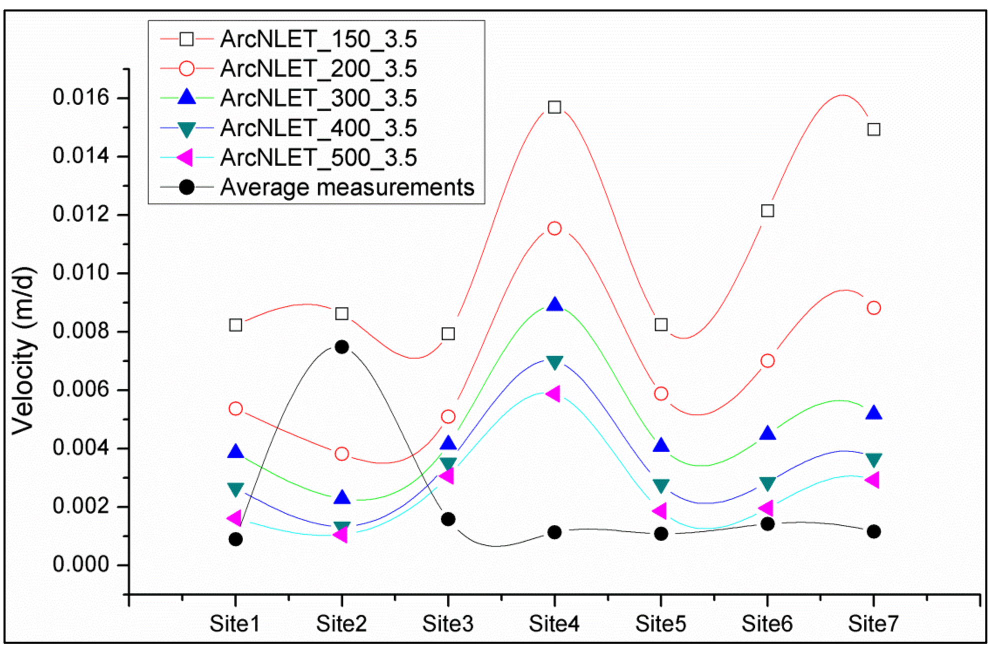

Figure 4-12. Average of observed seepage rates and simulated seepage rates with different smoothing factors (150 – 500) but the same hydraulic conductivity of 3.5 m/d, the average value for loamy sand.

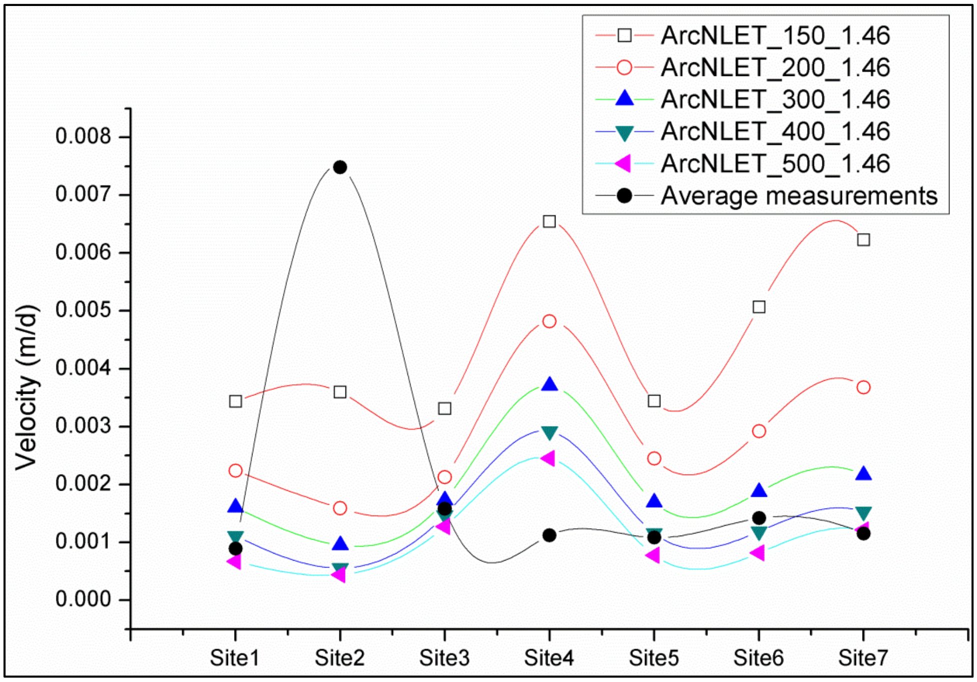

Figure 4-13. Average of observed seepage rates and simulated seepage rates with different smoothing factors (150 – 500) but the same hydraulic conductivity of 1.46 m/d, the minimum value for loamy sand.

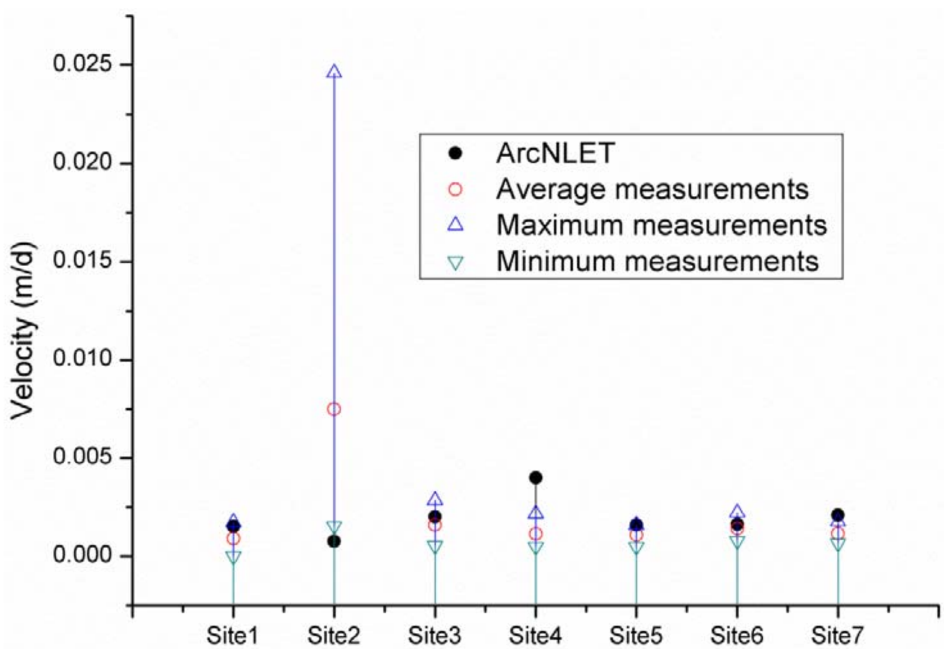

Figure 4-14. Average of observed seepage rates and simulated seepage rates with the smoothing factors of 400. In the ArcNLET simulation, the minimum values of sand and loamy sand are used for the areas, where sand and loamy sand sediments are identified by the soil samples (Figure 4-9).

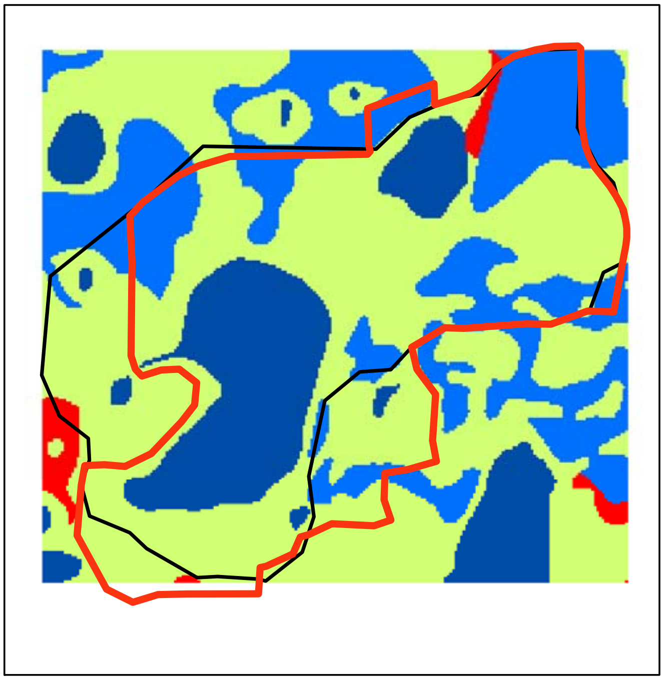

Figure 4-15. Heterogeneous hydraulic conductivity (m/d) of soil units of the Lake Roberts watershed. The value of hydraulic conductivity in the soil zone surrounding the lake is changed from 7.95 m/d to 2.0 m/d. The original and new watershed boundaries are delineated by the black and red polylines, respectively.

4.4. New Modeling Results Using Calibrated Flow Parameters

With the calibrated flow model parameters, ArcNLET modeling was conducted to estimate groundwater flow rate and nitrate load from septic to water bodies. Figure 4-16 plots the simulated flow paths obtained using the smoothing factor of 400. The flow pattern is similar the original one shown in Figure 4-5. However, comparing the histogram of the new flow velocity (Figure 4-17) with that of the original flow velocity (Figure 4-8), the new flow simulations are significantly smaller.

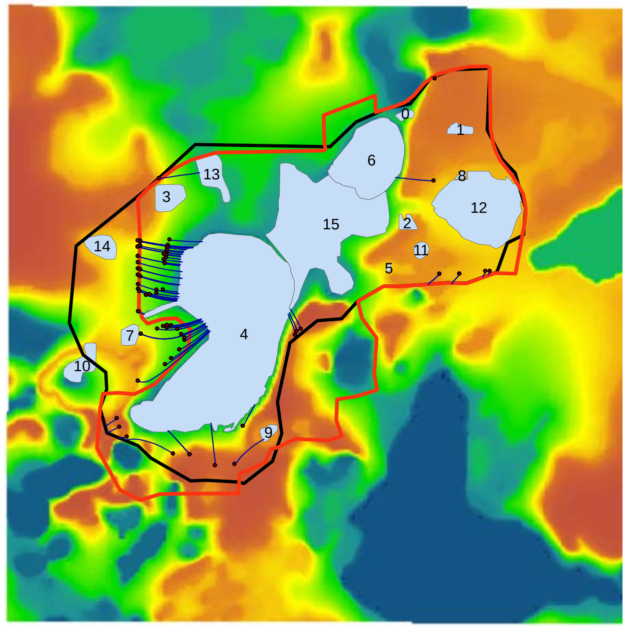

Figure 4-16. Simulated flow paths using the calibrated smoothing factor and hydraulic conductivity. The original and new watershed boundaries are delineated by the black and red polylines, respectively.

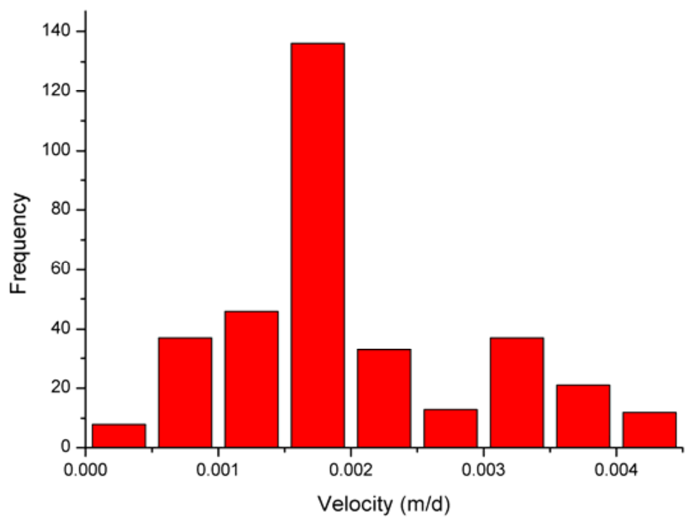

Figure 4-17. Histogram of extracted seepage velocity magnitude (m/d) along the perimeter of Lake Roberts. The seepage rate estimates are substantially smaller than those shown in Figures 4-7 and 4-8.

Figure 4-18 plots the simulated nitrogen plumes, and lists the water bodies that receive nitrogen load. The amount of load is reduced from 1413.54 g/d to 906.51 g/d for two reasons. First, the two plumes originally reaching waterbodies 6 and 13 (Figure 4-5) are terminated before reaching the waterbodies. This is not surprising, because the effect of denitrification becomes more significant due to the decrease of flow velocity. This is also the reason that the reduction ratio increase from 16.62% to 47.28% (Table 4-5).

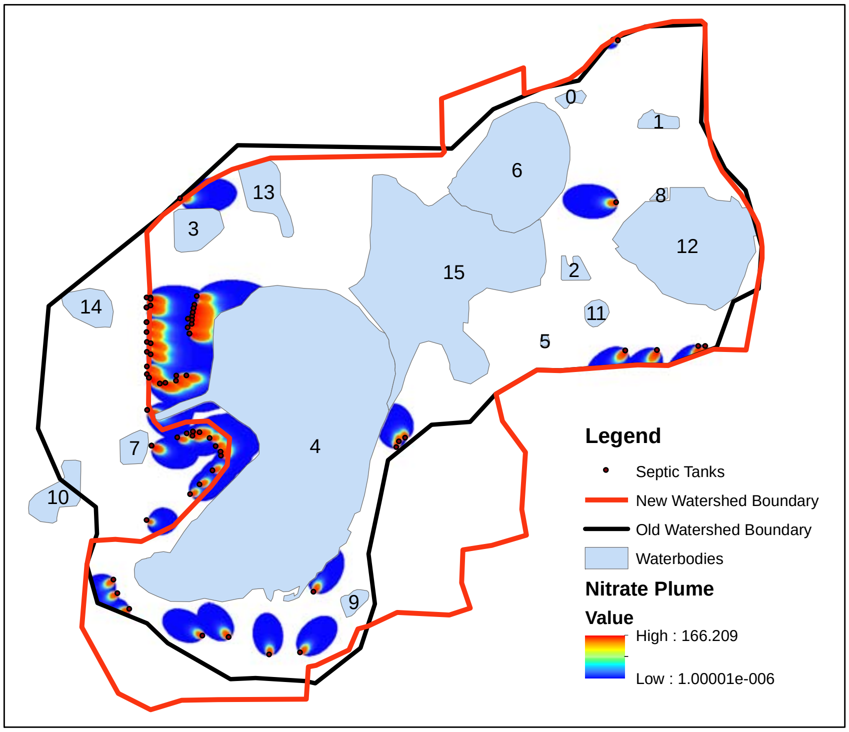

Figure 4-18. Simulated nitrogen plumes from septic systems to surface water bodies. The waterbodies (including marshes and swamps) are labeled with their FIDs. The original and new watershed boundaries are delineated by the black and red polylines, respectively.

Table 4-5. Simulated nitrogen for water bodies in the Lake Roberts watershed. Locations of the water bodies are shown in Figure 4-5.

Waterbody FID	Load (g/d)	Load (lb/yr)	Inflow Mass (g/d)	Reduction Ratio (%)
4	884.57	711.80	1622.74	45.49
15	21.94	17.65	24.22	9.42
sum	906.51	729.46	1719.62	47.28

While using the calibrated smoothing factor and hydraulic conductivity significantly affect the simulated flow path, flow velocity, and nitrogen load, they are not used for the other three watersheds, because the measured seepage rate is suspiciously small and it is unknown why the measurements at Site 2 are significantly larger than those at other sites. If the seepage rate measurements are considered to be reasonable, it is straightforward to use the calibrated smoothing factor for the other three watersheds. It is also possible to use small values of hydraulic conductivity for the other three watersheds, if necessary.

4.5. New Modeling Results with Updated Septic Tank Locations

Given that the setback distance of 150 feet between septic systems and surface waterbodies is used in the Orange County, the distances between septic systems and surface water bodies were examined. For the septic tanks with distances to waterbodies less than 150 feet, their locations were moved away in the direction perpendicular to the waterbodies to meet the requirement of setback distance. As shown in Figure 4-19, there are only four septic system locations were adjusted, and the adjustment is minor.

Using the ArcNLET parameters described above, the nitrogen transport was simulated. Figure 4-20 plotted the simulated plumes; the spatial distribution of the plumes is visually almost identical to that shown in Figure 4-18 with the original septic system locations.

This is reasonable when considering the minor adjustment of the septic system locations. The estimated nitrate load to the water bodies is listed in Table 4-6. The total nitrate load is 893.45 g/d, only 1.4% smaller than the load of 906.51 g/d (Table 4-5) calculated with the original septic systems locations. This is reasonable, because the four septic systems were moved away from the surface waterbodies. As a result, the slightly longer plumes are subject to denitrification. Subsequently, the removal rates of nitrate increase from 47.28% to 48.04%. While moving the septic systems further away from the waterbodies can slightly decrease the nitrate load to water bodies, the decrease is negligible.

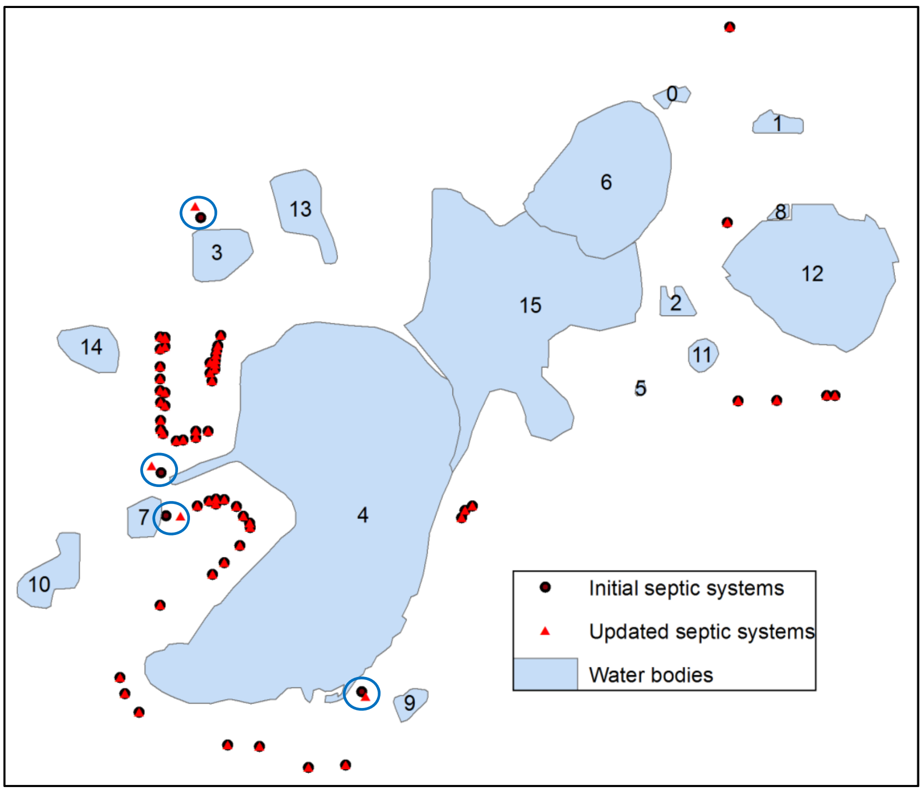

Figure 4-19. Original and updated septic system locations.

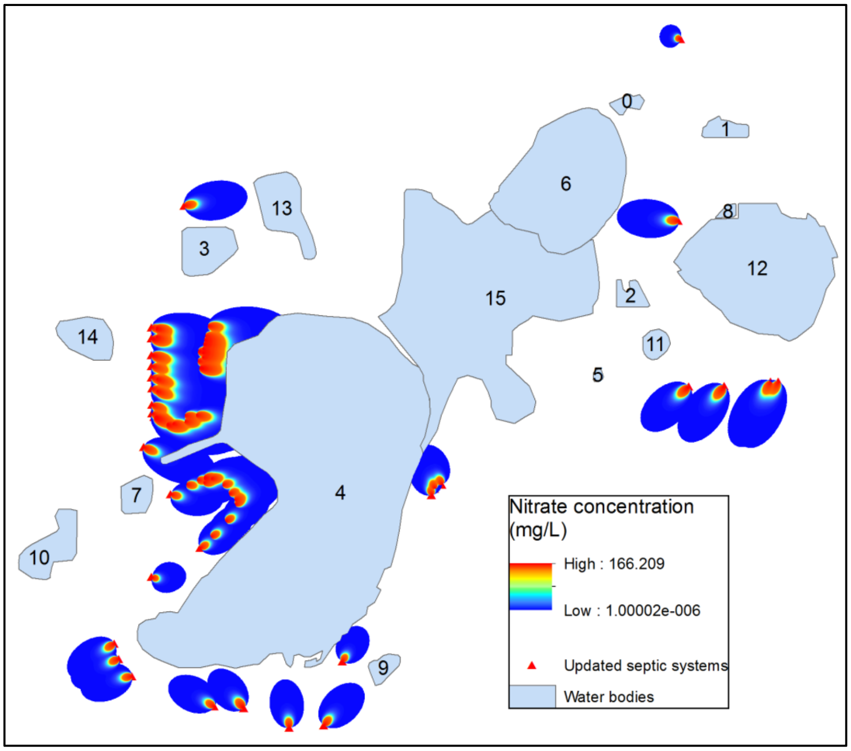

Figure 4-20. Simulated nitrogen plumes from updated septic system locations to surface water bodies. The waterbodies (including marshes and swamps) are labeled with their FIDs.

Table 4-6. Simulated nitrogen for water bodies in the Lake Roberts watershed with updated septic system locations. The locations of the water bodies are shown in Figure 4-20.

FID	M_out(g/d)	Load (lb/y)	M_in(g/d)	Reduction Ratio (%)
4	871.35	701.17	1622.74	46.30
9	0.00	0.00	24.22	100.00
6	0.00	0.00	24.22	100.00
13	0.00	0.00	24.22	100.00
15	22.10	17.79	24.22	8.74
Sum	893.45	718.95	1719.62	48.04

4.6. Impacts of Watershed Boundary on ArcNLET Modeling Results

Figure 4-21 is revised from Figure 4-20 with the original and new watershed boundaries added. The figure also include the DEM of the modeling domain shown in Figure 4-2. Since the ArcNLET simulation domain is substantially larger than the original and new watershed, the modeling results are not affected by the watershed boundaries. Although the new watershed is smaller than the original watershed at the west side of the modeling domain, the difference does not affect the ArcNLET-estimated nitrogen loading, because there is no loading to the three waterbodies (with FIDs of 7, 10, and 14). More importantly, at the west side of the lake, groundwater flows cross the new watershed boundary into the lake, as indicated by the seepage measurements and the simulated flow paths. Therefore, it is concluded that the new watershed boundary does not affect the ArcNLET-estimated nitrogen load.

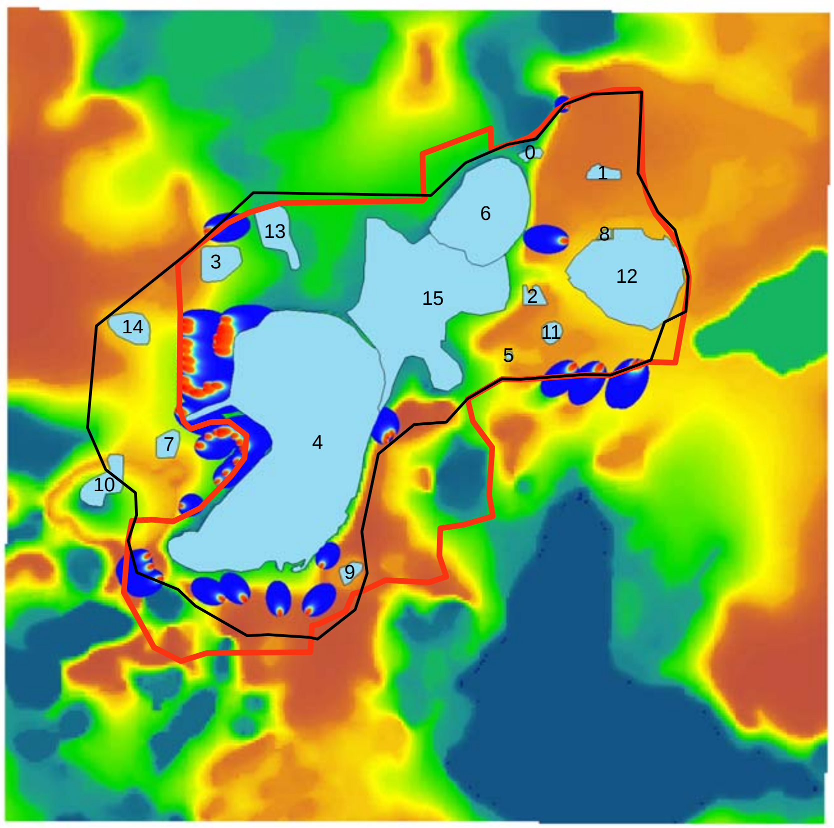

Figure 4-21. Simulated nitrogen plumes from updated septic system locations to surface water bodies. The waterbodies (including marshes and swamps) are labeled with their FIDs. The original and new watershed boundaries are delineated by the black and red polylines.

5. ARCNLET MODELING FOR LAKE WEIR

The ArcNLET modeling for Lake Weir has two components. Sections 5.1 – 5.4 include the modeling results obtained in 2014 when there were no observations of hydraulic head and/nitrogen concentration for calibration. After hydraulic head observations were provided in 2015 by the Marion County (through Kyeongsik Rhew at FDEP), the ArcNLET flow model was calibrated, and procedure of calibration was presented in Section 5.5. The calibrated smoothing factor is 50, the same as the one based on our previous modeling experience and used in the 2014 modeling. The County also provided an updated septic tank coverage file that contains 2,081 septic tanks, substantially larger than the original number of 485 septic tanks. The new modeling results of nitrogen loading are included in Section 5.6.

5.1. Geographic Data for Lake Weir

Lake wire is located in the southern Marion County, near the boundary between Marion, Sumter, and Lake Counties. As shown in Figure 3-1, Lake Weir is north to the other three lakes, about 28.57 km (17.75 miles) north to Lake Denham located in the Lake County, 54.28 km (33.73 miles) to Lake Marshall, and 66.40 km (41.26 miles) north to Lake Roberts. Figure 5-1 shows the boundary of the watershed where Lake Weir resides; the watershed boundary was downloaded from FDEP database and provided by Kyeongsik Rhew at FDEP. In addition to Lake Weir, the watershed also includes Little Lake Weir, several small waterbodies, and a few swamps and marshes; the polygon files of waterbodies and swamps and marshes were also provided by Kyeongsik Rhew. Following the previous ArcNLET modeling practice, the swamps and marshes were merged into waterbodies so that they also receive nitrogen load from the septic systems.

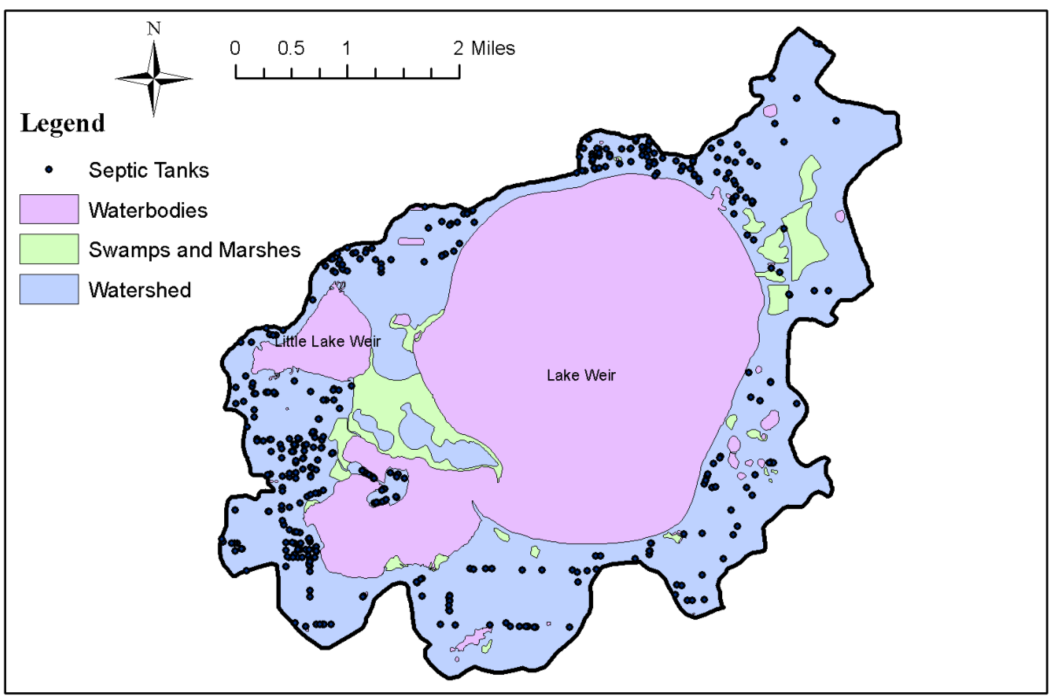

Figure 5-1. Watershed of Lake Weir and locations of septic tanks, waterbodies, and swamps and marshes. The swamps and marshes are merged into waterbodies later on for calibration of nitrogen load.

For the Lake Weir watershed and its vicinity, the USGS DEM database contains a set of data with the resolution of 1/3 arc-second (about 10m × 10m). Since the USGS data has higher resolution than FDEP data that has the resolution of 15 × 15m, the USGS DEM data was used in the modeling. The USGS dataset has four tiles (Figure 5-2), and the tiles were combined using the ArcGIS Mosaic to new raster function. Figure 5-3 plots the merged raster and clipped at the watershed and its vicinity. Comparing Figure 5-3 with Figure 5-1 shows that the resolution of 10m × 10m is able to reflect small waterbodies such as those in the area highlighted in Figure 5-3.

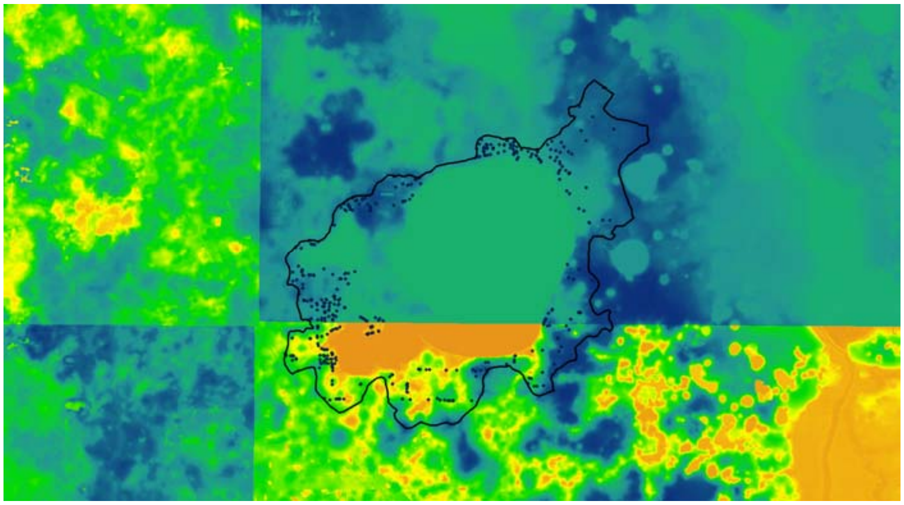

Figure 5-2. DEM at the Lake Weir watershed and its vicinity. The DEM data was downloaded from USGS website, and it was a combination of four tiles. Note that the symbology of the four sources of DEM data is not the same.

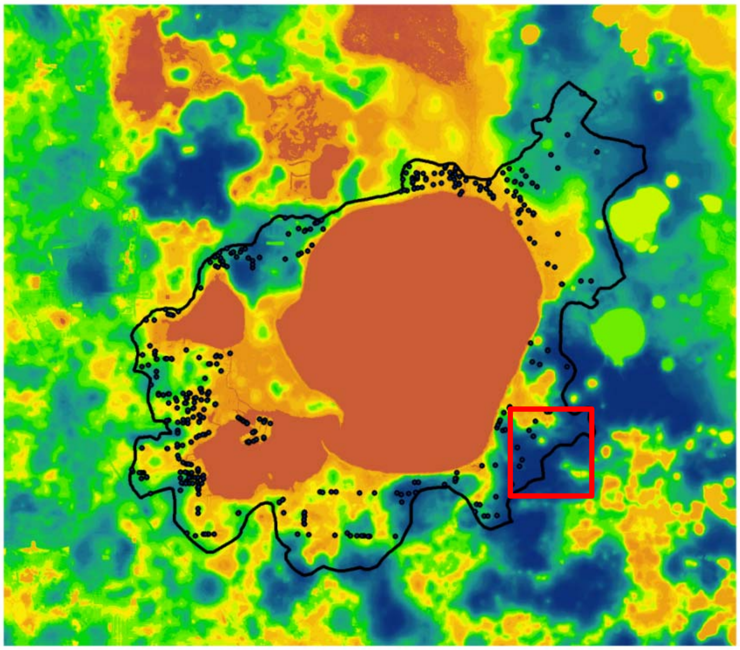

Figure 5-3. DEM merged using the ArcGIS Mosaic function and clipped for the watershed and its vicinity. The DEM resolution of 10m × 10m is able to reflect the small waterbodies such as those in the highlighted area.

Comparing Figure 5-3 with Figure 3-3 of Lake Marshall and Figure 4-2 of Lake Roberts shows that the DEM of Lake Weir is less smoothing than that of Lake Marshall and Lake Roberts. This poses challenges to ArcNLET modeling. As shown in Figure 5-4, the elevation map contains local valleys that are sinks of simulated groundwater flow. To resolve this problem, ArcNLET developed the sink filling function that fills the sinks and evaluates the groundwater velocity using the methods developed in surface hydrology. The resulting flow paths in the sink filling area may not be as smooth as in other areas where sink filling is not performed. The details of the sink filling function are referred to Section 2.3.2 of the ArcNLET technical manual (Rios et al., 2011).

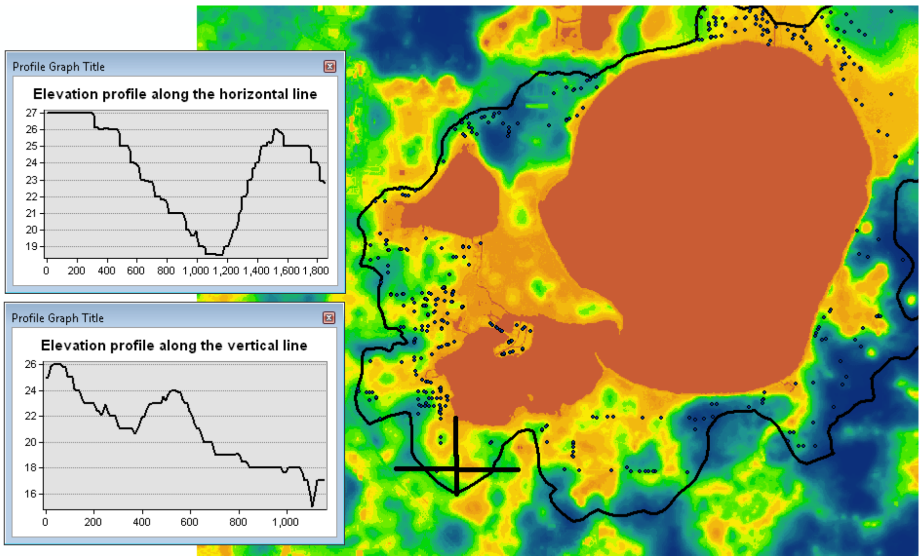

Figure 5-4. Elevation profiles along the horizontal and vertical lines marked on the elevation map. Local valleys (i.e., sinks) are observed at locations where waterbodies are absent. To handle the sinks, the sink filling function of ArcNLET was used in the modeling.

Figures 5-5 and 5-6 plot the heterogeneous spatial distributions of hydraulic conductivity and porosity, respectively, of the Lake Weir watershed. These data were obtained from the SSURGO database and aggregated from the horizons to components and to soil units by following the procedure descried in Wang et al. (2011). The values of hydraulic conductivity and porosity at the waterbody locations are assigned to zero in SSURGO. The parameter values in the south part of the watershed are more heterogeneous than in the north part. This may be related to the spatial variability of DEM.

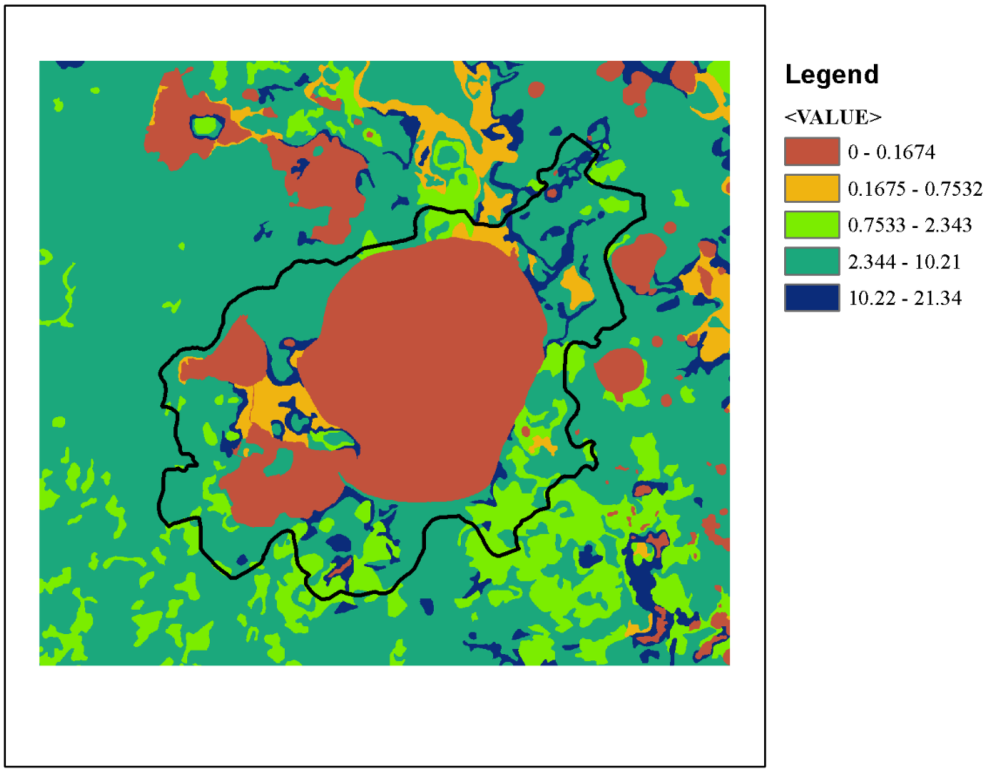

Figure 5-5. Heterogeneous hydraulic conductivity (m/d) of soil units of the Lake Weir watershed. The black polyline is the watershed boundary.

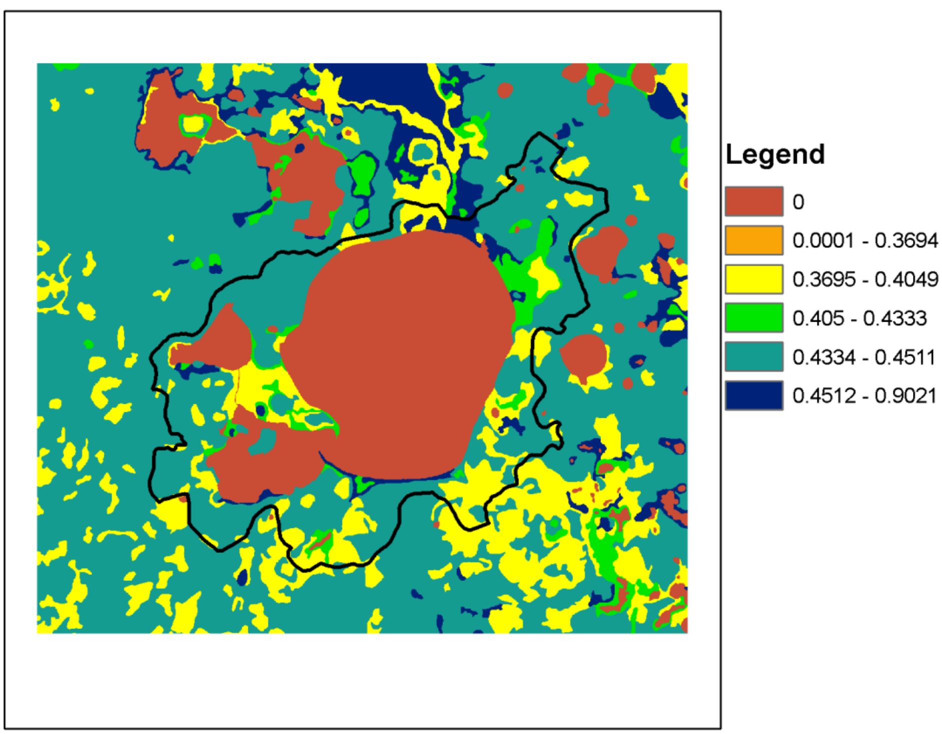

Figure 5-6. Heterogeneous porosity ([-]) of soil units of the Lake Weir watershed. The black polyline is the watershed boundary.

5.2. Nitrogen Load to Groundwater and Denitrification

For the Marion County, the nitrogen load (i.e., inflow mass rate) from a septic system to groundwater was estimate in the manner similar to that for the Orange County. However, the estimate is slightly different, because there are 2.41 persons per household in Marion County, according to the website (http://quickfacts.census.gov/qfd/states/12/12083.html). Therefore, the value of inflow mass rate is approximated as 12.63 g per person per day × 2.41 persons per household × 0.7 (the amount of nitrogen not lost in septic tanks) = 21.31 g/d. This is slightly smaller than the approximate of 24.22 g/d used for the Orange County.

Nitrate fate and transport (including denitrification) has been studied for the Silver Spring area in the Marion County (Hicks and Holland, 2012; O'Reilly et al., 2012a,b; Wanielista et al., 2011; Phelps, 2004). A number of hydrology and water quality data were obtained by Andrew M. O'Reilly and his colleagues, and more information is available at their project website, http://fl.water.usgs.gov/projects/oreilly_stormwaternitrogen/index.html. However, the extent of denitrification is not fully known due to spatial variability. For example, the O'Reilly group studied two sites: Hunter Trace and South Oak, whose locations are shown in Figure 5-7 and they are about 4 kilometer apart. According to Wanielista et al. (2011), denitrification occurs in the South Oak site but not in the Hunter Trace site, due to presence of oxygen in the latter site. Although the two sites are far from Lake Weir, the aerobic condition is likely to occur at the modeling site of this study, because nitrate transport from septic systems is always in shallow aquifer. Therefore, the relatively low decay coefficient of 0.001 d^{-1} was used in this study.

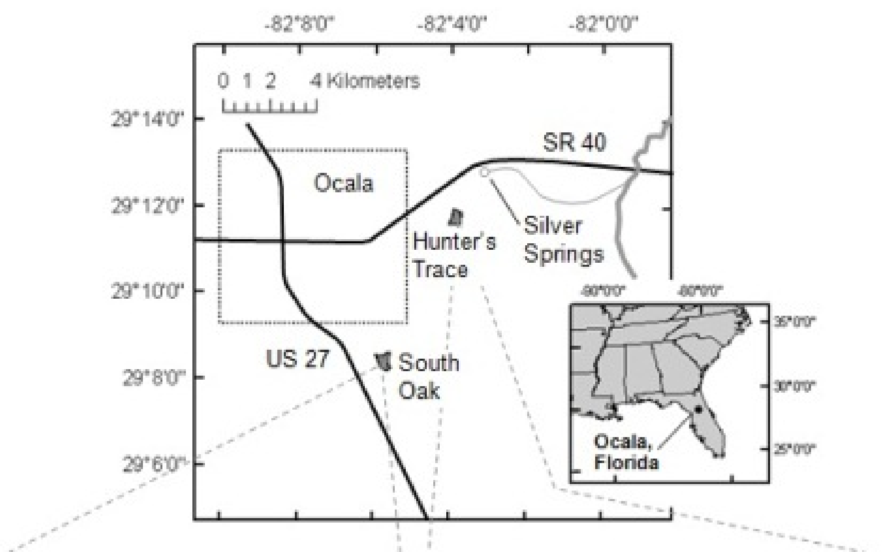

Figure 5-7. Study area showing locations of the South Oak and Hunter's Trace stormwater infiltration basins and monitoring sites. The figure and figure caption are copied from http://fl.water.usgs.gov/projects/oreilly_stormwaternitrogen/index.html.

5.3. Modify Waterbody Polygon

We found that the waterbody polygon does not agree with the DEM data. An example is shown in Figure 5-8. The left figure on the top row, copied from Google Earth, shows a canal that is connected with Lake Weir. However, the right figure on the top row shows that the canal was missing from the Lake Weir polygon with the FID of 19. The canal was incorporated into the lake polygon by using the ArcGIS edit function, and the revised lake polygon is shown at the bottom row of Figure 5-8. The waterbody FIDs change, because of adding and merging waterbodies. The change of FID does not affect the modeling results.

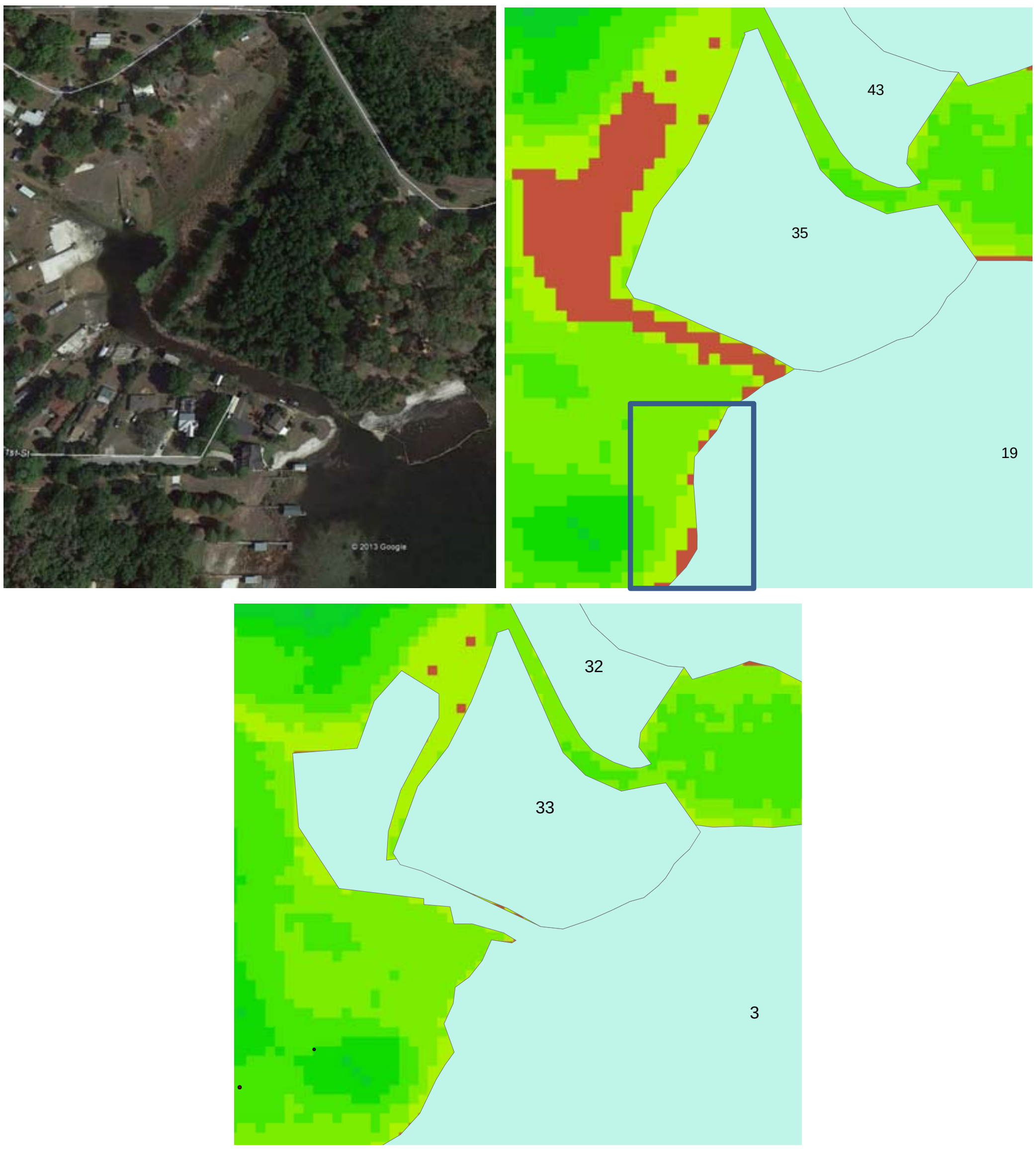

Figure 5-8. (Left of top row) Google Earth picture shows a canal. (Right on the top row) The canal is reflected in the DEM but not included as part of the waterbody polygon of Lake Weir (with FID of 19). (Bottom) revised waterbody polygon to incorporate the canal into the polygon.

The inconsistency between the waterbody polygon and the DEM is also reflected in the area shown in Figure 5-8, because the DEM data (in red) of waterbodies covers large areas than the waterbody polygon (in light blue). We assumed that the DEM data is more accurate and thus revised the waterbody polygon to be consistent with the DEM data. The manual revision may not be accurate, and water polygon with better accuracy is needed.

5.4. Modeling Results without Flow Model Calibration

With the data discussed above and information of model parameters described in Chapter 3, ArcNLET modeling was conducted. Figure 5-9 plots the simulated nitrogen plumes from the septic systems to the surface waterbodies. Table 5-1 lists the waterbodies that receive nitrogen load. The total amount of load is 3230.33 g/d, i.e., 2599.40 lb/year, which is about ten times as large as that at the watershed of Lake Marshall and twice as large as that at the watershed of Lake Roberts. This is not surprising, considering that the number of septic systems in the watersheds of Lake Weir, Lake Marshall, and Lake Roberts are 485, 47, and 83, respectively. The load in the watersheds of Lake Roberts is relatively higher than those in the other two watersheds because of the relatively large groundwater velocity and short distance between septic systems and waterbodies, as discussed above. Lake Weir (with FID of 3) and Little Lake Weir (with FID of 8) receive the largest and the second largest amount of load, respectively. The rest receiving waterbodies are swamps and small waterbodies. For example, as shown in Figure 5-9, the swamp with FID 32 receives the third largest amount of nitrogen load.

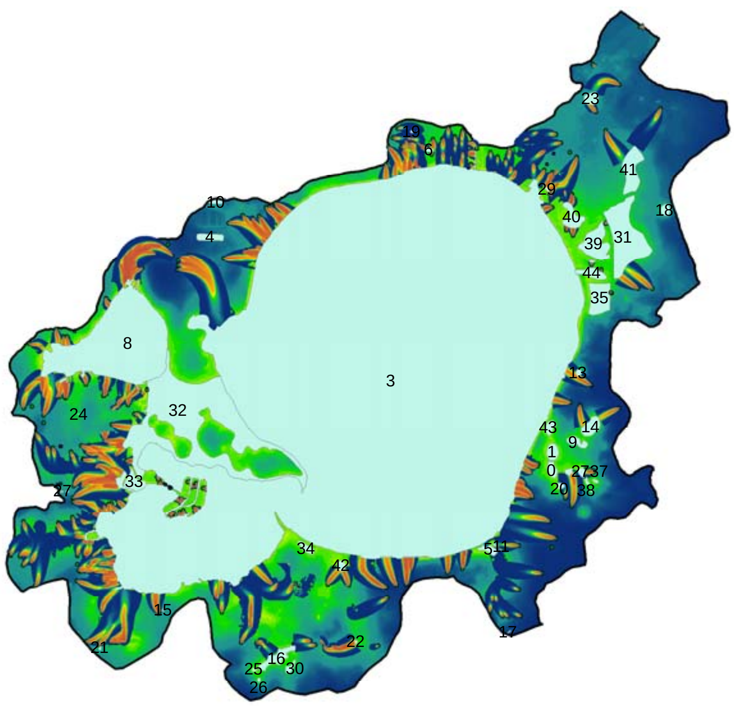

Figure 5-9. Simulated flow nitrogen plumes from septic systems to surface waterbodies. The background is DEM. The waterbodies (including marshes and swamps) are labeled with their FIDs.

Table 5-1. Simulated nitrogen loads to waterbodies in the Lake Weir watershed. Locations of the waterbodies are shown in Figure 5-9.

Waterbody FID	Inflow Mass (g/d)	Inflow Mass (lb/d)	Load (g/d)	Load (lb/yr)	Reduction Ratio (%)
3	6350.38	14.00	2101.84	1691.32	66.90
8	1193.36	2.63	395.88	318.56	66.83
32	447.51	0.99	195.38	157.22	56.34
29	191.79	0.42	137.37	110.54	28.38
40	149.17	0.33	112.77	90.74	24.40
6	127.86	0.28	51.97	41.82	59.35
35	42.62	0.09	40.62	32.69	4.69
31	63.93	0.14	35.13	28.27	45.05
42	106.55	0.23	25.80	20.76	75.79
22	127.86	0.28	23.47	18.89	81.64
11	42.62	0.09	21.16	17.02	50.36
44	21.31	0.05	21.14	17.01	0.77
28	21.31	0.05	20.90	16.82	1.93
23	42.62	0.09	15.31	12.32	64.08
12	63.93	0.14	15.00	12.07	76.53
14	42.62	0.09	10.50	8.45	75.35
27	149.17	0.33	2.89	2.32	98.07
41	42.62	0.09	2.47	1.99	94.21
16	42.62	0.09	0.61	0.49	98.56
5	191.79	0.42	0.12	0.10	99.94
Total	9461.64	20.86	3230.33	2599.40	65.86

As shown in Table 5-1, the overall nitrogen reduction ratio (due to denitrification) is about 66%, which is similar to that for the three waterbodies (with FIDs of 3, 8, and 32) that receive the top three amounts of load. The reduction ratio is similar to that for the watershed of Lake Marshall, but larger than that for the watershed of Lake Roberts. The reduction rate is high uncertain. In the report of Phelps (2004) for the Silver Spring basin, it was stated that "An attenuation by denitrification of 20 percent was estimated by Otis and others (1993); rates as high as 80 percent were reported by Horsley and others (1996)." However, it should be noted that these ratios are not specifically for the watershed of Lake Weir. More site-specific study is needed to determine more accurate estimate of the reduction ratio.

Figures 5-10 and 5-11 show respectively the ArcGIS- and EXCEL-generated descriptive statistics of the extracted seepage velocity magnitude along the perimeter of Lake Weir. The seepage velocity magnitude varies in five orders of magnitude from 0.0008 to 14.22 m/d. Comparing the statistics with those of Lake Marshall and Lake Roberts shows that the overall seepage to Lake Weir is significantly larger. This is attributed to the larger perimeter of Lake Weir and larger seepage velocity at certain locations of the lake perimeter.

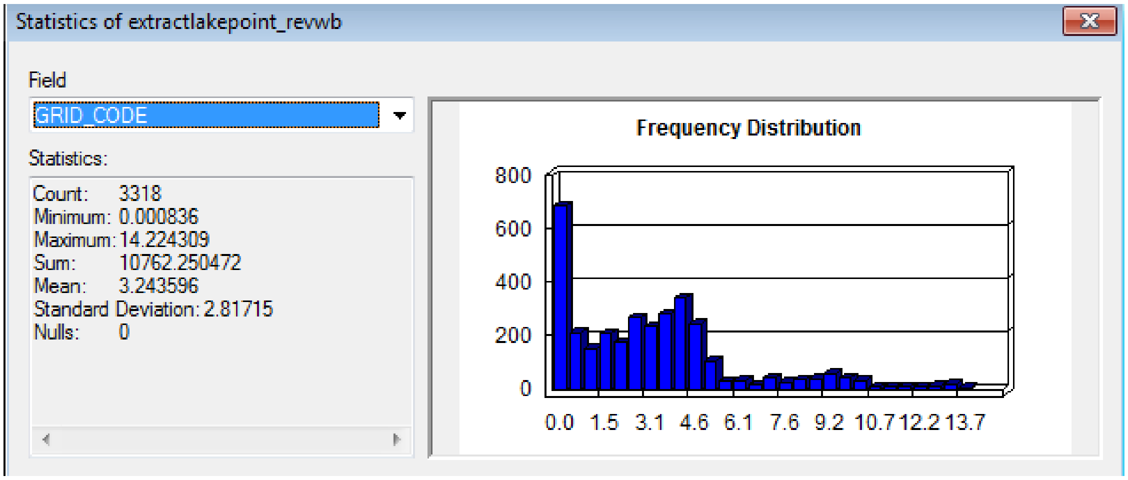

Figure 5-10. Statistics of extracted seepage velocity magnitude (m/d) along the perimeter of Lake Weir.

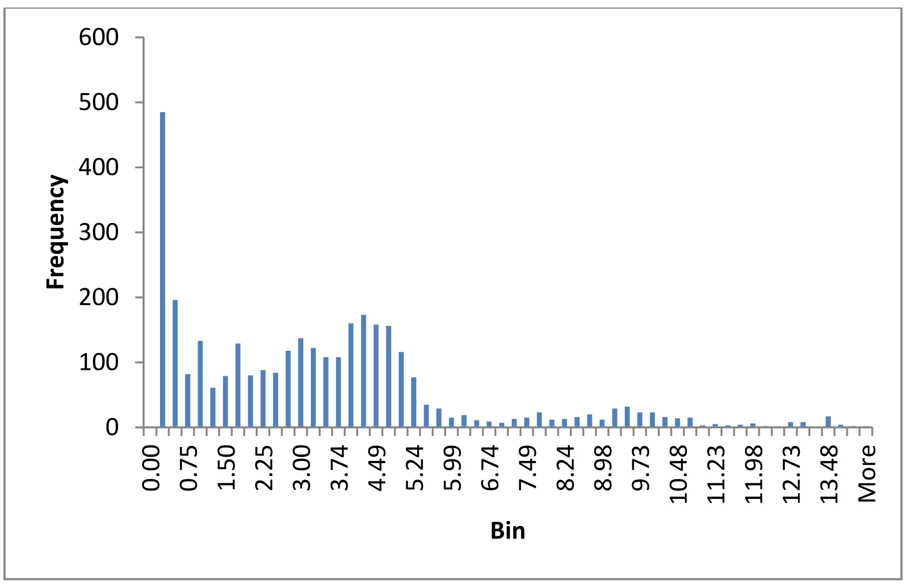

Figure 5-11. EXCEL-based histogram of extracted seepage velocity magnitude (m/d) along the perimeter of Lake Weir.

5.5. Flow Model Calibration Using Observations of Water Level Elevation

In April 2015, Kyeongsik Rhew at FDEP provided to us the monitoring data of water level elevation (i.e., hydraulic head) obtained by the Marion County at a landfill site located near Lake Weir (Figure 5-12). The water level elevation data are for both confined and unconfined aquifers. Since ArcNLET was developed for flow and transport in unconfined aquifers, only the data of the unconfined surficial aquifer were selected and used to calibrate the ArcNLET flow model. The locations of the selected 26 monitoring wells are shown in Figure 5-12.

Figure 5-12. Locations of observation wells of hydraulic head in surficial aquifer.

To understand spatio-temporal variability of hydraulic head, Figure 5-13 plots the time series of water level elevation in several wells that has a relatively large number of data for analysis. The data plotted in the figure were observed in the period of 12/1/2006 ~ 12/1/2011. Despite of the fluctuation, there are no significant trends presented within the time period of observations. It is therefore reasonable to use the average (over time) value of water level elevation at each well for model calibration later on.

All the selected wells shown in Figure 5-13 have a similar pattern of temporal variation. In particular, the magnitudes of water level elevation change are similar at wells DMW-47B, DMW-36B, DMW-10B, and DMW-18B. Considering that wells DMW-47B and DMW-36B are located in the south and the other wells in the north of the site, the similar pattern of temporal variation indicates that water table at the landfill site rises and/or falls at the same time with a similar rate. At well DMW-22B, water level elevation substantially decreased at the beginning and the end of the observation period, which may be attributed to measurement error or other unknown reasons such as small-scale heterogeneity.

Spatial variation of heterogeneity may cause difficulty for the model calibration. For example, the high water level elevation at well DMW-47B and low water level elevation at well DMW-11B indicate that the groundwater flow is not uniformly converging to Lake Weir. The monitoring data indicate an area of high water level elevation around well DMW-40C. The area may be considered as a groundwater divide, and groundwater flows in the southeast direction to Lake Weir and in the northwest direction to other areas of lower water level elevation. Special attention is therefore needed to handle the spatial variability of water table elevation during the calibration, as discussed below.

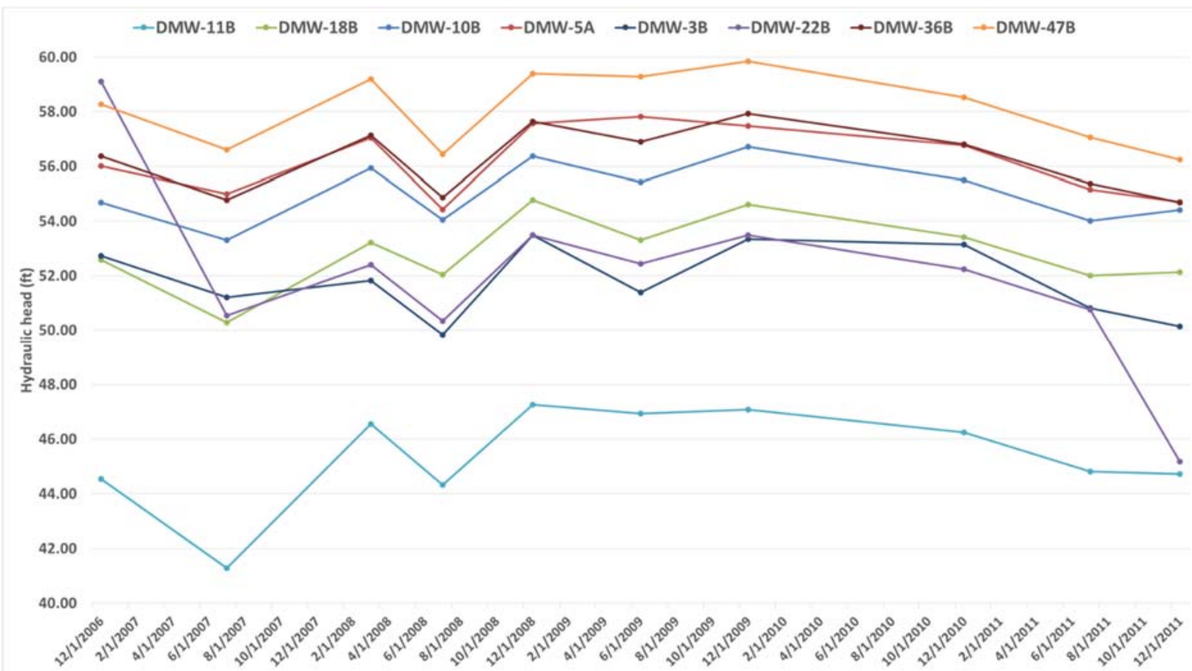

Figure 5-13. Time series of water level elevation (ft) at eight selected monitoring wells.

As explained in Chapter 2, the ArcNLET groundwater flow modeling involves three parameters: smoothing factor, hydraulic conductivity, and porosity. Since porosity always has small uncertainty, the SSURGO values are always used directly in ArcNLET modeling without calibration. While hydraulic conductivity is subject to calibration as shown in the last chapter for the Lake Roberts modeling, it is always preferred to calibrate smoothing factor before calibrating hydraulic conductivity. If reasonable model calibration is achieved by calibrating smoothing factor alone, there is no need to calibrate hydraulic conductivity. This is the case for the Lake Weir modeling. By adjusting the smoothing factor value, the goal of the ArcNLET flow model calibration based on water level elevation is to achieve 1:1 relation between the average water level elevation (over time) and smoothed DEM. The 1:1 relation indicates that the shape of smoothed DEM matches the shape of water table so that hydraulic gradient can be approximated by the gradient of smoothed DEM, as shown in Equation 2 of Chapter 2.

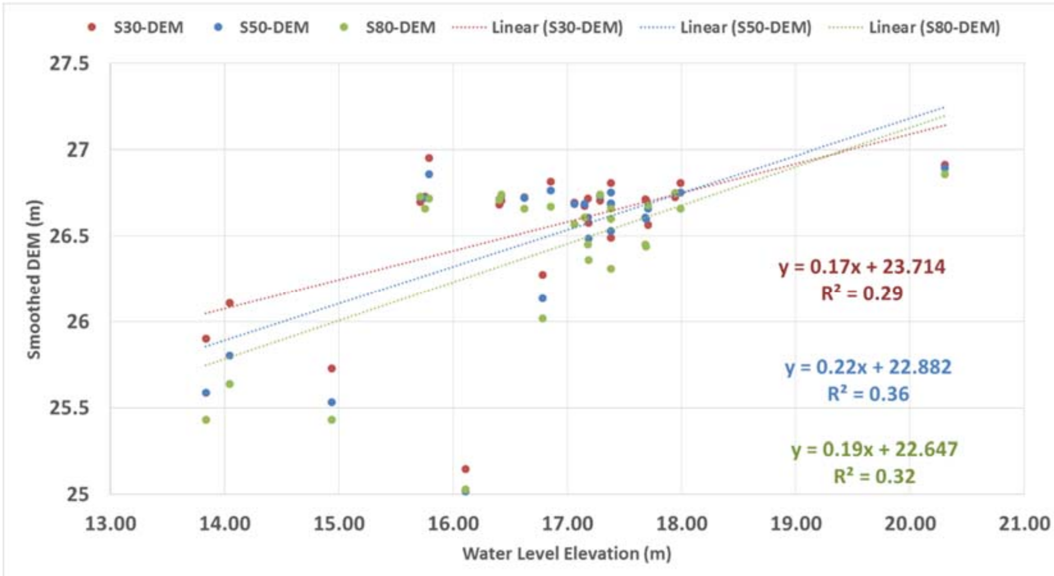

Figure 5-14. Linear regression lines between water level elevation at 26 monitoring wells and smoothed DEM with three smoothing factor values of 30, 50, and 80.

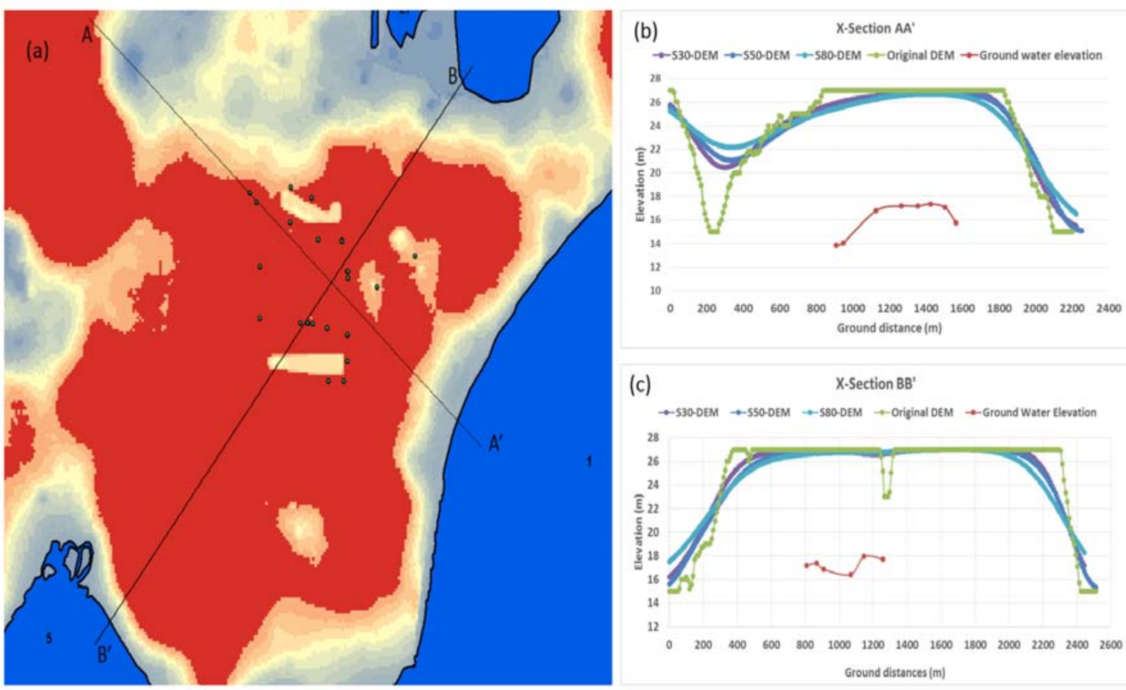

Figure 5-15. (a) Locations of cross-sections of AA’ and BB’ at the landfill site and its vicinity, (b) Smoothed DEM (with different smoothing factors), original DEM, and ground water elevation along cross-section AA’ (ground distance is zero at point A), and (c) Smoothed DEMs (with different smoothing factors), original DEM, and ground water elevation along cross-section BB’ (ground distance is zero at point B).

Figure 5-14 shows the relation between the average water level elevations at all the 26 monitoring wells and the corresponding smoothed DME for three different smoothing factors of 30, 50, and 80. The smoothing factor of 50 is based our modeling experience at other sites, and was used in the previous modeling presented in Sections 5.1 – 5.4. The figure shows that the relations are not 1:1, and this may be explained by Figure 5-15 that plots water level elevations, original DEM, and smoothed DME at two cross-sections. The two cross-sections AA' and BB' (Figure 5-15a) were chosen to be significantly larger than the landfill site to better understand the relation between water level elevation and smoothed DEM. To remove the impacts of the artificial height at the landfill, the original DEM was processed by assigning a value of 27m, the highest elevation of the natural land at the vicinity of the landfill site. In other words, if the land surface elevation at the landfill site is higher than 27m, it is replaced by 27m. The average water table elevations used for plotting Figure 5-15b are from the eight wells (DMW-11B, DMW-6B, DMW-10B, DMW-5A, DMW-57C, DMW-40C, DMW-65C, and DMW-50C) close to cross-section AA'. Figure 5-15b shows that, while the original DEM (after the processing to remove landfill height) is flat for the area where the monitoring wells are located, the water level elevations are not flat. Along the southeast direction, water level elevation increases first, becomes flat, and then decreases. The flat area may be a groundwater divide, away from which groundwater flows along the southeast and northwest directions, respectively, as discussed earlier. In comparison with the shape of the original DEM, the shapes of the smoothed DEM are closer to the shape of the water table elevation, suggesting the need of smoothing DEM. Figure 5-15c does not show the relation between smoothed DEM and average water level elvation (at wells DMW-74C, DMW-9A, DMW-40C, DMW-22B, DMW-24C, DMW-47C). This is not surprising, because groundwater flow direction should not be along the BB' cross-section, i.e., parallel to the lake shore in the northest and southwest directions. Therefore, calibrating the smoothing factor should be based on the data along the AA' cross-section.

For calibrating the smoothing factor, a cross-section similar to cross-section AA' was selected. This cross-section, as shown in Figure 5-16a, is not straight but passes several monitoring wells so that the direct relation between water table elevation and smoothed DEM can be obtained. Figure 5-16b shows that shape of the water level elevation agrees with the shapes of the smoothed DEM with the three different smoothing factors of 30, 50, and 80. To further examine the relation, Figure 5-16c plots the water level elevation on the second *y*-axis. The figure shows that the different smoothing factors give significantly different shapes of the smoothed DEM. To demonstrate the importance of selecting monitoring wells along the flow direction, we included on purpose monitoring well DMW-78C (Figure 5-16a) that is not along the flow direction toward the lake. Figure 5-16c shows that including this well deteriorates the agreement at the end of the cross-section. This is reflected quantitatively in Figure 5-17 that plots the linear trend lines between the smoothed DEM and water level elevation. When water level elevation at well DMW-78C is included in the regression, the regression coefficient is about 0.7 (Figure 5-17a); after the well is excluded from the regression, the coefficient increases to about 0.95 (Figure 5-17b). Therefore, well DMW-78C was not used for the calibration.

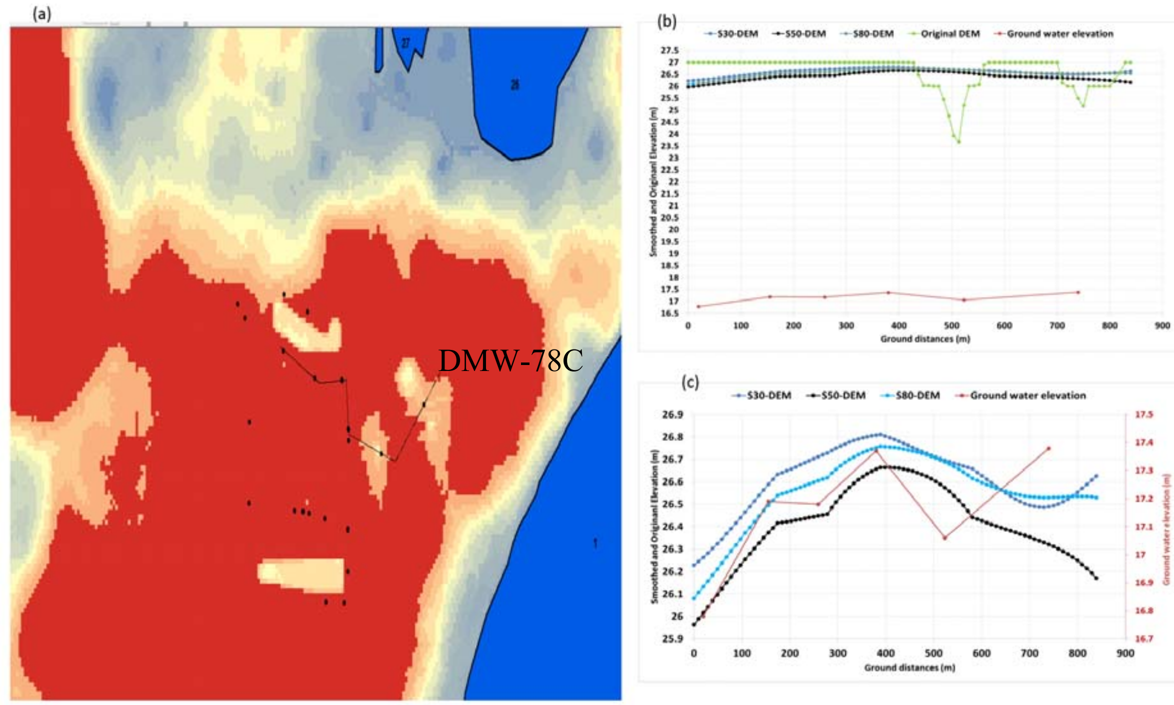

Figure 5-16. (a) Location of the cross-section of the selected wells for calibration, (b) Smoothed DEMs (with different smoothing factors), original DEM, and ground water elevation along the cross-section (ground distance starts from the most northwest well), and (c) replot of Figure (b) by plotting water level elvation on another y-axis to better evaluate the relation between water level elevation and smoothed DEMs.

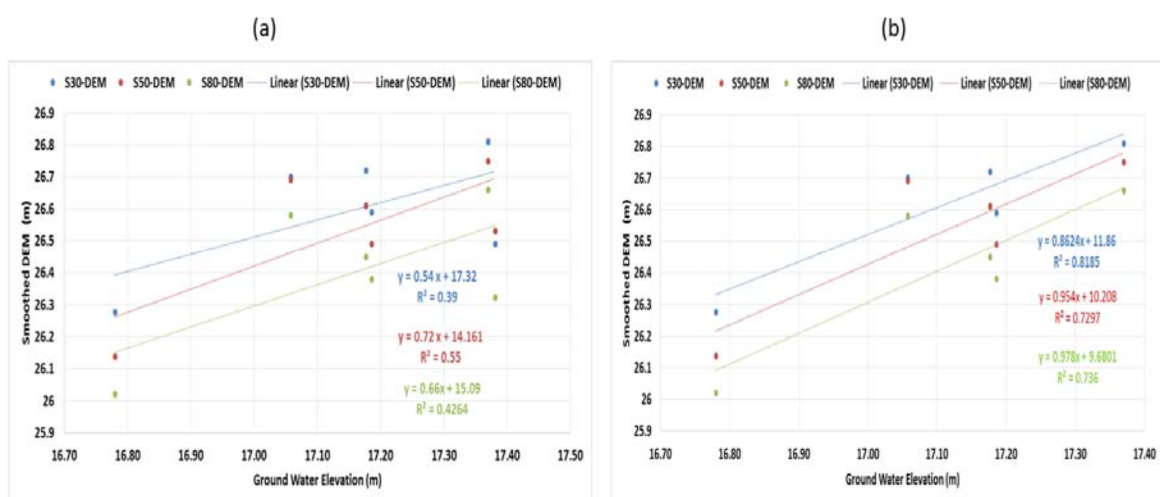

Figure 5-17. Linear regression lines between smoothed DEM with three smoothing factor values (30, 50, and 80) and water level elevation (a) at six monitoring wells including well DMW-78C and (b) at five monitoring wells excluding well DMW-78C. The regression slope becomes closer to 1 after excluding well DMW-78C.

For the three smoothing factors of 30, 50, and 80, the value of 50 was selected for two reasons. First, the regression coefficient (0.954) of this smoothing factor is better than that (0.862) of smoothing factor of 30, as shown in Figure 5-17b. Although the regression coefficient is the best for the smoothing factor of 80, the improvement is marginal in that the regression coefficient only increases from 0.954 to 0.978. More importantly, we were concerned that the smoothing factor of 80 may result in an over-smoothing, considering that the landfill site is a high land of the modeling domain. Because the calibrated smoothing factor is the same as the one used in the previous flow modeling presented in Sections 5.1 – 5.4, the flow modeling results are not changed.

5.6. New Modeling Results with Updated Septic Tank Locations

A new ArcNLET transport modeling was conducted to simulate the nitrogen load for the updated septic tank file provided by Kyeongsik Rhew at FDEP. The new file contains 2,081 septic tanks, substantially larger than the original number of 485 septic tanks. After comparing the new septic tank locations with the old locations shown in Figure 5-1, it was found that the new septic tank locations do not include the old septic tank locations, as illustrated in Figure 5-18. Therefore, this round of simulation with difference numbers and locations of septic tanks gives different nitrogen loading estimates from those listed in Table 5-1. In addition, it was found that some septic tanks are located in surface water bodies as shown in Figure 5-18(a). This happens often in the post ArcNLET modeling, because septic tank locations are assigned as geometric centers of parcels. If a parcel includes a pond or swamp (considered as a water body in ArcNLET modeling), its geometric center is likely within the pond or swamp. This problem of misplaced septic tank locations needs to be resolved, because septic tanks located in waterbodies are not included in ArcNLET modeling and the loading is underestimated, especially when septic tanks are close to waterbodies. To resolve this problem, we used Google Earth images to determine house locations and manually moved the septic tank locations. This is demonstrated in Figure 5-19(b).

The procedure of estimating nitrogen loading is the same as that described in Section 5.4. Figure 5-19 plots the simulated nitrogen plumes from the septic systems to the surface waterbodies. Table 5-2 lists the waterbodies that receive nitrogen load. The total amount of load is 16141.05 g/d (1299.72 lb/yr). The new load is about five times as large as the previous estimate of 3230.33 g/d (2599.40 lb/yr) listed in Table 5-1. This ratio is close to the ratio of 2081/485 = 4.3 between the numbers of new and original septic tanks. The load to Lake Weir (FID 3) is 8895.46 lb/yr, about 5.3 times as large as the original estimate of 1691.32 lb/yr listed in Table 5-1. This is reasonable considering the new septic tanks added around the lakeshore, as shown in Figure 5-18. This also explains the reason that the reduction ratio reduces from 65.85% (Table 5-1) to 60% (Table 5-2), because short travel paths correspond to smaller reduction ratio.

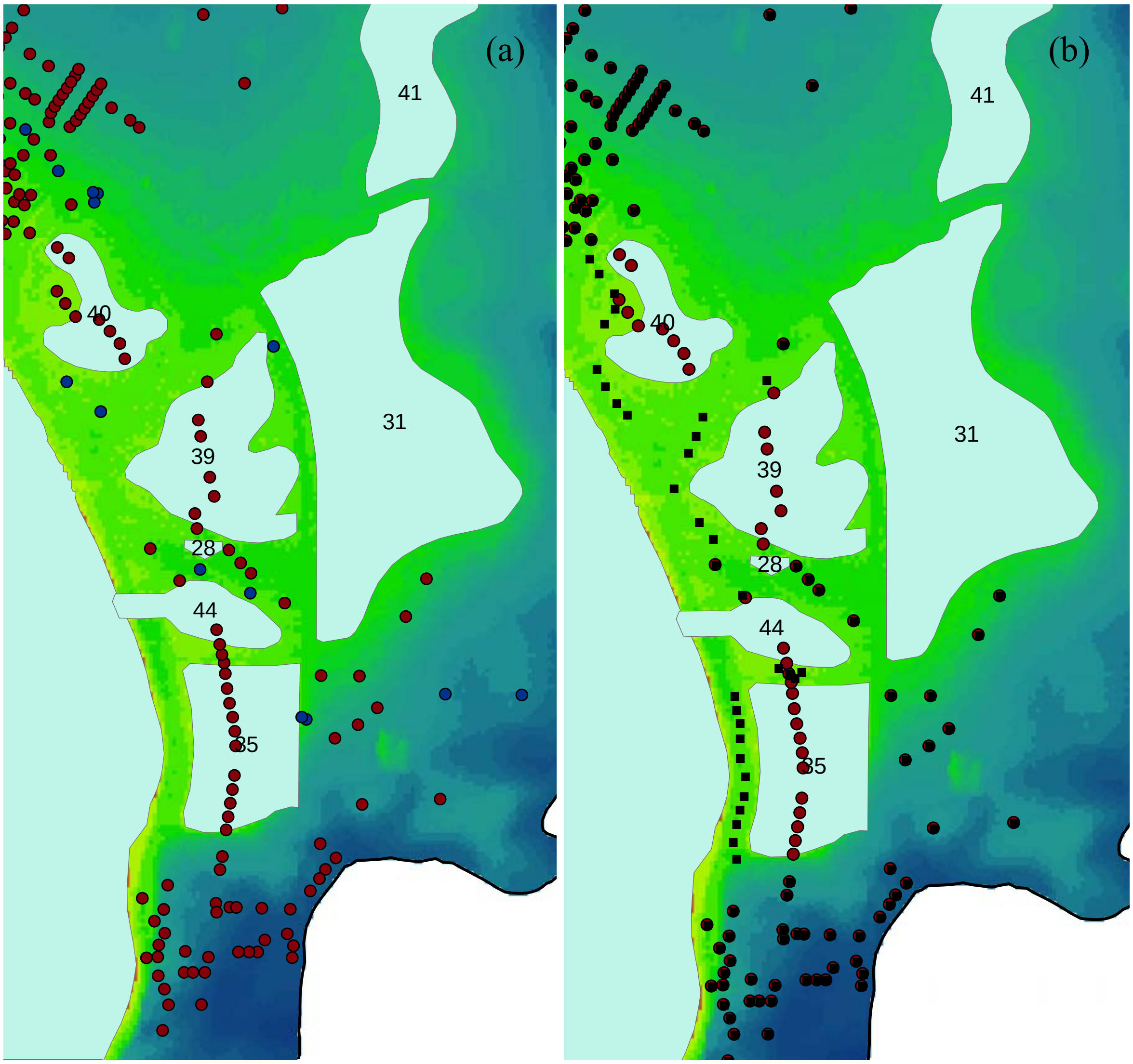

Figure 5-18. (a) Locations of original (blue) and new (red) septic tanks and (b) original and revised locations of the new septic tanks. The background color is DEM, and waterbodies (labeled by their FIDs). Figure (a) shows that the new septic tank locations do not include the original septic tank locations. Figure (b) illustrates the revised locations of the new septic tanks that are originally located in waterbodies.

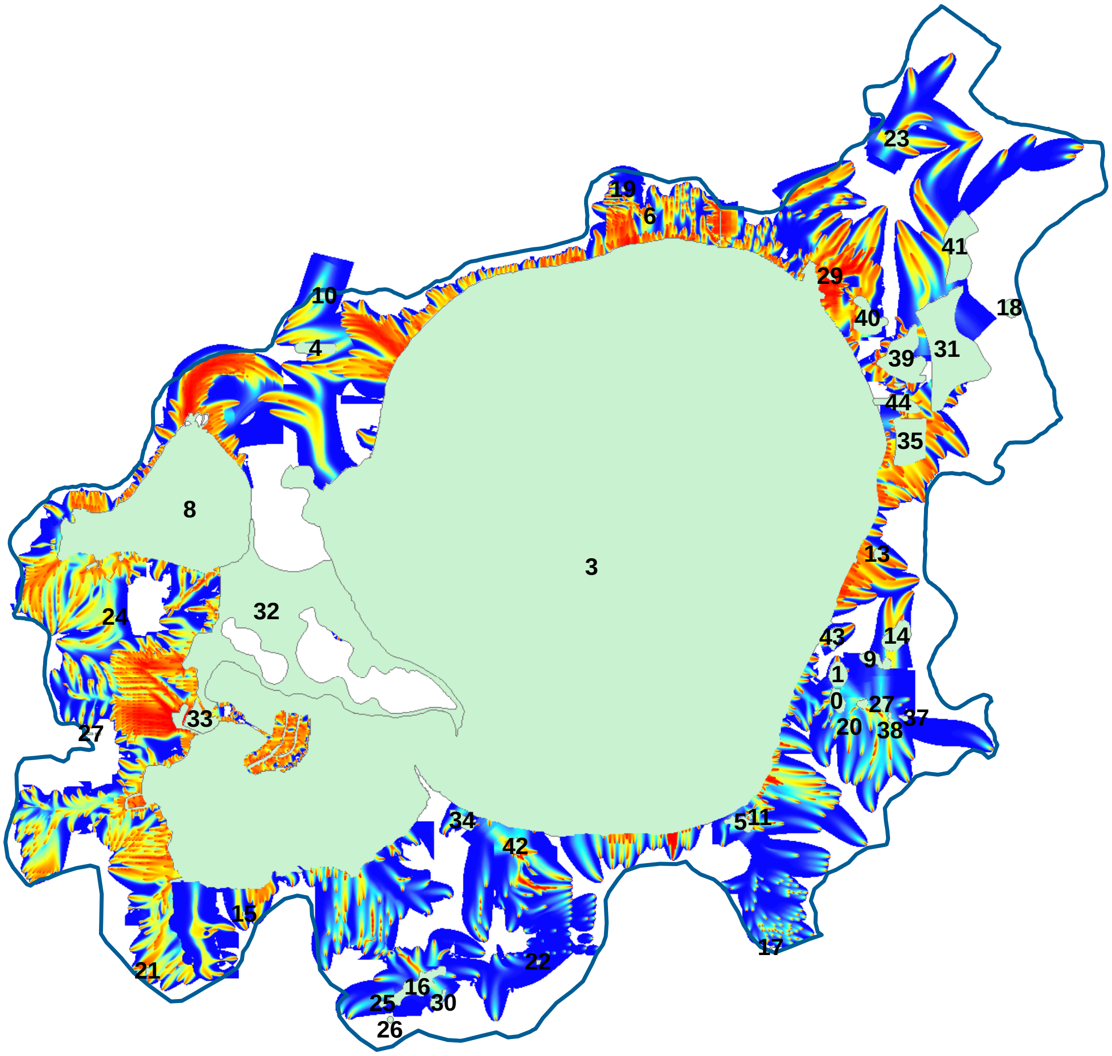

Figure 5-19. Simulated flow nitrogen plumes from septic systems to surface waterbodies. The background is DEM. The waterbodies (including marshes and swamps) are labeled with their FIDs

Table 5-2. Simulated nitrogen loads to waterbodies in the Lake Weir watershed from 2,081 septic tanks. Locations of the waterbodies are shown in Figure 5-19.

FID	Inflow Mass (g/d)	Inflow Mass (lb/d)	Load (g/d)	Load (lb/yr)	Reduction Ratio (%)
3	25849.03	57.00	11052.67	8895.46	57.24
8	5412.74	11.94	2216.96	1784.26	59.04
32	1981.83	4.37	667.71	537.39	66.31
29	937.64	2.07	557.41	448.62	40.55
35	447.51	0.99	240.03	193.18	46.36
42	1150.74	2.54	217.58	175.11	81.09
39	213.10	0.47	205.90	165.71	3.38
40	255.72	0.56	124.83	100.47	51.18
44	106.55	0.23	105.04	84.54	1.42
11	149.17	0.33	78.58	63.24	47.32
12	298.34	0.66	67.46	54.29	77.39
16	255.72	0.56	48.15	38.75	81.17
5	1470.39	3.24	45.69	36.77	96.89
0	191.79	0.42	43.44	34.96	77.35
23	170.48	0.38	40.94	32.95	75.98
28	42.62	0.09	40.46	32.57	5.06
31	127.86	0.28	39.64	31.90	69.00
20	85.24	0.19	38.95	31.35	54.30
34	42.62	0.09	36.26	29.19	14.92
36	42.62	0.09	33.51	26.97	21.38
13	42.62	0.09	32.55	26.20	23.62
1	34.15	0.08	30.67	24.68	10.18
43	42.62	0.09	29.27	23.56	31.32
14	63.93	0.14	27.78	22.36	56.55
27	149.17	0.33	27.38	22.04	81.64
6	191.79	0.42	24.59	19.79	87.18
33	21.31	0.05	21.11	16.99	0.95
41	213.10	0.47	14.69	11.82	93.11
21	85.24	0.19	14.55	11.71	82.93
4	21.31	0.05	8.93	7.18	58.12
10	42.62	0.09	7.63	6.14	82.10
22	63.93	0.14	0.41	0.33	99.35
19	21.31	0.05	0.29	0.23	98.65
Total	**40246.12**	**88.74**	**16141.05**	**12990.72**	**59.89**

6. ARCNLET MODELING FOR LAKE DENHAM

6.1. Modeling Site and Geographic Data

Lake Denham is located in the Lake County. As shown in Figure 3-1, Lake Denham is between Lake Weir and Lake Marshall. It is about 28.64 km (17.80 miles) southeast to Lake Weirl, and 30.82 km (19.15 miles) northwest to Lake Marshall. Figure 6-1 shows the boundary of the watershed where Lake Denham resides; the watershed boundary was downloaded from FDEP database and provided by Kyeongsik Rhew at FDEP. The lake is surrounded by the Okahumpka Swamp, and its southeast side intersects with the watershed boundary. In addition to the lake and the swamp, the watershed also includes a number of small waterbodies, and small swamps and marshes; the polygon files of waterbodies and swamps and marshes were also provided by Kyeongsik Rhew. Following the previous ArcNLET modeling practice, the swamps and marshes were merged into waterbodies so that they also receive nitrogen load from the septic systems.

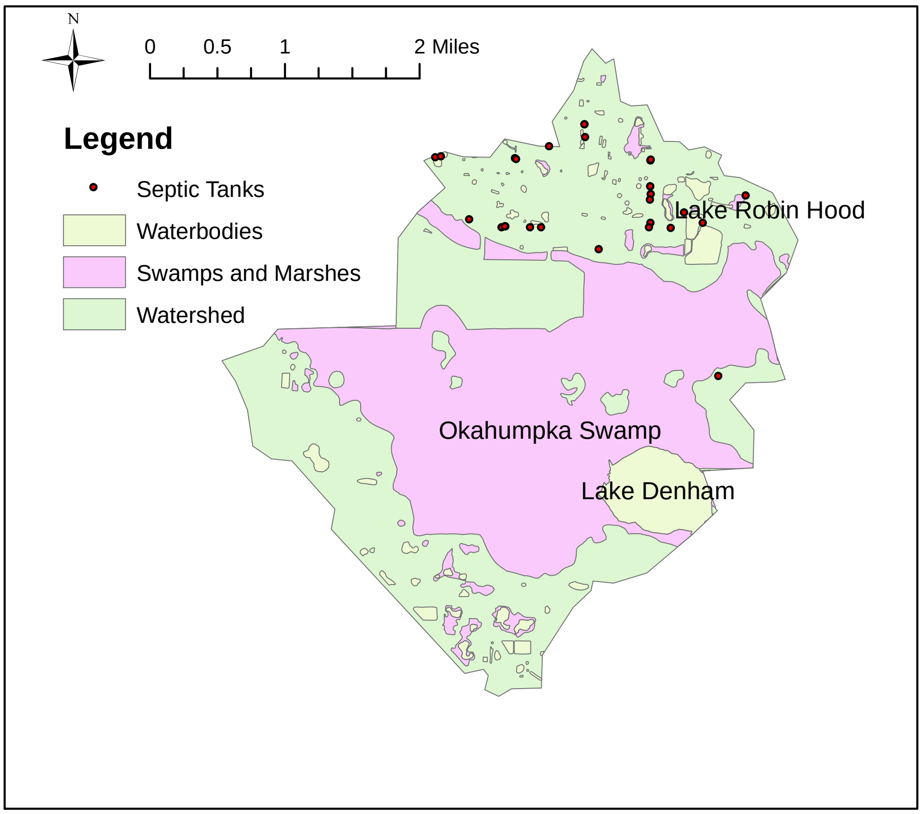

Figure 6-1. Watershed of Lake Denham and locations of septic tanks, waterbodies, and swamps and marshes. The swamps and marshes are merged into waterbodies later on for calculation of nitrogen load.

For the Lake Denham watershed and its vicinity, the USGS DEM database contains a set of data with the resolution of 1/9 arc-second (about 3m × 3m). Since the USGS data has higher resolution than FDEP data that has the resolution of 15 × 15m, the USGS DEM data was used in the modeling. As in the Lake Weir modeling, the USGS dataset has four tiles. The tiles were combined together, and Figure 6-2 plots the DEM clipped at the watershed and its vicinity. Figure 6-3 shows the zoomed-in DEM in the north part of the watershed. Comparing Figure 6-3with Figure 6-1 shows that the DEM can reflect the small waterbodies shown in Figure 6-1.

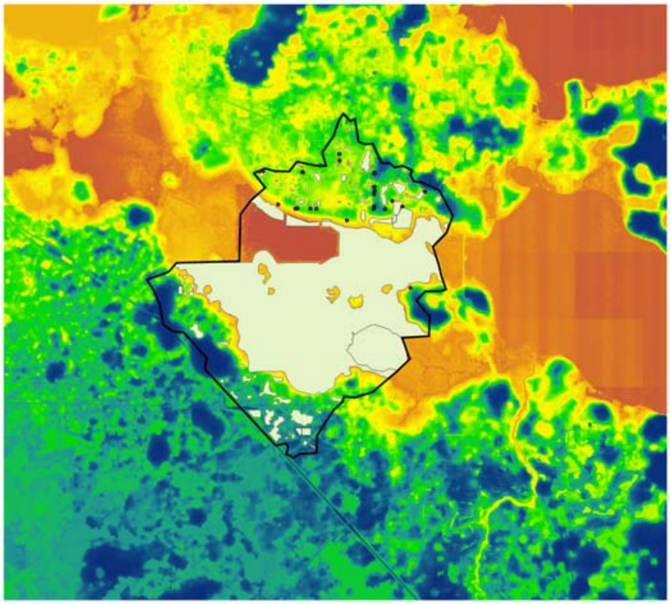

Figure 6-2. DEM merged using the ArcGIS Mosaic function and clipped for the watershed and its vicinity. The DEM resolution of 10m × 10m is able to reflect the small waterbodies such as those in the highlighted area.

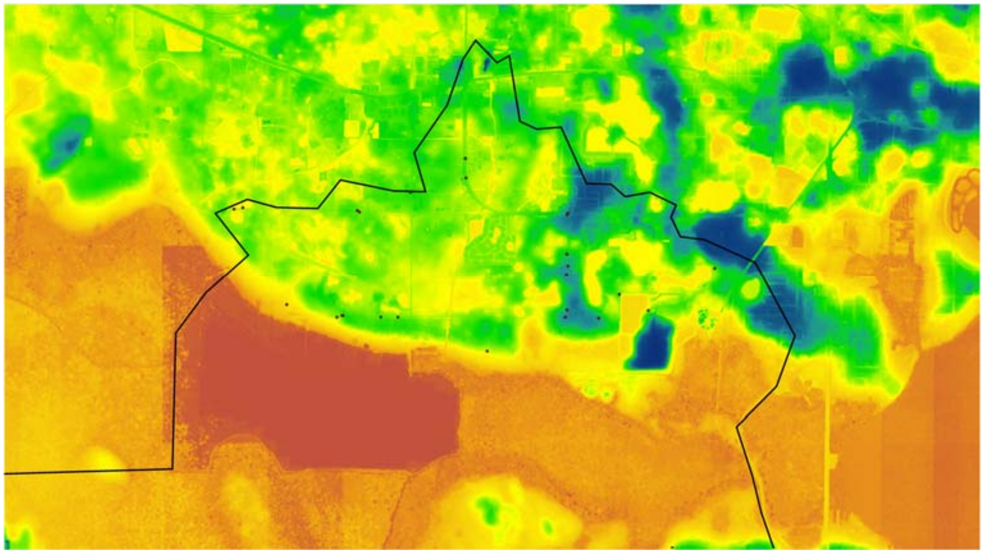

Figure 6-3. Zoomed-in DEM in the northern watershed. Comparing this figure with Figure 6-1 shows that the DEM can reflect the small waterbodies.

Figure 6-4 plots the heterogeneous spatial distributions of hydraulic conductivity of the Lake Denham watershed. The hydraulic conductivity data was obtained from the SSURGO database and aggregated from the horizons to components and to soil units by following the procedure descried in Wang et al. (2011). One may note the small white tail of the watershed shown in Figure 6-4 that is located in the Sumter County. Since we only processed the SSURGO data of the Lake County but the watershed covers both Lake and Sumter counties, hydraulic conductivity value is lacking in this small area. The ideal solution is to process the SSURGO database of the Sumter County to obtain the data, which however time consuming. Since the area is small and it is far away from the lake and the area of septic systems, we used ArcGIS raster calculate to add hydraulic conductivity value of the nearby area to the white tail and the entire thin tile at the left side of the domain. The results are shown in Figure 6-5. In the same manner, the porosity data was added to the white tail area of Figure 6-4, and the results are shown in Figure 6-6.

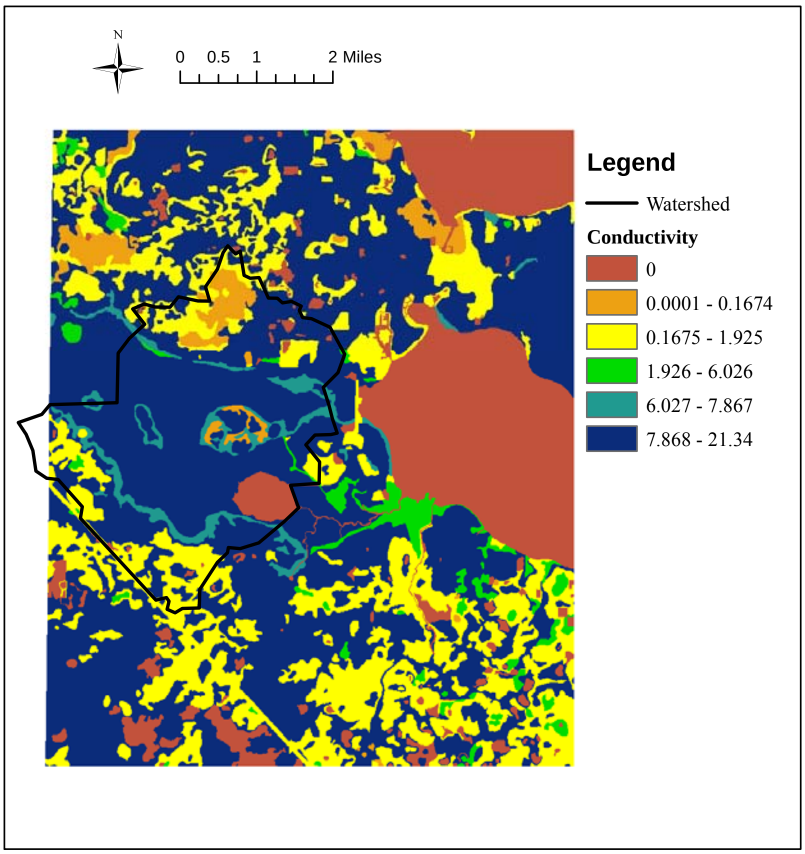

Figure 6-4. Heterogeneous hydraulic conductivity (m/d) of soil units of the Lake Denham watershed. The black polyline is the watershed boundary. The white tale of the watershed is located in the Sumter County, and there is no hydraulic conductivity data in the SSURGO database of the Lake County, where most of the watershed resides.

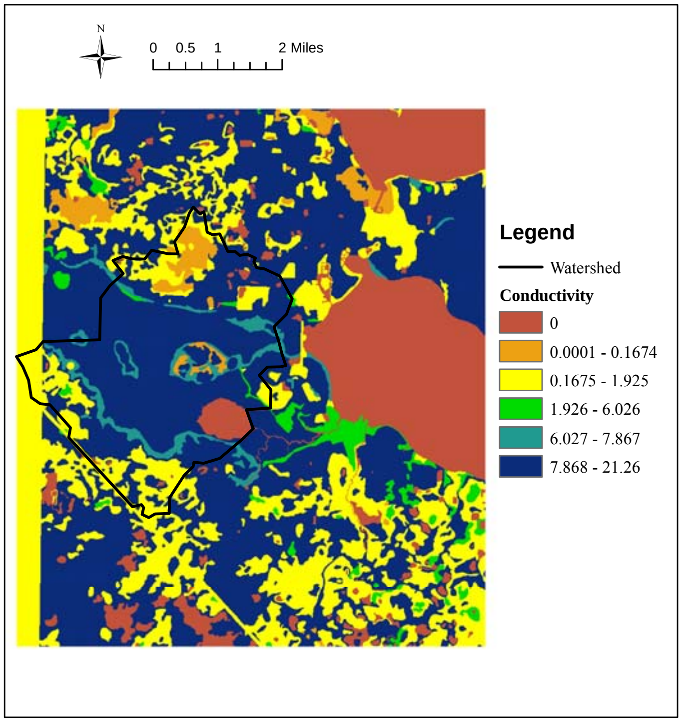

Figure 6-5. Heterogeneous hydraulic conductivity (m/d) of soil units of the Lake Denham watershed. The black polyline is the watershed boundary. The thin tile in yellow at the left side of domain contains hydraulic conductivity value added manually.

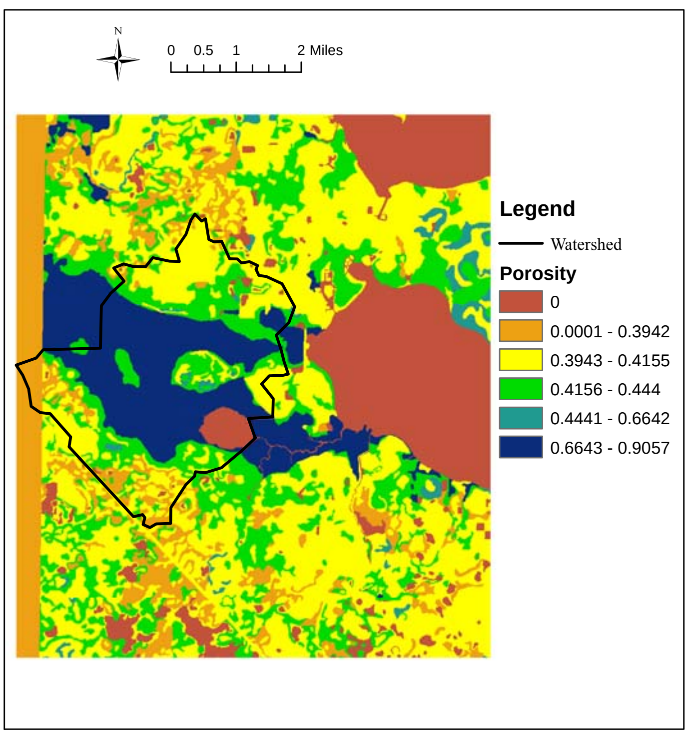

Figure 6-6. Heterogeneous porosity ([-]) of soil units of the Lake Denham watershed. The black polyline is the watershed boundary.

6.2. Nitrogen Load to Groundwater and Denitrification

For the Lake County, the nitrogen load (i.e., inflow mass rate) from a septic system to groundwater was estimate in the manner similar to that for the Orange County. However, the estimate is slightly different, because there are 2.51 persons per household in Lake County based on the data at the website of http://quickfacts.census.gov/qfd/states/12/12069.html. Therefore, the value of inflow mass rate is approximated as 4.61 kg per person per year × 2.51 persons per household × 0.7 (the amount of nitrogen not lost in septic tanks) = 8.10 kg/year = 22.19 g/d.

Regarding the decay coefficient, we did not find information specific to Lake County. Considering that Lake Denham is close to Lake Marshall, we used the value of 0.001 d^{-1}.

6.3. Modeling Results

Figure 6-7 plots the simulated nitrogen plumes from the septic systems to the surface waterbodies. Table 6-1 lists the waterbodies that receive nitrogen load. The total amount of load is 262.87 g/d, i.e., 211.53 lb/year. Since there is no septic system near Lake Denham, the lake does not receive any nitrogen load. Most of the load is to the small waterbodies in the northern part of the watershed. As shown in Table 5-1, the overall nitrogen reduction ratio (due to denitrification) is about 38%, which is relatively large due to the short distance between the septic systems and the waterbodies

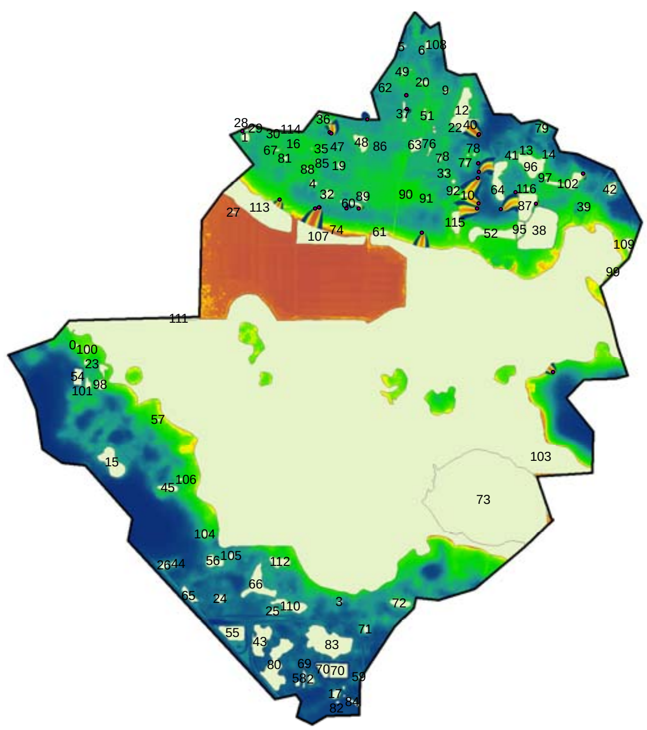

Figure 6-7. Simulated flow paths and nitrogen plumes from septic systems to surface waterbodies. The background is DEM. The waterbodies (including marshes and swamps) are labeled with their FIDs.

Table 6-1. Simulated nitrogen loads to surface waterbodies and groundwater (inflow mass) in the Lake Denham watershed. Locations of the waterbodies are shown in Figure 3-13.

Waterbody FID	Inflow Mass (g/d)	Inflow Mass (lb/d)	Load (g/d)	Load (lb/yr)	Reduction Ratio (%)
31	66.57	0.15	50.97	41.02	23.43
50	66.57	0.15	39.43	31.73	40.77
5	44.38	0.10	37.02	29.79	16.58
19	44.38	0.10	31.61	25.43	28.78
43	44.38	0.10	30.36	24.43	31.60
36	22.19	0.05	20.66	16.63	6.89
33	22.19	0.05	17.74	14.27	20.06
23	22.19	0.05	15.26	12.28	31.25
8	44.38	0.10	13.45	10.82	69.70
28	44.38	0.10	6.38	5.13	85.63
Total	421.61	0.93	262.87	211.53	37.65

Figures 6-8 and 6-9 show respectively the ArcGIS- and EXCEL-generated descriptive statistics of the extracted seepage velocity magnitude along the perimeter of Lake Weir. The seepage velocity magnitude is the smallest among the four lakes. It is not surprising, because the lake is surrounded by the the Okahumpka Swamp that is relatively flat.

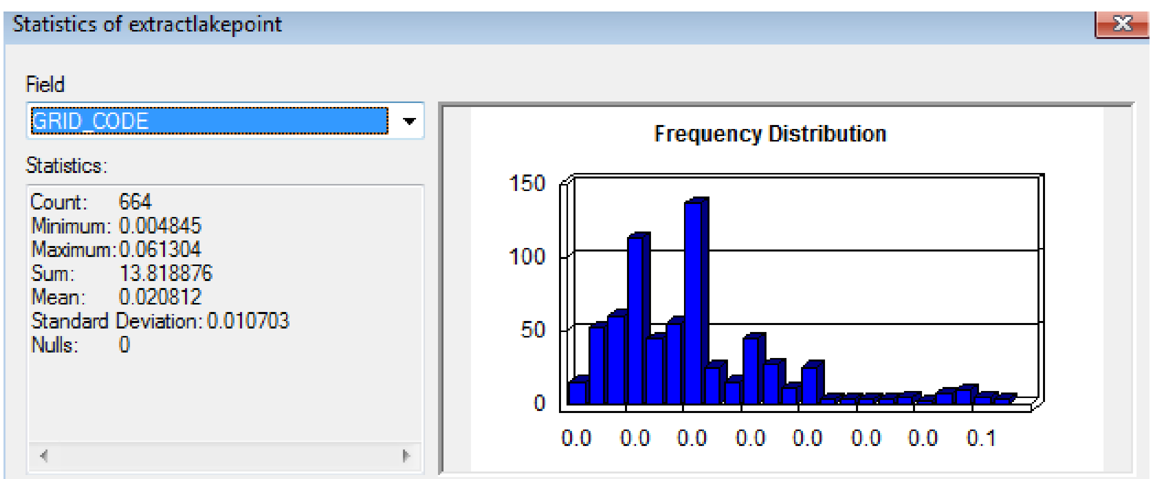

Figure 6-8. Statistics of extracted seepage velocity magnitude (m/d) along the perimeter of Lake Denham.

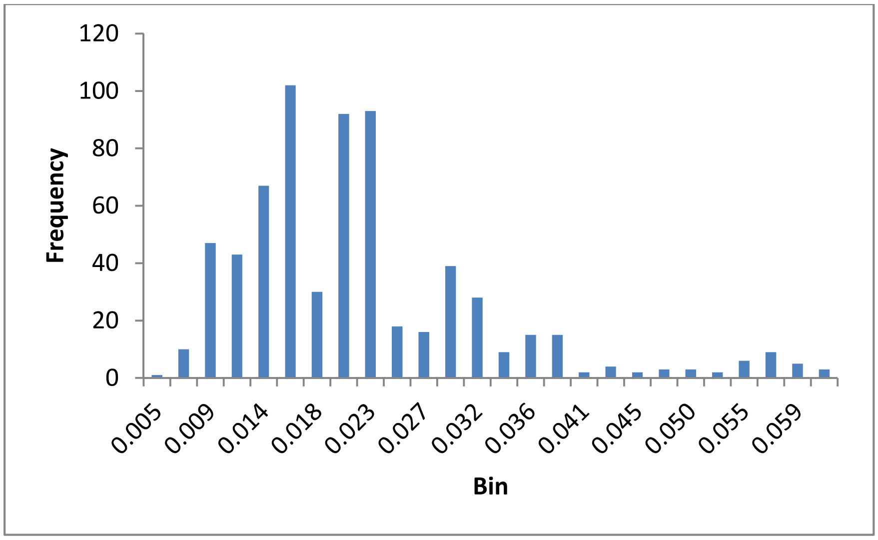

Figure 6-9. EXCEL-based histogram of extracted seepage velocity magnitude (m/d) along the perimeter of Lake Denham.

7. DISCUSSION AND CONCLUSION

To evaluate the estimated nitrogen loads, Table 7-1 lists the numbers of septic systems, the ArcNLET-estimated total loads (in the units of g/d and lb/yr), load (g/d) per septic system to the surface water bodies, and the reduction ratios for the four watersheds. The reduction ratio, as defined before, is the amount of denitrified nitrogen (i.e., the difference between the load to groundwater and the load to surface waterbodies) divided by the load to groundwater (i.e., the inflow mass, M_{in} in equation 5 of Section 2). The table shows that, while the total load is proportional to the number of septic systems, the relation between total load and number of septic systems is not linear. The relation depends on the amount of denitrification. For example, because of the small reduction ratio, the load per septic system is the largest for the Lake Roberts watershed. As a result, the total load in the Lake Roberts watershed is about half of the total load in the Lake Weir watershed, although the number of septic systems in the Lake Roberts watershed is only 1/8 of that in the Lake Weir watershed.

Table 7-1. Simulated nitrogen loads to surface waterbodies and nitrogen reduction ratios for the four watersheds.

Name	Number of septic systems	Total load (g/d)	Total load (lb/yr)	Load per septic systems (g/d)	Reduction ratio
Lake Marshall	47	319.92	257.43	6.81	62.26%
Lake Roberts	83	1413.54	1137.46	17.03	16.62%
Lake Weir	485	3230.33	2599.40	6.66	65.86%
Lake Denham	28	262.87	211.53	9.39	37.65%

Table 7-2. Nitrogen reduction ratio from the literature and this study.

Reference	Site Location	Nitrogen reduction ratio
Roeder (2008)	Wekiva Study Area, FL	70.0%
Valiela et al. (1997)	Waquoit Bay, MA	57.1%
Meile et al. (2010)	McIntosh County, GA	65-85 %
Ye and Sun (2013)	Port St. Lucie, FL	67.0%
	Stuart, FL	50.4%
	North River Shores, FL	11.7%
	Seagate Harbor, FL	10.8%
	Banner Lake, FL	64.6%
	Rio, FL	79.1%
	Hobe Sound, FL	70.5%
This Study	Lake Marshall	62.26%
	Lake Roberts	16.62%
	Lake Weir	65.86%
	Lake Denham	37.65%

The reduction ratios estimated in this study are comparable with those reported literature and those obtained in our modeling practice, which are listed in Table 7-2. The reduction ratios are determined by the flow path and flow velocity; large flow path and small flow velocity always lead to large amount of denitrification and thus large reduction ratio. For example, visual examination of the simulated flow paths and nitrogen contours shown in Figure 3-15and Figure 4-5 for the Lake Marshall watershed and Lake Roberts watershed, respectively, shows that the flow paths are shorter in the Lake Marshall watershed than in the Lake Roberts watershed. Ye and Sun (2013) showed that flow paths and velocities are closely related to soil drainage conditions given in the SSURGO database. The relation however has not been evaluated in this study.

The ArcNLET modeling of this study leads to the following major conclusions:

(1) Data and information needed to establish ArcNLET models for groundwater modeling and nitrogen load estimation are readily available in the four watersheds. The data are available in either the public domain (e.g., USGS websites) or FDEP database. Most of the data are site-specific, including DEM, waterbodies, septic locations, hydraulic conductivity, and porosity. Transport parameters are not site specific. The values of dispersivity, decay coefficient, inflow mass to groundwater, and source plane concentration are obtained from literature, as explained in Chapters 3 – 6.

(2) ArcNLET can simulate directions and magnitude of groundwater flows at each raster cell; using ArcGIS extraction tools to extract the simulated seepage velocity along lake perimeters can estimate groundwater seepage to the lakes. The average estimates is the largest for Lake Weir (3.244 m/d) and the smallest for Lake Denham (0.021 m/d). The estimates are consistent with the lake geometry. For example, the average seepage estimate is 0.391 m/d for Lake Marshall but only 0.121 m/d for Lake Roberts. This is consistent with the deeper slope of land surface around Lake Marshall than around Lake Roberts.

(3) ArcNLET can simulate nitrogen concentrations and nitrogen loads to surface water bodies. These values appear to be reasonable by comparing the reduction ratios with literature data.

(4) The seepage rate measurements at Lake Roberts are important to calibrate the ArcNLET flow model for estimating the smoothing factor and hydraulic conductivity. The results of flow and solute transport modeling before the calibration are significantly different from those after the calibration. Generally speaking, after the calibration, the ArcNLET-simulated flow velocity and nitrogen load become smaller. However, the calibrated smoothing factor is not used for the other three watersheds, because the measured seepage rate is suspiciously small and it is unknown why the measurements at one site are significantly larger than those at other sites. If the seepage rate measurements are considered to be reasonable, it is straightforward to use the calibrated smoothing factor for the other three watersheds. It is also possible to use small values of hydraulic conductivity for the other three watersheds, if necessary.

To better evaluate the flow and transport modeling results, it would be necessary to compare simulated water table shape with observed water table depth and to compare simulated nitrogen concentrations with field observations. If the model fit between model simulations and field observations is not satisfactory, it is necessary to adjust certain model parameters (e.g., the decay coefficient) to improve the model fit. This will also yield field-specific parameter values. Another way to evaluate reasonableness of the estimates is to compare the load estimate from septic systems with the total nitrogen load estimate. For example, a recent study (USEPA, 2013) for the Chesapeake Bay watershed indicates that septic systems contribute about 5% of the total nitrogen load. The comparison should be straightforward when the total load estimates for the watershed are available. If the percentage is not desired, parameter adjustment can be conducted to yield reasonable percentages.

8. REFERENCES

Anderson, D. (2006), A Review of Nitrogen Loading and Treatment Performance Recommendations for Onsite Wastewater Treatment Systems (OWTS) in the Wekiva Study Area, Hazen and Sawyer, P.C.

Blandford, T.N. and T.R. Birdie (1992), Ground-Water Flow and Solute Transport Modeling Study for Eastern Orange County, Florida and Adjoining Regions, HydroGeoLogic Report prepared for St. Johns River Water Management District, Orange County Public Utilities Division, and City of Cocoa, Special Publication SJ93-SP4.

Belanger, T.V. and M.T. Montgomery (1992), Seepage meter errors. Limnol. Oceanogr. 37: 1787–1795.

BMAP (2012), Basin Management Action Plan for the Implementation of Total Maximum Daily Loads for Nutrients and Dissolved Oxygen by the Florida Department of Environmental Protection in the Santa Fe River Basin, developed by the Florida Department of Environmental Protection Division of Environmental Assessment and Restoration Bureau of Watershed Restoration.

Byrme Sr., M.J., R.L. Smith, and D.A. Repert (2012), Potential for Denitrification near Reclaimed Water Application Sites in Orange County, Florida, 2009, U.S. Geological Survey Open File Report 2012-1123.

Cherkauer, D.A. and J.M. McBride (1988), A remotely operated seepage meter for use in large lakes and rivers. Ground Water. 26:165–171.

Carsel, R.F. and R.S. Parrish (1988), Developing Joint Probability Distributions of Soil Water Retention Characteristics. Water Resources Research, 24(5): 755-769.

Domenico, P.A. (1987), An analytical model for multidimensional transport of a decaying contaminant species. J Hydrol 91:49–58.

Erickson, D.R. (1981), A study of littoral groundwater seepage at Williams Lake, Minnesota, using seepage meters and wells. M.S. Thesis. Univ. of Minnesota, Minneapolis. A study of littoral groundwater seepage at Williams Lake, Minnesota, using seepage meters and wells. M.S. Thesis. Univ. of Minnesota, Minneapolis.

Gelhar, L.W., C. Welty, and K.R. Rehfeldt. (1992), A critical review of data on field-scale dispersion in aquifers. Water Resour. Res. 28: 1955–1974.

Fernandes, R. (2011), Statistical methods for estimating the denitrification rate. Florida State University, Master Thesis.

Harden, H., J. Chanton, R. Hicks, and E. Wade (2010), Wakulla County Septic Tank Study Phase II Report on Performance Based Treatment Systems.

Heinen, M (2006) Simplified denitrification models: Overview and properties. Geoderma 133(3-4):444–463

Hicks, R.W. and K. Holland (2012), Nutrient TMDL for Silver Springs, Silver Springs Group, and Upper Silver River (WBIDs 2772A, 2772C, and 2772E), Ground Water Management Section, Florida Department of Environmental Protection, Tallahassee, FL.

Horsley, S.W., Santos, D., and Busby, D., 1996, Septic system impacts for the Indian River Lagoon, Florida, available at http://water.epa.gov/type/watersheds/archives/upload/2004_05_11_watershed_Proceed_sess41-60.pdf, accessible as of 1/20/2014.

Kidmose, J., Engesgaard, P., Nilsson, B., Laier, T., Looms, M.C. (2011), Spatial distribution of seepage at a flow through lake: Lake Hampen, Western Denmark. Vadose Zone Journal, Special Issue, 10, 110-124.

Maggi, F., C. Gu, W.J. Riley, G.M. Hornberger, R.T. Venterea, T. Xu, N. Spycher, C. Steefel, N.L. Miller, C.M. Oldenburg (2008), A mechanistic treatment of the dominant soil nitrogen cycling processes: Model development, testing, and application. J Geophys Res. doi:10.1029/2007JG000578.

McCray, J.E., M. Geza, K.F. Murray, E.P Poeter, D. Morgan (2009), Modeling onsite wastewater systems at the watershed scale: a user's guide. Water Environment Research Foundation, Alexandria, VA.

McCray, JE, Kirkland SL, Siegrist RL, Thyne GD (2005) Model parameters for simulating fate and transport of on-site wastewater nutrients. Ground Water 43(4):628–639.

O'Reilly, A.M., N.-B. Chang, and M. P. Wanielista (2012a), Cyclic biogeochemical processes and nitrogen fate beneath a subtropical stormwater infiltration basin, Journal of Contaminant Hydrology, 133, 53–75.

O'Reilly, A.M., M.P. Wanielista, N.-B. Chang, Z. Xuan, W.G. Harris (2012b), Nutrient removal using biosorption activated media: Preliminary biogeochemical assessment of an innovative stormwater infiltration basin, Science of the Total Environment, 432, 227–242.

Otis, R.J., Anderson, D.L., and Apfel, R.A., 1993, Onsite sewage disposal system research in Florida: Report prepared for Florida Department of Health and Rehabilitative Services, Contract No. LP-596, Ayres and Associates, Tampa, Fla., 57 p.

Phelps, G.G. (2004), Chemistry of Ground Water in the Silver Spring Basin, Florida, with an Emphasis on Nitrate, U.S. Geological Survey, Reston, Virginia, Scientific Investigations Report 2004-5144

Reddy, K.R., P.D. Sacco, and D.A. Graetz (1980), Nitrate reduction in an organic soil-water system, Journal of Environmental Quality, 9(2), 283-288.

Rios, J.F. (2010), A GIS-Based Model for Estimating Nitrate Fate and Transport from Septic Systems in Surfacial Aquifers, Master Thesis, Florida State University, Tallahassee, FL.

Rios, J.F., M. Ye, and L. Wang (2011a), uWATER-PA: Ubiquitous WebGIS Analysis Toolkit for Extensive Resources - Pumping Assessment, Ground Water, 49(6), 776-780, DOI: 10.1111/j.1745-6584.2011.00872.x.

Rios, J.F., M. Ye, L. Wang, and P. Lee (2011b), ArcNLET: An ArcGIS-Based Nitrate Load Estimation Toolkit, User's Manual, Florida State University, Tallahassee, FL., available online at http://people.sc.fsu.edu/~mye/ArcNLET/users_manual.pdf.

Rios, J.F., M. Ye, L. Wang, P.Z. Lee, H. Davis, and R.W. Hicks (2013a), ArcNLET: A GIS-based software to simulate groundwater nitrate load from septic systems to surface water bodies, Computers and Geosciences, 52, 108-116, 10.1016/j.cageo.2012.10.003.

Rios, J.F., M. Ye, and H. Sun (2013b), ArcNLET 2.0: New ArcNLET Function of Monte Carlo Simulation for Uncertainty Quantification, Florida State University, Tallahassee, FL.

Rosenberry, D.O. and M.A. Menheer (2006), A system for calibrating seepage meters used to measure flow between groundwater and surface water. Sci. Invest. Rep. 2006-5053. USGS, Reston, VA.

Srinivasan V, Clement TP, Lee KK (2007) Domenico solution – is it valid? Ground Water 45(2):136–146.

Sumner, D.M. and L.A. Bradner (1996), Hydraulic Characteristics and Nutrient Transport and Transformation Beneath a Rapid Infiltration Basin, Reedy Creek Improvement District, Orange County, Florida, U.S. Geological Survey, Water-Resources Investigations Report, 95-4281.

Ursin, E.L. and E. Roeder (2008), An assessment of nitrogen contribution from onsite wastewater treatment systems (OWTS) in the Wekiva study area of central Florida. In National Onsite Wastewater Recycling Association (NOWRA) Nitrogen Symposium. Florida Department of Health, Tallahassee.

U.S. EPA (2003), Voluntary National Guidelines for Management of Onsite and Clustered (Decentralized) Wastewater Treatment Systems. U.S. Environmental Protection Agency.

U.S. EPA. (2010), Water Quality Standards for the State of Florida's Lakes and Flowing Waters; Proposed Rule. Released by EPA on January 14, 2010. http://edocket.access.gpo.gov/2010/pdf/2010-1220.pdf.

U.S. EPA (2013), A Model Program for Onsite Management in the Chesapeake Bay Watershed, Office of Wastewater Management, U.S. Environmental Protection Agency.

Valiela, I. and J.E. Costa (1988), Eutrophication of Buttermilk Bay, a Cape Cod coastal embayment: Concentrations of nutrients and watershed nutrient budgets. Environmental Management 12, no. 4: 539–553.

Valiela, I., G. Collins, J. Kremer, K. Lajtha, M. Geist, B. Seely, J. Brawley, C.H. Sham (1997) Nitrogen loading from coastal watersheds to receiving estuaries: new method and application, Ecological Applications, 7(2), 358–380.

Valiela, I., M. Geist, J. McClelland, and G. Tomasky (2000), Nitrogen loading from watersheds to estuaries: Verification of the Waquoit Bay Nitrogen Loading Model. Biogeochemistry 49, no. 3: 277–293.

Wang, L., M. Ye, J.F. Rios, and P. Lee (2011), ArcNLET: An ArcGIS-Based Nitrate Load Estimation Toolkit, Application Manual, Florida State University, Tallahassee, FL., available online at http://people.sc.fsu.edu/~mye/ArcNLET/application_manual.pdf.

Wang L, Ye M, J.F. Rios, Lee P (2012). Sensitivity analysis and uncertainty assessment for ArcNLET-estimated nitrate load from septic systems to surface water bodies. http://people.sc.fsu.edu/~mye/ArcNLET/ArcNLETSensitivityUncertainty.pdf

Wang, L., M. Ye, J.F. Rios, R. Fernandes, P.Z. Lee, and R.W. Hicks (2013), Estimation of nitrate load from septic systems to surface water bodies using an ArcGIS-based software, Environmental Earth Sciences, doi:10.1007/s12665-013-2283-5.

Wanielista, M., N.-B. Chang, Z. Xuan, L. Naujock, and P. Biscardi (2011), Nitrogen Transport and Transformation Beneath Stormwater Retention Basins in Karst Areas and Effectiveness of Stormwater Best Management Practices for Reducing Nitrate Leaching to Ground Water Marion County, Florida, Florida Department of Environmental Protection, FDEP Report # S0316.

West, MR, Kueper, BH, Ungs, MJ (2007) On the use and error of approximation in the Domenico (1987) solution. Ground Water 45(2): 126–135.

Ye, M, Sun H (2013), Estimation of Nitrogen Load from Removed Septic Systems to Surface Water Bodies in the City of Port St. Lucie, the City of Stuart, and Martin County, Technical report submitted to Florida Department of Environmental Protection, Florida State University, Tallahassee, FL., Under review.

Appendix A

Table A-1. Percentages of particle size components at location SS-1.

Field ID SS-1

Sample ID	Ref. Method	Component		Resutlt (%)	type*	Soil Type
1597666	SOP-BB15 SOP-BB15-5	Sediment % Organic		2.2		Sand
		Sediment Particle Size, %	>2.0mm	1	Gravel	
		Sediment Particle Size, %	0.5-2.0mm	12.4	Coarse sand	
		Sediment Particle Size, %	0.25-0.5mm	31.8	Median sand	
		Sediment Particle Size, %	0.125-0.25mm	40.9	Fine sand	
		Sediment Particle Size, %	0.063-0.125mm	5.18	Very fine sand	
		Sediment Particle Size, %	<0.063mm	9.74	Silt	

Table A-2. Percentages of particle size components at location SS-2.

Field ID SS-2

Sample ID	Ref. Method	Component		Resutlt (%)	Type*	Soil Type
1597667	SOP-BB15 SOP-BB15-5	Sediment % Organic		2.8		Loamy sand
		Sediment Particle Size, %	>2.0mm	1	Gravel	
		Sediment Particle Size, %	0.5-2.0mm	9.66	Coarse sand	
		Sediment Particle Size, %	0.25-0.5mm	17.9	Median sand	
		Sediment Particle Size, %	0.125-0.25mm	39.4	Fine sand	
		Sediment Particle Size, %	0.063-0.125mm	10.4	Very fine sand	
		Sediment Particle Size, %	<0.063mm	22.7	Silt	

Table A-3. Percentages of particle size components at location SS-3.

Field ID SS-3

Sample ID	Ref. Method	Component		Resutlt (%)	Type*	Soil Type
1597668	SOP-BB15 SOP-BB15-5	Sediment % Organic		1		Sand
		Sediment Particle Size, %	>2.0mm	1	Gravel	
		Sediment Particle Size, %	0.5-2.0mm	7.14	Coarse sand	
		Sediment Particle Size, %	0.25-0.5mm	23.8	Median sand	
		Sediment Particle Size, %	0.125-0.25mm	51.1	Fine sand	
		Sediment Particle Size, %	0.063-0.125mm	7.93	Very fine sand	

		Sediment Particle Size, %	<0.063mm	9.99	Silt	

Table A-4. Percentages of particle size components at location SS-4.

Field ID SS-4

Sample ID	Ref. Method	Component		Resutlt (%)	Type*	Soil Type
1597669	SOP-BB15 SOP-BB15-5	Sediment % Organic		1.6		Sand
		Sediment Particle Size, %	>2.0mm	1	Gravel	
		Sediment Particle Size, %	0.5-2.0mm	3.59	Coarse sand	
		Sediment Particle Size, %	0.25-0.5mm	21.8	Median sand	
		Sediment Particle Size, %	0.125-0.25mm	53.7	Fine sand	
		Sediment Particle Size, %	0.063-0.125mm	9.46	Very fine sand	
		Sediment Particle Size, %	<0.063mm	11.4	Silt	

Table A-5. Percentages of particle size components at location SS-5.

Field ID SS-5

Sample ID	Ref. Method	Component		Resutlt (%)	Type*	Soil Type
1597670	SOP-BB15 SOP-BB15-5	Sediment % Organic		1		Sand
		Sediment Particle Size, %	>2.0mm	1	Gravel	
		Sediment Particle Size, %	0.5-2.0mm	3.23	Coarse sand	
		Sediment Particle Size, %	0.25-0.5mm	23.9	Median sand	
		Sediment Particle Size, %	0.125-0.25mm	56.4	Fine sand	
		Sediment Particle Size, %	0.063-0.125mm	7.62	Very fine sand	
		Sediment Particle Size, %	<0.063mm	8.87	Silt	

Table A-6. Percentages of particle size components at location SS-6.

Field ID SS-6

Sample ID	Ref. Method	Component		Resutlt (%)	Type*	Soil Type
1597666	SOP-BB15 SOP-BB15-5	Sediment % Organic		1.1		Sand
		Sediment Particle Size, %	>2.0mm	1	Gravel	

		Sediment Particle Size, %	0.5-2.0mm	3.86	Coarse sand	
		Sediment Particle Size, %	0.25-0.5mm	24.8	Median sand	
		Sediment Particle Size, %	0.125-0.25mm	53.6	Fine sand	
		Sediment Particle Size, %	0.063-0.125mm	7.83	Very fine sand	
		Sediment Particle Size, %	<0.063mm	9.89	Silt	

Table A-7. Percentages of particle size components at location SS-7.

Field ID SS-7

Sample ID	Ref. Method	Component		Resutlt (%)	Type*	Soil Type
1597667	SOP-BB15 SOP-BB15-5	Sediment % Organic		2.3		Loamy sand
		Sediment Particle Size, %	>2.0mm	1.8	Gravel	
		Sediment Particle Size, %	0.5-2.0mm	7.05	Coarse sand	
		Sediment Particle Size, %	0.25-0.5mm	18.2	Median sand	
		Sediment Particle Size, %	0.125-0.25mm	47	Fine sand	
		Sediment Particle Size, %	0.063-0.125mm	10.3	Very fine sand	
		Sediment Particle Size, %	<0.063mm	17.4	Silt	

Table A-8. Percentages of particle size components at location SS-8.

Field ID SS-8

Sample ID	Ref. Method	Component		Resutlt (%)	Type*	Soil Type
1597668	SOP-BB15 SOP-BB15-5	Sediment % Organic		3.3		Sand
		Sediment Particle Size, %	>2.0mm	1	Gravel	
		Sediment Particle Size, %	0.5-2.0mm	11.3	Coarse sand	
		Sediment Particle Size, %	0.25-0.5mm	22.2	Median sand	
		Sediment Particle Size, %	0.125-0.25mm	45.7	Fine sand	
		Sediment Particle Size, %	0.063-0.125mm	8.72	Very fine sand	
		Sediment Particle Size, %	<0.063mm	12	Silt	

Table A-9. Percentages of particle size components at location SS-9.

Field ID SS-9

Sample ID	Ref. Method	Component		Resutlt (%)	Type*	Soil Type
1597669	SOP-BB15 SOP-BB15-5	Sediment % Organic		1		Sand
		Sediment Particle Size, %	>2.0mm	1	Gravel	
		Sediment Particle Size, %	0.5-2.0mm	11	Coarse sand	
		Sediment Particle Size, %	0.25-0.5mm	21.6	Median sand	
		Sediment Particle Size, %	0.125-0.25mm	44.5	Fine sand	
		Sediment Particle Size, %	0.063-0.125mm	11.3	Very fine sand	
		Sediment Particle Size, %	<0.063mm	11.6	Silt	

Table A-10. Percentages of particle size components at location SS-10.

Field ID SS-10

Sample ID	Ref. Method	Component		Resutlt (%)	Type*	Soil Type
1597670	SOP-BB15 SOP-BB15-5	Sediment % Organic		4		Loamy sand
		Sediment Particle Size, %	>2.0mm	1	Gravel	
		Sediment Particle Size, %	0.5-2.0mm	16.6	Coarse sand	
		Sediment Particle Size, %	0.25-0.5mm	18.7	Median sand	
		Sediment Particle Size, %	0.125-0.25mm	30.2	Fine sand	
		Sediment Particle Size, %	0.063-0.125mm	12.8	Very fine sand	
		Sediment Particle Size, %	<0.063mm	21.6	Silt	

Table A-11. Percentages of particle size components at location SS-11.

Field ID SS-11

Sample ID	Ref. Method	Component		Resutlt (%)	Type*	Soil Type
1597666	SOP-BB15 SOP-BB15-5	Sediment % Organic		1		Sand
		Sediment Particle Size, %	>2.0mm	1	Gravel	
		Sediment Particle Size, %	0.5-2.0mm	5.46	Coarse sand	
		Sediment Particle Size, %	0.25-0.5mm	24.4	Median sand	
		Sediment Particle Size, %	0.125-0.25mm	53.5	Fine sand	
		Sediment Particle Size, %	0.063-0.125mm	8.77	Very fine sand	
		Sediment Particle Size, %	<0.063mm	7.9	Silt	

Table A-12. Percentages of particle size components at location SS-12.

Field ID SS-12

Sample ID	Ref. Method	Component		Resutlt (%)	Type*	Soil Type
1597667	SOP-BB15 SOP-BB15-5	Sediment % Organic		3.7		Loamy sand
		Sediment Particle Size, %	>2.0mm	1	Gravel	
		Sediment Particle Size, %	0.5-2.0mm	6.64	Coarse sand	
		Sediment Particle Size, %	0.25-0.5mm	19.2	Median sand	
		Sediment Particle Size, %	0.125-0.25mm	40.1	Fine sand	
		Sediment Particle Size, %	0.063-0.125mm	9.14	Very fine sand	
		Sediment Particle Size, %	<0.063mm	24.9	Silt	

Table A-13. Percentages of particle size components at location SS-13.

Field ID SS-13

Sample ID	Ref. Method	Component		Resutlt (%)	Type*	Soil Type
1597668	SOP-BB15 SOP-BB15-5	Sediment % Organic		1		Sand
		Sediment Particle Size, %	>2.0mm	1	Gravel	
		Sediment Particle Size, %	0.5-2.0mm	2.65	Coarse sand	
		Sediment Particle Size, %	0.25-0.5mm	24.1	Median sand	
		Sediment Particle Size, %	0.125-0.25mm	58.5	Fine sand	
		Sediment Particle Size, %	0.063-0.125mm	8.33	Very fine sand	
		Sediment Particle Size, %	<0.063mm	6.41	Silt	

Table A-14. Percentages of particle size components at location SS-14.

Field ID SS-14

Sample ID	Ref. Method	Component		Resutlt (%)	Type*	Soil Type
1597669	SOP-BB15 SOP-BB15-5	Sediment % Organic		1		Sand
		Sediment Particle Size, %	>2.0mm	1	Gravel	
		Sediment Particle Size, %	0.5-2.0mm	9.38	Coarse sand	
		Sediment Particle Size, %	0.25-0.5mm	25.2	Median sand	
		Sediment Particle Size, %	0.125-0.25mm	49.1	Fine sand	
		Sediment Particle Size, %	0.063-0.125mm	8.84	Very fine sand	
		Sediment Particle Size, %	<0.063mm	7.53	Silt	

Table A-15. Percentages of particle size components at location SS-15.

Field ID SS-15

Sample ID	Ref. Method	Component		Resutlt (%)	Type*	Soil Type
1597670	SOP-BB15 SOP-BB15-5	Sediment % Organic		1.7		Sand
		Sediment Particle Size, %	>2.0mm	1	Gravel	
		Sediment Particle Size, %	0.5-2.0mm	3.05	Coarse sand	
		Sediment Particle Size, %	0.25-0.5mm	22.5	Median sand	
		Sediment Particle Size, %	0.125-0.25mm	56.1	Fine sand	
		Sediment Particle Size, %	0.063-0.125mm	8.68	Very fine sand	
		Sediment Particle Size, %	<0.063mm	9.7	Silt	

* Daniel Hillel, Environmental soil physics. Academic Press.1998, P61&P64